SYNTHESIS, CHARACTERIZATION AND APPLICATIONS OF PALM FATTY ACID FUNCTIONALIZED MAGNETIC NANOPARTICLES AS NEW ADSORBENTS

SITI KHALIJAH BINTI MAHMAD ROZI

FACULTY OF SCIENCE
UNIVERSITY OF MALAYA
KUALA LUMPUR

2018

University of Malaya

SYNTHESIS, CHARACTERIZATION AND APPLICATIONS OF PALM FATTY ACID FUNCTIONALIZED MAGNETIC NANOPARTICLES AS NEW ADSORBENTS

SITI KHALIJAH BINTI MAHMAD ROZI

THESIS SUBMITTED IN FULFILMENT OF THE REQUIREMENTS FOR THE DEGREE OF DOCTOR OF PHILOSOPHY

DEPARTMENT OF CHEMISTRY
FACULTY OF SCIENCE
UNIVERSITY OF MALAYA
KUALA LUMPUR

2018

University of Malaya

University of Malaya

UNIVERSITY OF MALAYA
ORIGINAL LITERARY WORK DECLARATION

Name of Candidate: **Siti Khalijah Binti Mahmad Rozi**

Matric No: **SHC 140090**

Name of Degree: **Doctor of Philosophy**

Title of Thesis ("this Work"):

Synthesis, Characterization and Applications of Palm Fatty Acid Functionalized Magnetic Nanoparticles as New Adsorbents

Field of Study: **Analytical Chemistry**

I do solemnly and sincerely declare that:

(1) I am the sole author/writer of this Work;
(2) This Work is original;
(3) Any use of any work in which copyright exists is done by way of fair dealing and for permitted purposes and any excerpt or extract from, or reference to or reproduction of any copyright work has been disclosed expressly and sufficiently and the title of the Work and its authorship have been acknowledged in this Work;
(4) I do not have any actual knowledge nor do I ought reasonably to know that the making of this work constitutes an infringement of any copyright work;
(5) I hereby assign all and every rights in the copyright to this Work to the University of Malaya ("UM"), who henceforth shall be owner of the copyright in this Work and that any reproduction or use in any form or by any means whatsoever is prohibited without the written consent of UM having been first had and obtained;
(6) I am fully aware that if in the course of making this Work I have infringed any copyright whether intentionally or otherwise, I may be subject to legal action or any other action as may be determined by UM.

Candidate's Signature Date:

Subscribed and solemnly declared before,

Witness's Signature Date:

Name:

Designation:

SYNTHESIS, CHARACTERIZATION AND APPLICATIONS OF PALM FATTY ACID FUNCTIONALIZED MAGNETIC NANOPARTICLES AS NEW ADSORBENTS

ABSTRACT

In this study, three new adsorbents were synthesized, free fatty acids from hydrolysis of triacylglycerol of palm cooking oil functionalized magnetic nanoparticles (MNP@FFAs-PCO), free fatty acids from waste palm cooking oil functionalized magnetic nanoparticles (MNP@FFAs-WPCO) and free fatty acids from waste palm cooking oil functionalized magnetic nanoparticles immobilized on the surface of the graphene oxide (MNP@FFAs-WPCO-GO) for the preconcentration and remediation of organic pollutants from various sample matrices. The structure of MNP@FFAs-PCO and MNP@FFAs-WPCO were characterized by XRD, TEM, FT-IR, FESEM, VSM, EDX, BET, TGA analyses and water contact angle measurement. The obtained results prove the successful synthesis of these adsorbents. Furthermore, it was also revealed that MNP@FFAs-WPCO has a larger surface area and higher hydrophobicity compared to MNP@FFAs-PCO. The synthesized MNP@FFAs-PCO and MNP@FFAs-WPCO were used as adsorbent for magnetic solid phase extraction (MSPE) of polycyclic aromatic hydrocarbons (PAHs) and for the removal of oil from aqueous media. The MNP@FFAs-PCO and MNP@FFAs-WPCO showed a low limit of detection (LOD) ranging from 0.01 to 0.05 ng mL^{-1} and 0.001 to 0.05 ng mL^{-1}, respectively and limit of quantification (LOQ) in the range of 0.03-0.16 ng mL^{-1} and 0.004-0.2 ng mL^{-1}, respectively. The application of MNP@FFAs-PCO and MNP@FFAs-WPCO were successfully studied on the leachate and sludge from a landfill site. The MNP@FFAs-PCO recorded good recovery (81.1-119.3%) with satisfactory precision (%RSD: 3.1–13.6) while MNP@FFAs-WPCO showed satisfactory recovery (72.3–119.9%) with acceptable precision (%RSD: 4.8–11.8). The MNP@FFAs-PCO and MNP@FFAs-WPCO were also found to be able to adsorb 3.50 times and 4.31 times of

University of Malaya

oil higher than their own weight, respectively. In this study, it was found that MNP@FFAs-WPCO showed an excellent MSPE performance as it provided lower LOD for all selected PAHs and good oil sorption capacity in comparison with the performance MNP@FFAs-PCO. The third adsorbent, MNP@FFAs-WPCO-GO was characterized by FT-IR, XRD, FESEM, TGA, TEM, VSM and EDX analyses to confirm its structure. It was successfully applied as a MSPE adsorbent for simultaneous separation of selected PAHs and phthalate esters (PAEs). It has good performance with low LODs ranging from 0.02 – 0.93 ng mL^{-1} for PAHs and 0.56 – 0.97 ng mL^{-1} for PAEs with LOQs in the range of 0.07 to 3.10 ng mL^{-1} for PAHs and 1.86 to 3.20 ng mL^{-1} for PAEs. The MNP@FFAs-WPCO-GO was successfully studied on apple, cabbage and landfill sludge samples. High recoveries (81.5 – 118.2% for PAEs) and (86.7 – 118.8% for PAHs) with satisfactory precision (%RSD: 2.1 to 9.9 for PAEs, 1.5 to 11.0 for PAHs) were obtained.

Keywords: Magnetic nanoparticles, free fatty acids, graphene oxide, organic pollutants

University of Malaya

SINTESIS, PENCIRIAN DAN APLIKASI MAGNETIK NANOZARAH YANG BERFUNGSIKAN ASID LEMAK SAWIT SEBAGAI PENJERAP BARU

ABSTRAK

Dalam kajian ini, tiga penjerap baru telah disintesis iaitu magnetik nanozarah yang berfungsikan asid lemak bebas daripada hidrolisis triasilgliserol minyak masak sawit (MNP@FFAs-PCO), magnetik nanozarah yang berfungsikan asid lemak bebas daripada sisa buangan minyak masak sawit (MNP@FFAs-WPCO), magnetik nanozarah yang berfungsikan asid lemak bebas daripada sisa buangan minyak masak sawit yang diimobilisasikan ke atas permukaan grafin oksida (MNP@FFAs-WPCO-GO) untuk pra-pemekatan dan pemulihan pencemar organik dari pelbagai sampel matrik. Struktur MNP@FFAs-PCO dan MNP@FFAs-WPCO dikenalpasti oleh XRD, TEM, FT-IR, FESEM, VSM, EDX, BET, TGA analisis dan pengukuran sudut sentuh air. Keputusan yang diperolehi dari pencirian kedua-dua penjerap ini membuktikan kedua-dua penjerap ini telah berjaya disintesis. Selain itu, hasil dari analisa ini juga menemukan bahawa penjerap MNP@FFAs-WPCO mempunyai kawasan permukaan yang luas dan ia sangat bersifat hidrofobik berbanding penjerap MNP@FFAs-PCO. Penjerap MNP@FFAs-PCO dan MNP@FFAs-WPCO yang telah disintesis digunakan sebagai penjerap untuk pengekstrakan fasa pepejal bermagnetik (MSPE) bagi polisiklik hidrokarbon aromatik (PAHs) dan penyingkiran minyak daripada media akueus. Kedua-dua penjerap MNP@FFAs-PCO dan MNP@FFAs-WPCO masing-masing telah menunjukkan had pengesanan yang rendah (LOD) di antara 0.01-0.05 ng mL^{-1} dan 0.001 to 0.05 ng mL^{-1}dengan had kuantifikasi (LOQ) adalah di antara 0.03-0.16 ng mL^{-1} dan 0.004-0.2 ng mL^{-1}. Kedua-dua penjerap ini telah berjaya diaplikasi terhadap sampel alam sekitar seperti larut resapan dan enapcemar dari tapak pelupusan. Keputusan yang diperolehi menunjukkan MNP@FFAs-PCO mencatat kebolehdapatan semula yang bagus (81.1-119.3%) dengan kepersisan yang bagus (%RSD: 3.1–13.6) manakala MNP@FFAs-

University of Malaya

WPCO menunjukkan kebolehdapatan semula yang memuaskan (72.3–119.9%) dengan kepersisan yang boleh diterima (%RSD: 4.8–11.8). Di samping itu, kedua-dua penjerap MNP@FFAs-PCO and MNP@FFAs-WPCO ini didapati masing-masing boleh menyerap 3.50 dan 4.31 kali ganda minyak lebih tinggi dari berat mereka sendiri. Hasil keputusan eksperimen menunjukkan MNP@FFAs-WPCO mempamerkan prestasi yang cemerlang sebagai penjerap MSPE dimana ia memberikan LOD yang lebih rendah untuk PAHs yang dipilih untuk kajian ini dan kapasiti penyerapan minyak yang bagus berbanding prestasi yang ditunjukkan oleh penjerap MNP@FFAs-PCO. Penjerap yang ketiga iaitu MNP@FFAs-WPCO-GO telah dianalisa oleh FT-IR, XRD, FESEM, TGA, TEM, VSM and EDX untuk mengesahkan strukturnya. Penjerap in telah berjaya digunakan sebagai penjerap MSPE untuk pemisahan serentak PAHs dan ftalat ester (PAEs). Ia menunjukkan LOD yang rendah di antara 0.02 – 0.93 ng mL^{-1} untuk PAHs dan 0.56 – 0.97 ng mL^{-1} untuk PAEs dengan LOQ di antara 0.07 - 3.10 ng mL^{-1} untuk PAHs dan 1.86 - 3.20 ng mL^{-1} untuk PAEs. Penjerap MNP@FFAs-WPCO-GO telah berjaya diaplikasi terhadap sampel seperti epal, kobis dan enapcemar dari tapak pelupusan. Kebolehdapatan semula yang tinggi (86.7 – 118.8% untuk PAHs) dan (81.5 – 118.2% untuk PAEs) dengan kepersisan yang memuaskan (%RSD: 2.1 to 9.9 for PAEs; 1.5 to 11.0 for PAHs) telah diperolehi.

Kata kunci: Magnetik nanozarah, asid lemak bebas, grafin oksida, pencemar organik

University of Malaya

ACKNOWLEDGEMENTS

First of all, I am grateful to The Almighty God for establishing me to complete this thesis. This thesis would not have been possible without the opportunity given to me by the University of Malaya and the inspiration and constant support given by my kind supervisors, Associate Prof. Dr. Sharifah Binti Mohamad and Dr. Ninie Suhana Binti Abdul Manan. They have also provided me with invaluable supervision, advice and guidance. I gratefully appreciate their contributions of time, ideas and support to make my Ph.D. program productive and exciting.

I would like to thank my family, foremostly my mother, Fatimah Binti Hashim and my father Mahmad Rozi Bin Man, whose love and encouragement supported me throughout this journey. I would also like to take this opportunity to express my gratitude to my labmates and the staffs of Department of Chemistry for their supports.

Finally, I would like to thank the Department of Chemistry for providing me a conducive environment for carrying out my research and University of Malaya for PPP Grant (PG042-2015A). I also gratefully acknowledge the Ministry of Higher Education of Malaysia and School of Bioprocess Engineering, University of Malaysia Perlis (UniMaP) for fellowship funding.

University of Malaya

TABLE OF CONTENTS

Abstract iii
Abstrak v
Acknowledgements vii
Table of Contents viii
List of Figures xii
List of Tables..xxi
List of Symbols and Abbreviations xxiii

CHAPTER 1: INTRODUCTION 1
1.1 Background of study 1
1.2 Objectives of the research 6
1.3 Outline of thesis 6

CHAPTER 2: LITERATURE REVIEW 8
2.1 Magnetic nanoparticles 8
  2.1.1 Surface modification strategies of magnetic iron oxide 10
2.2 Fatty acids modified magnetic iron oxide 11
  2.2.1 Palm oil...13
  2.2.2 Waste palm oil 15
2.3 Graphene oxide modified magnetic iron oxide 16
2.4 Applications of functionalized magnetic nanoparticles as adsorbent ...18
  2.4.1 Magnetic solid phase extraction (MSPE) application 19
    2.4.1.1 Polycyclic aromatic hydrocarbons (PAHs) 20
    2.4.1.2 Phthalate esters (PAEs) 26
  2.4.2 Remediation of oil 29

University of Malaya

CHAPTER 3: METHODOLOGY **33**

3.1 Chemicals, materials and reagents 33

3.2 Instruments 33

3.2.1 GC conditions 34

3.2.2 HPLC conditions 35

3.2.2.1 Liquid chromatographic conditions for separation of PAHs 35

3.2.2.2 Liquid chromatographic conditions for simultaneous separation of PAHs and PAEs 35

3.3 Preparation of new adsorbents 36

3.3.1 Synthesis of MNP@FFAs-PCO 36

3.3.1.1 Hydrolysis of triacylglycerol of palm cooking oil 36

3.3.1.2 Preparation of MNPs 37

3.3.1.3 Preparation of MNP-APTES 37

3.3.1.4 Preparation of MNP@FFAs-PCO 37

3.3.2 Synthesis of MNP@FFAs-WPCO 38

3.3.3 Synthesis of MNP@FFAs-WPCO-GO 40

3.3.3.1 Preparation of Graphene oxide (GO) 40

3.3.3.2 Preparation of MNP@FFAs-WPCO-GO 40

3.4 The applications of new adsorbents 41

3.4.1 MSPE study 41

3.4.1.1 Optimization of MSPE procedure 41

3.4.1.2 Adopted extraction conditions 42

3.4.1.3 Reusability study 43

3.4.1.4 Method validation 43

3.4.1.5 Real samples application 44

3.4.2 Oil removal procedure 46

University of Malaya

3.4.2.1 Optimization of oil adsorption procedure 46

3.4.2.2 Adopted removal conditions 46

3.4.2.3 Reusability study 47

CHAPTER 4: RESULTS AND DISCUSSION 48

4.1 Introduction... 48

4.2 Free fatty acids from palm cooking oil functionalized magnetic nanoparticles (MNP@FFAs-PCO) and its applications 51

4.2.1 Physicochemical properties of MNP@FFAs-PCO 51

4.2.2 Applications of the MNP@FFAs-PCO 61

4.2.2.1 MSPE performance 61

4.2.2.2 Oil removal efficiency... 71

4.3 Free fatty acids from waste palm cooking oil functionalized magnetic nanoparticles (MNP@FFAs-WPCO) and its applications... 78

4.3.1 Physicochemical properties of MNP@FFAs-WPCO 78

4.3.2 Applications of the MNP@FFAs-WPCO 89

4.3.2.1 MSPE performance 89

4.3.2.2 Oil removal application 102

4.4 Free fatty acids from waste palm cooking oil functionalized magnetic nanoparticles immobilized on the surface of graphene oxide (MNP@FFAs-WPCO-GO) and its application.. 110

4.4.1 Characterizations of MNP@FFAs-WPCO-GO 110

4.4.2 Application of the MNP@FFAs-WPCO-GO....................................... 116

CHAPTER 5: CONCLUSIONS AND FUTURE DIRECTION 130

5.1 Conclusion 130

5.2 Future direction.. 131

University of Malaya

References 132

List of Publications and Papers Presented 146

University of Malaya

LIST OF FIGURES

Figure 2.1 : TEM images of Fe_3O_4 nanoparticles with diameter of (A) 7 nm and (B) 19 nm obtained from co-precipitation method (adapted from Kim *et al*., 2005) 9

Figure 2.2 : The main structure of functionalized iron oxide nanoparticles (if iron oxide nanoparticles are always assumed as the core) (adapted from Wu *et al*., 2008) 10

Figure 2.3 : Common chemical moieties for the anchoring of functional groups at the surface of iron oxide magnetic nanoparticles (Dias *et al*., 2011) 11

Figure 2.4 : Palm oil exports to the world consumption year 2011 (Awalludin *et al*., 2015) 13

Figure 2.5 : The hydrolysis reaction of TAG palm oil 14

Figure 2.6 : The schematic route of preparation graphene oxide from oxidation of graphite (Nodeh *et al*., 2016) 17

Figure 2.7 : Schematic illustration of the adsorption-desorption process 19

Figure 2.8 : The schematic procedure of MSPE for different analyte preconcentration from aqueous media 20

Figure 2.9 : Digital photograph images of removal of lubricating oil from water surface by magnetic nanocomposites under magnetic field (a-d) (adapted from Chen *et al*., 2013) 31

Figure 3.1 : The preparation scheme of (A) Free fatty acids (B) MNPs (C) MNP-APTES and (D) MNP@FFAs-PCO or MNP@FFAs-WPCO (R = the alkyl chain of the free fatty acids) 39

Figure 3.2 : The preparation scheme of MNP@FFAs-WPCO-GO 41

Figure 4.1 : FT-IR spectra of (A) MNPs (B) MNP-APTES and (C) MNP@FFAs-PCO 52

University of Malaya

Figure 4.2 : XRD patterns of (A) MNPs (B) MNP-APTES and (C) MNP@FFAs-PCO 53

Figure 4.3 : EDX spectra of (A) MNPs (B) MNP-APTES and (C) MNP@FFAs-PCO 54

Figure 4.4 : TGA thermograms of (A) MNPs (B) MNP-APTES and (C) MNP@FFAs-PCO 55

Figure 4.5 : TEM images of (A) MNPs (B) MNP-APTES and (C) MNP@FFAs-PCO; FESEM images of (D) MNPs (E) MNP-APTES and (F) MNP@FFAs-PCO; and diameter distributions of (G) MNPs (H) MNP-APTES and (I) MNP@FFAs-PCO 56

Figure 4.6 : N_2 adsorption-desorption isotherms of (A) MNPs; (B) MNP-APTES and (C) MNP@FFAs-PCO 57

Figure 4.7 : The magnetization hysteresis loops of MNPs, MNP-APTES and MNP@FFAs-PCO. The inset shows photographs of magnetic nanoparticles dispersed in solution (left) and separated from water solution under an external magnetic field (right) 58

Figure 4.8 : Optical image of a water droplet placed on (A) MNPs and (B) MNP@FFAs-PCO (C); the water contact angle on MNP@FFAs-PCO after corrosion/heat treatment (70 °C & 90 °C) and time storage (30 days) at ambient temperature and (D) Relationship between pH of water droplet on water CA on the MNP@FFAs-PCO surface 59

Figure 4.9 : Top and side view for situation of MNP@FFAs-PCO particles (A-B) floating under mechanical stirring, and (C-D) static on water surface after one night 60

Figure 4.10 : Comparison of the extraction efficiencies of PAHs between MNPs, MNP-APTES and MNP@FFAs-PCO. (Amount of the adsorbents (*i.e.*, MNPs, MNP-APTES and MNP@FFAs-PCO) = 10 mg, desorption solvent = *n*-hexane, volume of desorption solvent = 2.0 mL, extraction time = 10 min, desorption time = 5 min, sample pH = 6.5 and sample volume = 15 mL) 62

University of Malaya

Figure 4.11 : The illustration of the adsorption of targeted PAHs toward hydrophobic frameworks of MNP@FFAs-PCO during MSPE procedure (R = the alkyl chain of the free fatty acid) 62

Figure 4.12 : The effect amount of sorbent on the extraction efficiency of PAHs. (Desorption solvent = *n*-hexane, volume of desorption solvent = 2.0 mL, extraction time = 10 min, desorption time = 5 min, sample pH = 6.5 and sample volume = 15 mL) 63

Figure 4.13 : The effect of (A) desorption solvent. (Amount of MNP@FFAs-PCO = 15 mg, volume of desorption solvent = 2.0 mL, extraction time = 10 min, desorption time = 5 min, sample pH = 6.5 and sample volume = 15 mL) and (B) volume of desorption solvent (Amount of MNP@FFAs-PCO = 15 mg, desorption solvent = *n*-hexane, extraction time = 10 min, desorption time = 5 min, sample pH = 6.5 and sample volume = 15 mL) on the extraction efficiency of PAHs 64

Figure 4.14 : The effect of (A) extraction time (Amount of MNP@FFAs-PCO = 15 mg, desorption solvent = *n*-hexane, volume of desorption solvent = 2.0 mL, desorption time = 5 min, sample pH = 6.5 and sample volume = 15 mL) and (B) desorption time (Amount of MNP@FFAs-PCO = 15 mg, desorption solvent = *n*-hexane, volume of desorption solvent = 2.0 mL, extraction time = 15 min, sample pH = 6.5 and sample volume = 15 mL) on the extraction efficiency of PAHs 65

Figure 4.15 : The effect of pH of the sample on the extraction efficiency of PAHs. (Amount of MNP@FFAs-PCO = 15 mg, desorption solvent = *n*-hexane, volume of desorption solvent = 2.0 mL, extraction time = 15 min, desorption time = 10 min, and sample volume = 15 mL) 66

Figure 4.16 : The effect of sample volume on the extraction efficiency of PAHs. (Amount of MNP@FFAs-PCO = 15 mg, desorption solvent = *n*-hexane, volume of desorption solvent = 2.0 mL, extraction time = 15 min, desorption time = 10 min and sample pH = 6.5) 67

Figure 4.17 : Reusability cycles of MNP@FFAs-PCO for extraction of PAHs 68

University of Malaya

Figure 4.18 : HPLC-DAD chromatograms of the PAHs after extraction using proposed MSPE: Non-spiked (A); and 100 ng $mL^{-1}$of each PAHs spiked leachate sample (B) (1) FLT, (2) Pyr, (3) Cry, and (4) BaP 70

Figure 4.19 : Comparison of the adsorption capacity of MNPs, MNP-APTES and MNP@FFAs-PCO. (Amount of the adsorbents (*i.e.*, MNPs, MNP-APTES and MNP@FFAs-PCO) = 15 mg, contact time = 60 min and pH of the aqueous solution = 7) 71

Figure 4.20 : The effect of adsorbent dosage on the adsorption capacity of oil. (Contact time = 60 min and pH of the aqueous solution = 7) 72

Figure 4.21 : The effect of contact time on the adsorption capacity of oil. (Amount of MNP@FFAs-PCO = 10 mg, and pH of the aqueous solution = 7) 73

Figure 4.22 : The effect of pH on the adsorption capacity of oil. (Amount of MNP@FFAs-PCO = 10 mg and contact time = 30 min) 74

Figure 4.23 : Oil-adsorption capacity of MNP@FFAs-PCO after different oil-adsorption cycles 75

Figure 4.24 : EDX spectra of (A) MNP@FFAs-PCO and (B) oil loaded MNP@FFAs-PCO; (C) FT-IR spectra of MNP@FFAs-PCO and oil loaded MNP@FFAs-PCO and (D) TGA thermogram of oil loaded MNP@FFAs-PCO 76

Figure 4.25 : Adsorption capacity of the MNP@FFAs-PCO for the adsorption of selected oil. (Amount of MNP@FFAs-PCO = 10 mg, contact time = 30 min and pH of the aqueous solution = 7) 77

Figure 4.26 : FT-IR spectrum of MNP@FFAs-WPCO 80

Figure 4.27 : XRD pattern of MNP@FFAs-WPCO 81

Figure 4.28 : EDX spectra of (A) MNP@FFAs-WPCO and (B) MNP@FFAs-PCO 82

University of Malaya

Figure 4.29 : TGA thermograms of (A) MNP@FFAs-WPCO and (B) MNP@FFAs-PCO 82

Figure 4.30 : TEM images of (A) MNP@FFAs-WPCO and (B) MNP@FFAs-PCO; FESEM images of (C) MNP@FFAs-WPCO and (D) MNP@FFAs-PCO (A-C); and diameter distributions of (E) MNP@FFAs-WPCO and (F) MNP@FFAs-PCO 84

Figure 4.31 : N_2 adsorption-desorption isotherms of (A) MNP@FFAs-WPCO and (B) MNP@FFAs-PCO 85

Figure 4.32 : VSM magnetization curves of (A) MNP@FFAs-WPCO and (B) MNP@FFAs-PCO 86

Figure 4.33 : The optical image of water droplet on the prepared (A) MNP@FFAs-WPCO; (B) MNP@FFAs-PCO substrate (water was dyed with methylene blue for a clear observation). (C- G) Approach, contact, deformation, and departure process of a water droplet suspending on a syringe with respect to MNP@FFAs-WPCO surface. The arrows represent the moving direction of the substrate 87

Figure 4.34 : (A) The relationship between pH of water droplet and water CA on the MNP@FFAs-WPCO surface; (B) water contact angle of MNP@FFAs-WPCO after corrosion, heat treatments for 72 hours and time storage (30 days) at ambient temperature 88

Figure 4.35 : Side and top view for situation of MNP@FFAs-WPCO particles (A-B) floating by mechanical stirring and (C-D) static on water surface after one night 88

Figure 4.36 : Comparison of the extraction efficiencies of PAHs between MNP@FFAs-WPCO and MNP@FFAs-PCO. (Amount of the adsorbents (*i.e.*, MNP@FFAs-PCO and MNP@FFAs-WPCO) = 10 mg, organic eluent = *n*-hexane, volume of organic eluent = 2.0 mL, extraction time = 10 min, desorption time = 5 min, sample pH = 6.5 and sample volume = 15 mL) 90

Figure 4.37 : The effect of adsorbent dosage on the extraction efficiency of PAHs. (Organic eluent = *n*-hexane, volume of organic eluent = 2.0 mL, extraction time = 10 min, desorption time = 5 min, sample pH = 6.5 and sample volume = 15 mL) 91

University of Malaya

Figure 4.38 : The effects of (A) organic eluent (Amount of MNP@FFAs-WPCO = 25 mg, volume of organic eluent = 2.0 mL, extraction time = 10 min, desorption time = 5 min, sample pH = 6.5 and sample volume = 15 mL) and (B) volume of organic eluent (Amount of the MNP@FFAs-WPCO = 25 mg, organic eluent = ethyl acetate, extraction time = 10 min, desorption time = 5 min, sample pH = 6.5 and sample volume = 15 mL) 92

Figure 4.39 : The effect of (A) extraction time (Amount of the MNP@FFAs-WPCO = 25 mg, organic eluent = ethyl acetate, volume of organic eluent = 2.5 mL, desorption time = 5 min, sample pH = 6.5 and sample volume = 15 mL) and (B) desorption time (Amount of the MNP@FFAs-WPCO = 25 mg, Organic eluent = ethyl acetate, volume of organic eluent = 2.5 mL, extraction time = 25 min, sample pH = 6.5 and sample volume = 15 mL) 93

Figure 4.40 : The effect of solution pH on the extraction efficiency of PAHs. (Amount of the MNP@FFAs-WPCO = 25 mg, Organic eluent = ethyl acetate, volume of organic eluent = 2.5 mL, extraction time = 25 min, desorption time = 25 min and sample volume = 15 mL) 94

Figure 4.41 : The effect of sample volume on the extraction efficiency of PAHs. (Amount of the MNP@FFAs-WPCO = 25 mg, organic eluent = ethyl acetate, volume of organic eluent = 2.5 mL, extraction time = 25 min, desorption time = 25 min and sample pH = 6.5) 95

Figure 4.42 : Reusability of the MNP@FFAs-WPCO for extraction of PAHs 95

Figure 4.43 : HPLC-DAD chromatograms of the PAHs after extraction using proposed MSPE: Non-spiked (A); and 50 ng mL^{-1} of each PAHs spiked leachate sample (B) (1) Flu (2) FLT, (3) Pyr, (4) Cry, and (5) BaP 99

Figure 4.44 : Comparison of the adsorption capacity of MNP@FFAs-WPCO and MNP@FFAs-PCO. (Amount of the adsorbents (*i.e.*, MNP@FFAs-PCO and MNP@FFAs-WPCO) = 15 mg, contact time = 60 min and pH of the aqueous solution = 7) 102

University of Malaya

Figure 4.45 : The effect of adsorbent dosage on the adsorption capacity of oil. (Contact time = 60 min and pH of the aqueous solution = 7) 103

Figure 4.46 : The effect of contact time on the adsorption capacity of oil. (Amount of MNP@FFAs-WPCO = 12 mg and pH of the aqueous solution = 7) 103

Figure 4.47 : The effect of pH on the adsorption capacity of oil. (Amount of MNP@FFAs-WPCO = 12 mg and contact time = 50 min) 104

Figure 4.48 : Oil-adsorption capacity of MNP@FFAs-WPCO after different oil-removal cycles 105

Figure 4.49 : EDX spectra of (A) MNP@FFAs-WPCO; (B) oil loaded of MNP@FFAs-WPCO and (C) oil loaded of MNP@FFAs-PCO; (D) FT-IR spectra of (i) MNP@FFAs-WPCO; (ii) oil loaded of MNP@FFAs-PCO and (iii) oil loaded of MNP@FFAs-WPCO; (D) TGA thermogram of (i) oil loaded of MNP@FFAs-WPCO and (ii) oil loaded of MNP@FFAs-PCO 106

Figure 4.50 : Oil adsorption capacity of the MNP@FFAs-WPCO. (Amount of MNP@FFAs-WPCO = 12 mg, contact time = 50 min and pH of the aqueous solution = 7) 106

Figure 4.51 : FT-IR spectra of (A) GO; (B) MNP@FFAs-WPCO and (C) MNP@FFAs-WPCO-GO 111

Figure 4.52 : XRD patterns of (A) GO; (B) MNP@FFAs-WPCO and (C) MNP@FFAs-WPCO-GO 112

Figure 4.53 : EDX spectra of (A) MNP@FFAs-WPCO and (B) MNP@FFAs-WPCO-GO 113

Figure 4.54 : TGA curves of (A) MNP@FFAs-WPCO and (B) MNP@FFAs-WPCO-GO 114

Figure 4.55 : FESEM images of (A) GO; (B) MNP@FFAs-WPCO and (C) MNP@FFAs-WPCO-GO; and TEM images of (D) MNP@FFAs-WPCO and (E) MNP@FFAs-WPCO-GO 115

University of Malaya

Figure 4.56 : The magnetization hysteresis loops of (A) MNP@FFAs-WPCO and (B) MNP@FFAs-WPCO-GO 116

Figure 4.57 : The study mass ratio of MNP@FFAs-WPCO to GO on the extraction efficiency of (A) PAEs and (B) PAHs. (Desorption solvent = methanol, volume of desorption solvent = 1.5 mL, extraction time = 10 min, desorption time = 10 min, sample pH = 6.5 and sample volume = 15 mL) 117

Figure 4.58 : Comparison of the extraction efficiencies of (A) PAEs and (B) PAHs between MNP@FFAs-WPCO and MNP@FFAs-WPCO-GO. (Amount of the adsorbent (*i.e.*, MNP@FFAs-WPCO and MNP@FFAs-WPCO-GO) = 15 mg, desorption solvent = methanol, volume of desorption solvent = 1.5 mL, extraction time = 10 min, desorption time = 10 min, sample pH = 6.5 and sample volume = 15 mL) 118

Figure 4.59 : Proposed mechanism of interactions between MNP@FFAs-WPCO-GO and mixture of PAHs and PAEs 118

Figure 4.60 : The effect of adsorbent dosage on the extraction efficiency of mixture PAEs and PAHs. (Desorption solvent = methanol, volume of desorption solvent = 1.5 mL, extraction time = 10 min, desorption time = 10 min, sample pH = 6.5 and sample volume = 15 mL) 119

Figure 4.61 : The effect of (A) organic eluent (Amount of MNP@FFAs-WPCO-GO = 20 mg, volume of desorption solvent = 1.5 mL, extraction time = 10 min, desorption time = 10 min, sample pH = 6.5 and sample volume = 15 mL) and (B) Volume of organic eluent (Amount of MNP@FFAs-WPCO-GO = 20 mg, desorption solvent = acetone, extraction time = 10 min, desorption time = 10 min, sample pH = 6.5 and sample volume = 15 mL) on the extraction efficiency of mixture PAEs and PAHs 120

Figure 4.62 : The effects of (A) extraction time (Amount of MNP@FFAs-WPCO-GO = 20 mg, desorption solvent = acetone, volume of desorption solvent = 2.0 mL, desorption time = 10 min, sample pH = 6.5 and sample volume = 15 mL) and (B) desorption time (Amount of MNP@FFAs-WPCO-GO = 20 mg, desorption solvent = acetone, volume of desorption solvent = 2.0 mL, extraction 121

University of Malaya

time = 10 min, sample pH = 6.5 and sample volume = 15 mL) on the extraction efficiency of mixture PAEs and PAHs

Figure 4.63 : The effect of solution pH on the extraction efficiency of mixture PAEs and PAHs. (Amount of MNP@FFAs-WPCO-GO = 20 mg, desorption solvent = acetone, volume of desorption solvent = 2.0 mL, extraction time = 10 min, desorption time = 10 min and sample volume = 15 mL) 122

Figure 4.64 : The effect of sample volume on the extraction efficiency of mixture PAEs and PAHs. (Amount of MNP@FFAs-WPCO-GO = 20 mg, desorption solvent = acetone, volume of desorption solvent = 2.0 mL, extraction time = 10 min, desorption time = 10 min and sample pH = 6.5) 123

Figure 4.65 : Reusability of the MNP@FFAs-WPCO-GO for extraction of mixture PAEs and PAHs 124

Figure 4.66 : Chromatogram of landfill sludge using MNP@FFAs-WPCO-GO as the MSPE adsorbent spiked with (a) 100 ng mL^{-1} of DPP, BBP, Flu and DCHP and 10 ng mL^{-1} of FLT and Cry and (b) unspiked landfill sludge 126

University of Malaya

LIST OF TABLES

Table 2.1 : Typical fatty acid composition (%) for palm oil source 14

Table 2.2 : Structure and properties of PAHs investigated in this work 22

Table 2.3 : Modified magnetic adsorbents for the enrichment of PAHs 25

Table 2.4 : Structure and properties of PAEs investigated in this work 27

Table 2.5 : Modified magnetic adsorbents for enrichment of PAEs 30

Table 2.6 : Modified magnetic adsorbents for removal of oil 32

Table 4.1 : Fatty acids compositions obtained from hydrolysis of triacylglycerol palm cooking oil 51

Table 4.2 : TGA analysis of MNPs, MNP-APTES and MNP@FFAs-PCO 55

Table 4.3 : Analytical performance for HPLC-DAD determination of PAHs using MNP@FFAs-PCO 69

Table 4.4 : The recoveries and standard deviations of PAHs in real environmental samples with a spiked concentration of 5 ng mL^{-1}, 10 ng mL^{-1}, and 100 ng mL^{-1} for each analyte 70

Table 4.5 : The physical properties of experimental oils 77

Table 4.6 : Fatty acids compositions obtained from hydrolysis of triacylglycerol palm cooking oil and waste palm cooking oil 79

Table 4.7 : TGA analysis of MNP@FFAs-WPCO and MNP@FFAs-PCO 83

Table 4.8 : Analytical performance data of the proposed methods MNP@FFAs-WPCO-MSPE and MNP@FFAs-PCO-MSPE 97

University of Malaya

Table 4.9 : The recoveries and standard deviations of PAHs in real environmental samples with spiked concentration of 0.5 ng mL^{-1}, 5 ng mL^{-1} and 50 ng mL^{-1} for each analyte 99

Table 4.10 : Comparison of %Recovery, %RSDs and LOD of the current work with other reported MSPE adsorbents 101

Table 4.11 : Comparison of the oil sorption uptake of various reported adsorbents 108

Table 4.12 : TGA analysis of MNP@FFAs-WPCO and MNP@FFAs-WPCO-GO 114

Table 4.13 : Analytical performance for HPLC-DAD determination of PAEs and PAHs using MNP@FFAs-WPCO-GO 125

Table 4.14 : The recoveries and standard deviations of PAEs and PAHs in real apple, cabbage and landfill sludge samples 126

Table 4.15 : Comparison of the developed MSPE adsorbent with other literature MSPE adsorbents for determination of PAEs and PAHs 128

University of Malaya

LIST OF SYMBOLS AND ABBREVIATIONS

APTES	:	(3-aminopropyl)triethoxysilane
BaP	:	Benzo(a)pyrene
BBP	:	Benzyl butyl phthalate
BET	:	Brunauer-Emmett-Teller
Cry	:	Crysene
DCHP	:	Dicyclohexyl phthalate
DMF		N,N-dimetylformamide
DPP	:	Dipropyl phthalate
EDX	:	Energy Dispersive X-ray Spectroscopy
FESEM	:	Field Emission Scanning Electron Microscopy
FFAs	:	Free Fatty Acids
FLT	:	Fluoranthene
Flu	:	Fluorene
FT-IR	:	Fourier Transform Infrared Spectroscopy
GC	:	Gas Chromatography
GO	:	Graphene Oxide
HPLC	:	High Performance Liquid Chromatography
LOD	:	Limit of Detection
LOQ	:	Limit of Quantification
MNP@FFAs-PCO	:	Free fatty acids from hydrolysis of triacylglycerol of palm cooking oil functionalized magnetic nanoparticles
MNP@FFAs-WPCO	:	Free fatty acids from waste palm cooking oil functionalized magnetic nanoparticles

University of Malaya

MNP@FFAs-WPCO-GO	:	Free fatty acids from waste palm cooking oil functionalized magnetic nanoparticles immobilized on the surface of the graphene oxide
MNP-APTES	:	(3-aminopropyl)triethoxysilane functionalized magnetic nanoparticles
MNPs	:	Magnetic nanoparticles
MSPE	:	Magnetic solid phase extraction
PAEs	:	Phthalate Esters
PAHs	:	Polycyclic Aromatic Hydrocarbons
PCO	:	Palm Cooking Oil
Pyr	:	Pyrene
RSD	:	Relative Standard Deviation
TAG	:	Triacylglycerol
TEM	:	Transmission Electron Microscopy
TGA	:	Thermogravimetric Analysis
UAE	:	Ultrasound-Assisted Extraction
VSM	:	Vibrating sample Magnetometer
WCA	:	Water Contact Angle analysis
WPCO	:	Waste Palm Cooking Oil
XRD	:	X-ray Diffraction

University of Malaya

CHAPTER 1: INTRODUCTION

1.1 Background of study

Magnetic nanoparticles (MNPs) have been demonstrated to have a great potential in the decontamination of diverse matrices due to its advantages such as low toxicity, high surface area, low cost and superparamagnetic property (Du *et al*., 2012; Gill *et al*., 2007). The surface of MNPs can be easily functionalized to achieve selective sample extraction and treatment (Sen *et al*., 2006). MNPs with surface modifications typically exhibit high number of surface active sites, high adsorption efficacy and selectivity as well as high sensitivity for removal and determination of contaminants in complex sample matrices.

Recently, MNPs have received considerable attention as adsorbents for environmental remediation (Takafuji *et al*., 2004). In this regard, adsorption process by magnetic solid adsorbent is one of the effective method for treatment of the pollutants in our environment due to its high efficiency, cost effective and rapid separation as magnetic adsorbent can readily be collected after the adsorption of target contaminants onto it by using simple external magnet (Moazed & Viraraghavan, 2005; Jawad *et al*., 2017).

MNPs also been extensively used in analytical applications (Lu *et al*., 2007). MNPs have been used in sample preparation technique prior analysis. This is because direct determination of contaminants in real samples seem incompatible with available instrumentation techniques such as high performance liquid chromatography (HPLC) and gas chromatography (GC) due to their sensitivity and selectivity which are not sufficient for direct determination of the pollutants at trace level in complex sample matrices (Bai *et al*., 2010). The samples must be preconcentrated and interfering species must be removed before satisfactory separation can be obtained. Therefore, a new mode of solid phase extraction (SPE) called magnetic solid phase extraction (MSPE) which is based on the use of magnetic adsorbent, has been successfully applied to solve different analytical

University of Malaya

problems (Seddon *et al*., 2000). This sample preparation technique offers comparably rapid isolation as the magnetic adsorbent can readily be collected after the adsorption of target analytes onto it by using an external magnet (Liu *et al*., 2012).

Unfortunately, MNPs suffer from several drawbacks, including being unstable in acidic environments, suffering agglomeration in aqueous media, ready oxidation upon exposure to air and poor extraction efficiency for hydrophobic organic compounds due to their highly hydrophilic nature (Liu *et al*., 2008). To overcome these problems, the MNPs should be coated with a suitable protective layer. This may include grafting or coating with small organic molecules, surfactants, polymers or even biomolecules. In this study, we focus on the modifying agents with low cost, simple preparation process and high adsorption efficiency for the modification of the MNPs surface. In this regard, free fatty acids (FFAs) from palm oil are suitable candidate as the coating agent for functionalization of MNPs. The chemical structure of FFAs, consists of long alkyl chains, making them excellent hydrophobizing agents for the selective extraction of the hydrophobic pollutants from complex matrices.

FFAs which could be found naturally in palm oil can be used as economical and eco-friendly hydrophobizing agents in modifying the surface of MNPs, turning it into a new highly hydrophobic adsorbent which can be used for the determination and remediation of hydrophobic organic pollutants from the real samples. Palm oil production is vital for the economy of Malaysia as our country is one of the biggest producers and exporters of palm oil and palm oil products. Palm oil based product has been selected in this research due to its easy availability and high amount of FFAs mainly palmitic acid and oleic acid (Japir *et al*., 2016). High amounts of FFAs can easily be obtained from the hydrolysis triacylglycerol (TAG) of palm oil. The increasing interest on use of oleo based product as starting material for production of new adsorbent is justifiable as these materials are low cost and environmentally friendly.

University of Malaya

As FFAs from palm oil functionalized MNPs have good hydrophobic interaction with hydrophobic organic pollutants from real samples, its application was further extended for determination simultaneous of wide range polarities of organic pollutants in real samples. Thus, FFAs functionalized MNPs is introduced into the surface of graphene oxide (GO) to enhance the adsorption of these pollutants. GO has a single sheet formed lamellar structure surface, containing abundant hydrophilic groups with hydroxyl, epoxide and carboxylic groups on its surface (Pan *et al*., 2014). It has large delocalized π-electron systems with high surface area. Therefore with the combinations of FFAs and GO, the adsorption of wide range of organic compounds is mainly driven through hydrogen bonding, hydrophobic and π-π interactions. In addition, GO can enhance the dispersion of the FFAs functionalized MNPs in aqueous matrices.

The scope of this research is to design new magnetic adsorbents functionalized with FFAs from palm oil. The successful synthesis of new adsorbents were further confirmed by X-Ray diffraction (XRD), transmission electron microscopy (TEM), Fourier transform infrared spectroscopy (FT-IR), energy dispersive X-Ray spectroscopy (EDX), thermogravimetric analysis (TGA), Brunauer-Emmett-Teller (BET), water contact angle (WCA), field emission scanning electron microscopy (FESEM), transmission electron microscopy (TEM) and vibrating sample magnetometer (VSM) analyses. The synthesized materials were introduced as new adsorbents for separation and determination as well as remediation of the selected of pollutants from real samples.

Herein, we report the synthesis of first adsorbent, magnetic nanoparticles functionalized with FFAs obtained from hydrolysis of TAG palm cooking oil, (MNP@FFAs-PCO). In this regard, palm cooking oil has been chosen in this study because it is one of the main palm oil based product which is easily available in our market. The presence of high FFAs in palm cooking oil are easily obtained from hydrolysis of TAG of palm cooking oil. As the major FFAs in palm cooking oil, mainly

University of Malaya

C16 and C18:1, suggesting MNP@FFAs-PCO has a very good hydrophobic framework which can interact well with hydrophobic pollutants via hydrophobic interaction. Literature survey reveals that surprisingly very little attention has been paid so far, to use oleo based materials in analytical and environmental field. Therefore, the designed adsorbent, MNP@FFAs-PCO is developed and utilized as a potential MSPE adsorbent for enrichment of polycyclic aromatic hydrocarbons (PAHs) from landfill leachate and sludge samples. In addition, we investigate its applicability in trapping oily contaminants from aqueous matrices.

Waste palm cooking oil is spent oil that has been used for cooking and cannot be reused as they pose a significant health hazard. They must be properly disposed of lest they leach into the environment and pollute it. We can exploit this waste because it has high content of FFAs that was produced by hydrolytic processes between the oil itself and water from the food during cooking. Thus, FFAs can be directly obtained from waste palm cooking and the TAG of oil does not need to be further hydrolyzed. The idea to use FFAs from waste palm cooking oil as modifying agent to functionalize the surface of MNPs for decontamination and detection of pollutants seems to be an innovative and valuable approach. In this section, inspired by excellent adsorption toward PAHs as well as oil and hierarchical structure of MNP@FFAs-PCO that containing of long alkyl chain of FFAs, the second material, MNP@FFAs-WPCO was fabricated by using FFAs which obtained from waste palm cooking oil as the hydrophobizing agent in modifying the surface of MNPs, turning it into a new highly hydrophobic adsorbent for adsorption of lipophilic PAHs and oil from the environmental samples. The utilization of waste palm cooking oil for fabrication of MNP@FFAs-WPCO, suggesting the source of preparation of this adsorbent is economical, solving environmental problem and easily available. The proposed adsorbent, MNP@FFAs-WPCO exhibited superhydrophobicity,

University of Malaya

superoleophilicity and great adsorption capability of PAHs and oil from polluted environment.

As MNP@FFAs-WPCO showed excellent adsorption toward oil and PAHs molecules, its utilization is further extended for the simultaneous determination of various organic pollutants in the real samples. It was then discovered that in most cases, the pollutants in our environment exist as complicated mixture with a wide range of polarities, depending on its content. Unfortunately, the previous adsorbent, MNP@FFAs-WPCO only provided hydrophobic interaction which limits its use as the adsorbent for wide range polarities of organic pollutants because of its very hydrophobic surface which only allow it to trap the hydrophobic molecules (*i.e.,* PAHs and oil) that floating at the air-water interface. Therefore, its extraction efficiency is reduced as it affects the effectiveness in sample preparation technique. To overcome this, FFAs from waste palm cooking oil functionalized magnetic nanoparticles immobilized on the surface of the graphene oxide (MNP@FFAs-WCPO-GO) was fabricated. The newly prepared MNP@FFAs-WCPO-GO is used as a MSPE adsorbent for simultaneous determination of PAHs and phthalate esters (PAEs) from various environmental and food matrices. This adsorbent is a combination of GO which are sp^3 hybridized carbons with hydroxyl, epoxy and carboxyl groups and long alkyl chains of FFAs originating from waste palm cooking oil. The combination of long alkyl chains FFAs and GO hybrid offer better interactions with selected organic pollutants compared to the previous adsorbent which only provide hydrophobic interactions, suggesting that there are many adsorption sites for organic pollutants which suitable for trapping of various organic contaminants in our real samples. In addition, the introduction of GO on the surface of MNP@FFAs-WPCO enhances the dispersion of MNP@FFAs-WPCO in aqueous media.

University of Malaya

1.2 Objectives of the research

The objectives of this study are as follow:

(i) To synthesize and characterize the new adsorbents:
  a. Free fatty acids from hydrolysis of triacylglycerol of palm cooking oil functionalized magnetic nanoparticles (MNP@FFAs-PCO).
  b. Free fatty acids from waste palm cooking oil functionalized magnetic nanoparticles (MNP@FFAs-WPCO).
  c. Free fatty acids from waste palm cooking oil functionalized magnetic nanoparticles immobilized on the surface of the graphene oxide (MNP@FFAs-WPCO-GO).

(ii) To develop and apply the synthesized materials, MNP@FFAs-PCO and MNP@FFAs-WPCO as adsorbents for oil removal from aqueous solution and magnetic solid phase extraction (MSPE) of polycyclic aromatic hydrocarbons (PAHs) from landfill leachate and sludge samples.

(iii) To develop and apply MNP@FFAs-WPCO-GO as a magnetic solid phase extraction (MSPE) adsorbent for the extraction and simultaneous determination of selected polycyclic aromatic hydrocarbons (PAHs) and phthalate esters (PAEs) from fruit, vegetable and landfill sludge samples.

University of Malaya

1.3 Outline of thesis

This thesis is divided into five chapters. Chapter 1 consists of a brief introduction on the research background and provides the objectives of the research. A review of related literature is presented in Chapter 2. Chapter 3 discusses the experimental procedure for the synthesis of new adsorbents (*i.e.*, MNP@FFAs-PCO, MNP@FFAs-WPCO and MNP@FFAs-WPCO-GO). In addition, this chapter presents the optimized procedure for MSPE of selected pollutants (*i.e.,* PAHs and PAEs) and oil removal application. Chapter

4 is subdivided into 3 sections, the first section reports the characterization of FFAs from hydrolysis of TAG of palm cooking oil functionalized magnetic nanoparticles (MNP@FFAs-PCO). It also presents the optimization of MSPE for the extraction of targeted PAHs as well as oil removal. The second section presents the characterization of FFAs from waste palm cooking oil functionalized magnetic nanoparticles (MNP@FFAs-WPCO). The new adsorbent is compared with MNP@FFAs-PCO in terms of performance. Third section presents a detailed study on FFAs obtained from waste palm cooking oil functionalized magnetic nanoparticles immobilized on the surface of the graphene oxide (MNP@FFAs-WPCO-GO). The optimizations and performances of MSPE method for the simultaneous extraction of targeted PAHs and PAEs using MNP@FFAs-WPCO-GO also are discussed in this section. Finally, the conclusion and recommendations for future works is provided in Chapter 5.

University of Malaya

CHAPTER 2: LITERATURE REVIEW

2.1 Magnetic nanoparticles

Magnetic nanoparticles (MNPs) are nanoparticles that can be affected by a magnetic field. In the last decade, MNPs have attracted significant interest for its potential in applications such as water treatment, bio-separation, drug delivery, environmental science, engineering, material science as well as the separation and purification of waste stream (Wilhelm *et al*., 2003). MNPs typically contain iron, nickel, cobalt, and their oxides (Li *et al*., 2013)

Among the various types of MNPs, iron oxides such as magnetite (Fe_3O_4), maghemite (γ-Fe_2O_3) and hematite (α-Fe_2O_3) are common and attractive because of their biocompatibility, great saturation magnetization and magnetic susceptibility (Maity & Agrawal, 2007). Magnetite (Fe_3O_4) has been heavily studied due to its advantages such as having the best saturation magnetization among the iron oxides, low cost and toxicity and a high specific surface area (Gill *et al*., 2007; Petcharoen & Sirivat, 2012; Ahmadi *et al*., 2018). Because of its unique properties, Fe_3O_4 nanoparticles is commonly used in biotechnology (Kumar *et al*., 2010), magnetic separation and as catalyst (Chen *et al*., 2013).

Most of these applications need the nanoparticles to be uniform in shape and size and be easily dispersible (Jang & Lim, 2010). The nanoparticles must be in the range of 30–50 nm in order to exist as single domain particles and achieve superparamagnetic behaviour (Mürbe *et al*., 2008). The size and shape of iron oxide nanoparticles are generally influenced by its synthesis method. Various approaches have been developed to synthesize iron oxides including sonochemical synthesis (Kim *et al*., 2005), the chemical co-precipitation (Zhang *et al*., 2006), hydrothermal synthesis (Wan *et al*., 2005) and thermal decomposition (Asuha *et al*., 2011). Among them, chemical co-precipitation

University of Malaya

has been widely used to produce iron oxide nanoparticles because of its ease and scale up capabilities (Tartaj *et al.*, 2005). This method involves mixing of Fe^{2+} and Fe^{3+} in a highly basic solution at elevated or room temperature. Equation 2.1 shows the magnetite nanoparticles synthesis route using co-precipitation process.

$$Fe^{2+} + 2Fe^{3+} + 8OH^{-} \longrightarrow Fe_3O_4 + 4H_2O \tag{2.1}$$

Typically, this approach results in water dispersible and biocompatible magnetic nanoparticles with a spherical shape and sub 25 mm size (Figure 2.1).

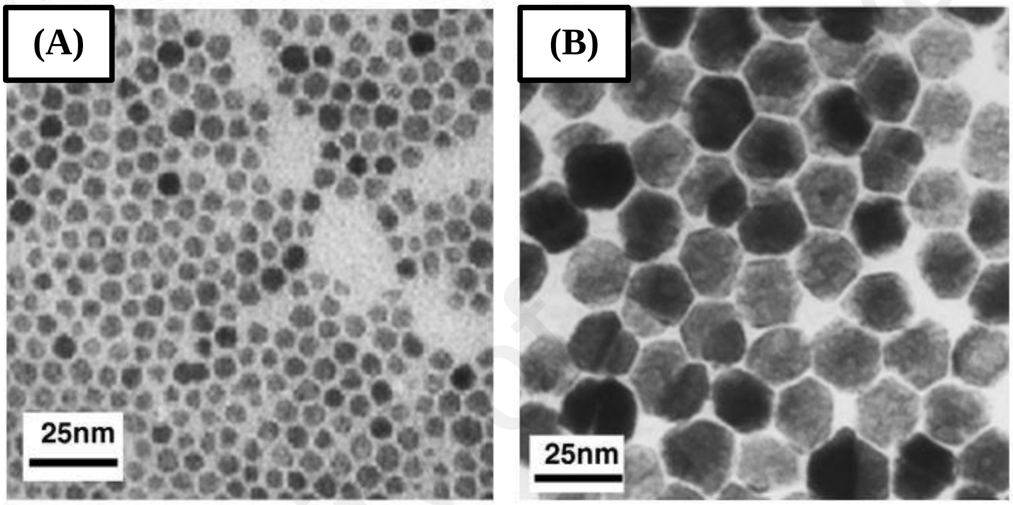

Figure 2.1: TEM images of Fe_3O_4 nanoparticles with diameter of (A) 7 nm and (B) 19 nm obtained from co-precipitation method (adapted from Kim *et al.*, 2005)

A disadvantage that must be overcome is that the iron oxide nanoparticles in the carrier liquid agglomerate because of acting Van der Waals forces (Wang *et al.*, 2013). This is exacerbated by the magnetic iron oxide nanoparticles possessing high surface energies due to their large surface area to volume ratio. Because of this, they tend to agglomerate seriously in order to reduce their surface energies. Furthermore, the bare iron oxide nanoparticles are highly reactive and susceptible to oxidation by air (Maity & Agrawal, 2007), both resulting in the loss in its dispersibility and magnetism. They are also by themselves poor extractors for hydrophobic pollutants due to their highly hydrophilic nature (Liu *et al.*, 2008). To overcome these problems, the surface of the iron oxide

University of Malaya

nanoparticles can be coated with a protective layer to prevent agglomeration and oxidation by air.

2.1.1 Surface modification strategies of magnetic iron oxide

Generally, the structure of the functionalized iron oxide can take one of three forms; core-shell, matrix, or $\text{shell}_{a\text{-}}$ core–shell_b (Figure 2.2). As a core-shell structure, the iron oxide becomes the core and it is coated by a layer of organic material that becomes the shell. The matrix structure is subdivided into two types; shell core and mosaic. Typically, the shell-core structure has the core layer made out of organic nanoparticles and it is coated with iron oxide nanoparticles as the shell. The mosaic structure has multiple discrete iron oxide nanoparticles that are uniformly distributed within the organic framework. The third structure, shell_a core–shell_b is simply another layer of organic material coated on the core–shell_b structure. Shell_a may or may not be different from shell_b.

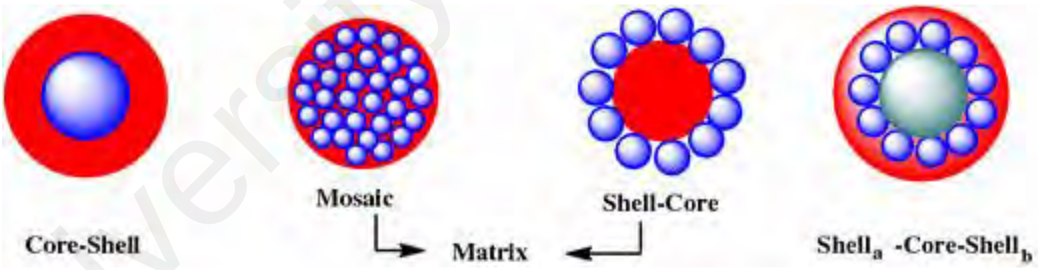

Figure 2.2: The main structure of functionalized iron oxide nanoparticles (if iron oxide nanoparticles are always assumed as the core) (adapted from Wu *et al.*, 2008)

Typically, organic compounds are often used to passivate the surface of the iron oxide nanoparticles so that it can remain stable under normal environmental conditions. This can be achieved by surface modification with appropriate organic functional groups such as the carboxyl, silane and amino groups (Figure 2.3). The organic coating improves

University of Malaya

biocompatibility of the compound and does not detract from the magnetic property of magnetic iron oxide nanoparticles.

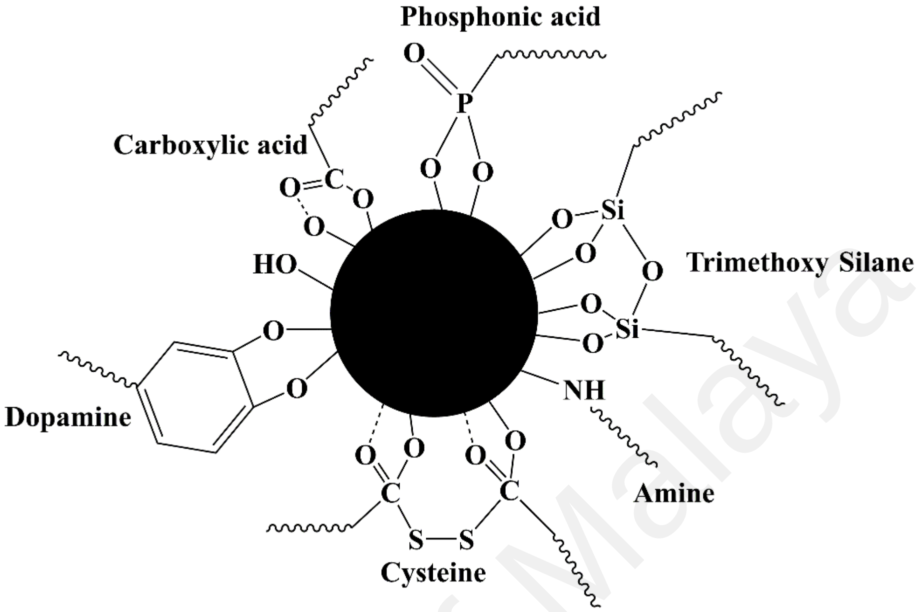

Figure 2.3: Common chemical moieties for the anchoring of functional groups at the surface of iron oxide magnetic nanoparticles (Dias *et al.*, 2011)

Recently, silanes, octadecylsilane, *n*-octadecylphosphonic acid, triphenylamine, polymers and graphene have been used as modifying agents in order to increase the stability of MNP as a dispersion in aqueous media (Wu *et al.*, 2008). Among these, fatty acids and graphene oxide are particularly attractive as modifying agents for magnetite. They can be considered ideal materials for coating simply for their versatility.

2.2 Fatty acids modified magnetic iron oxide

Fatty acids are commonly used as a surfactant to stabilize the magnetic iron oxide nanoparticles through the formation of strong chemical bonds between the carboxylic acid and, or strong physical adsorption on the amorphous iron oxide nanoparticles (Lu *et al.*, 2007). The iron oxide nanoparticles modified with fatty acid is classified as oil soluble type. The single or double layer of fatty acid creates steric repulsion which

University of Malaya

balances out the magnetic and Van der Waals attractive forces acting on the nanoparticles. Thus, oil functionalization prevents or at least decreases the agglomeration of magnetic iron oxide and therefore increases its dispersibility. Oleic acid ($CH_3(CH_2)_7CH=CH\ (CH_2)_7CO_2H$) has a C18 tail with a cis-double-bond in the middle, which is particularly attractive as it forms a kink that is beneficial for effective stabilization. It already has been widely used to form a dense, protective monolayer on iron nanoparticles, allowing highly uniform and monodisperse particles in water (Wu *et al*., 2008).

Zhang *et al*. (2006) synthesized monodisperse magnetic nanoparticles of 7 nm and 19 nm via seed-mediated high temperature thermal decomposition of iron(III) acetylacetonate ($Fe(acac)_3$) precursor. They then coated the nanoparticles with oleic acid and investigated the interfacial interactions between the oleic acid and magnetite. They confirmed by Fourier transform infrared spectra (FT-IR) and X-ray photoelectron spectroscopy (XPS) analyses that the oleic acid molecules were chemically adsorbed on the magnetic nanoparticles surface. They also found the existence of chelating bidentate interactions between the COO^- groups of oleic acid and the iron atoms. Furthermore, transmission electron microscopy (TEM) analysis revealed that the oleic acid provided the particles with better isolation and dispersibility.

Petcharoen & Sirivat (2012) investigated the use of hexanoic and oleic acid as coating agents during the initial crystallization phase of magnetite. The structure of their final product was elucidated by Fourier transform-infrared spectroscopy, (FT-IR), field-emission scanning electron microscopy (FESEM), vibrating sample magnetometer (VSM) and X-ray diffraction (XRD). It had a cubic spinel structure and spherical morphology with the particle size ranging from 10 to 40 nm. They found that their oleic acid modified magnetite can be well dispersed in aqueous solution stably for over a week.

University of Malaya

Naturally, it is desirable to minimize material cost to reduce overall production cost of the adsorbent. Palm oil is a cheap and abundant source of free fatty acids. However, its use as starting material for developing pollutant adsorbers and detectors has only been weakly explored despite its great potential. Hence, our research focuses on the use of free fatty acids from palm cooking oil for the removal of organic pollutants from aqueous media.

2.2.1 Palm oil

Malaysia is the major exporter of palm oil based oleochemicals in the global market, providing 38% of all palm oil consumed in 2011. This numbers can be clearly verified in Figure 2.4. It was forecasted that in years to come, the demand will be higher with the increasing demand of world total oils and fats. Figure 2.4 shows the percentage breakdown of oil exports by country. It was forecasted that in years to come, the demand for oleochemicals will increase.

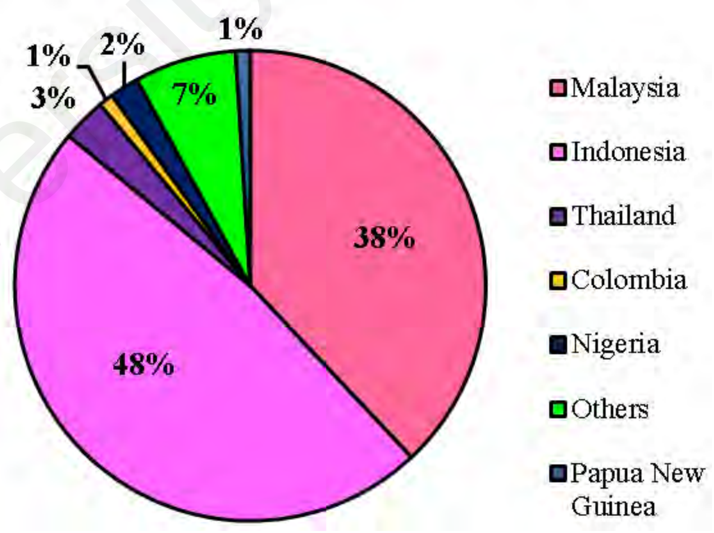

Figure 2.4: Palm oil exports by source for year 2011 (Awalludin *et al*., 2015)

University of Malaya

Palm oil is sourced from economical and very perennial oil palm trees. The oil is semi-solid at room temperature and in its virgin form, it is bright orange-red in colour due to the high content of carotene. Palm oil and its derivatives have good resistance to oxidation and heat making them ideal for use in cooking. Like all fats, it is a mixture of TAGs each composed of one moiety glycerol and three moieties of saturated or unsaturated fatty acids that may have different carbon chain length (Zhang *et al*., 2012). Typical fatty acid compositions found in palm oil are summarized in Table 2.1 (Lam *et al*., 2010). Free fatty acids can be obtained from hydrolysis of TAG palm oil. The reaction is shown in Figure 2.5.

Table 2.1: Typical fatty acid composition (%) for palm oil source

Fatty acid		Fatty acid composition (%)
Lauric	C 12:0	0.1
Myristic	C 14:0	1.0
Palmitic	C 16:0	42.8
Stearic	C 18:0	4.5
Oleic	C 18:1	40.5
Linoleic	C 18:2	10.1
Linolenic	C 18:3	0.2

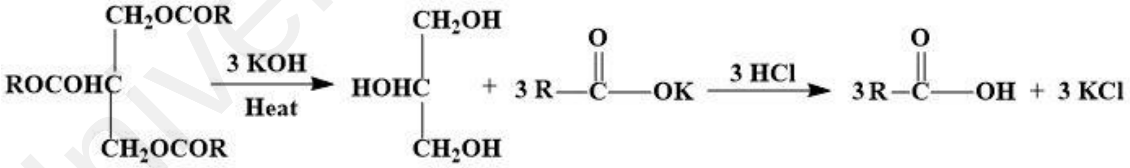

Figure 2.5: The hydrolysis reaction of TAG palm oil

The long alkyl chains of FFAs, make them an excellent hydrophobizing agent to tune the hydrophilic surface of magnetic iron oxide for selective extraction organic pollutants from real samples. Presently, only very limited studies have been carried out on the applications of oleo based materials in analytical and environmental fields. Some studies have used fatty hydroxamic acid synthesized from palm olein for analytical application. Suhendra *et al*. (2010) studied the separation and preconcentration of Cu(II) ion by fatty

University of Malaya

hydroxamic acids immobilized onto Amberlite Xad–4 resin. Isha and co-workers designed a chemical sensor for trace V(V) ions using palm-based fatty hydroxamic acid immobilized in polymethylmethacrylate (Isha *et al*., 2006) and polyvinyl chloride (Isha *et al*., 2007). Mohamad *et al*. (2008) used fatty hydrazides synthesized from palm olein for the extraction and separation of Mo(VI) from acidic media using liquid–liquid extraction technique. As the utilizations of the oleo based materials have been rarely reported for analytical and environmental applications, therefore, it is a good idea to explore FFAs from palm oil as raw material to develop adsorbent for treating and determination of organic pollutants.

2.2.2 Waste palm oil

Today, frying is a popular cooking technique widely used as it typically results in food with good taste, attractive colour and better presentation. The oil that had been used in frying is generally not reused many times as it poses a health risk to humans. Therefore, besides its niche use in the production of biodiesel and fertilizer, it is discarded as waste and must be managed. The European Union by itself produces 700,000-1,000,000 tonnes of waste cooking oil each year (Kulkarni & Dalai, 2006).

Improper management of waste cooking oil will eventually lead to the discharge of untreated waste cooking oil to the environment as a pollutant. Waste cooking oils contain harmful peroxides, aldehydes and polymers that had resulted from the thermolysis, hydrolysis, and oxidation of oil during the cooking process (Lam *et al*., 2010). Waste oil can damage plants and on water, it forms a layer on the surface that prevents oxygen from reaching marine biota, killing them. The oil also increases the chemical oxygen demand (COD) due to the degradation product of waste oil. Carcinogenic compounds in waste oil are consumed by the sea creatures and is passed on to humans through the food chain (Kulkarni & Dalai, 2006). Another problem is that when waste oil is poured down the

University of Malaya

kitchen sink, it will coat the drain walls and over the course of time, the oil will build up and eventually clog the drain. This will incur labor and other processing costs to fix the drain. Hence, waste cooking oil must be disposed safely or be used in a way so that is not harmful to human beings and the environment (Kulkarni & Dalai, 2006). In this regard, the utilization of spent cooking oil as a source of free fatty acids can offset waste oil that would otherwise must be disposed of and at the same time add value to it.

Waste cooking oil is an economical source for FFAs as they are already produced in the oil during the cooking process. Water from the food being cooked seeps into the oil and together with the high heat from cooking, causes the hydrolysis of TAG in the oil into FFAs, glycerol, monoglycerides and diglycerides (Zhang *et al*., 2012). The long C16 and C18 alkyl chain FFAs in waste palm cooking oil are very good extractors of organic pollutants. The idea of using waste palm cooking oil for analysis and extraction of hydrophobic pollutants is innovative and warrants further exploration.

2.3 Graphene oxide modified magnetic iron oxide

Graphene oxide (GO) obtained from the simple oxidation of graphite (Figure 2.6) has oxygen functional groups such as carboxyl, epoxy and hydroxyl groups which render it strongly hydrophilic and readily dispersible in water (Yang *et al*., 2012). In water, GO can act as a weak acid cation exchange resin because of the ionizable carboxyl groups, allowing surface complexation with metal ions or positively charged organic molecules. This property makes GO attractive for use as adsorbent for the retention and preconcentration of environmental pollutants. Moreover, the large specific area of GO makes it an excellent material for the modification of the surface of iron oxide.

University of Malaya

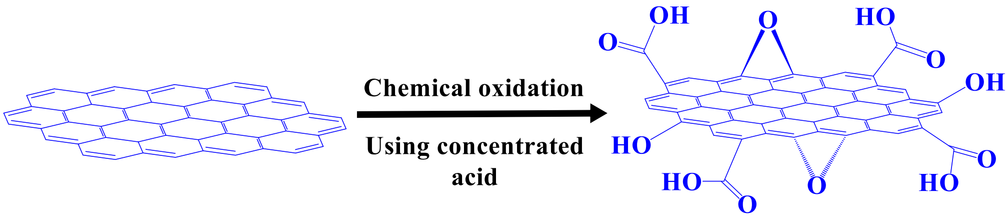

Figure 2.6: The schematic route of preparation graphene oxide from oxidation of graphite (Nodeh *et al.*, 2016)

Recently, researchers have succeeded in developing nanocomposites of magnetic iron oxide and GOs through methods such as chemical precipitation (Yang *et al.*, 2009), covalent bonding (He *et al.*, 2010) and electrostatic interactions (Liu *et al.*, 2012). Kassaee *et al.* (2011) managed to prepare and characterize a magnetic GO composite through a simple and effective one pot co-precipitation of $FeCl_3.6H_2O$ and $FeCl_2.4H_2O$ in the presence of GO nanosheets. The successful synthesis of this nanocomposite was confirmed by FT-IR, XRD, SEM and TEM analyses. The Fe_3O_4 nanoparticles were only 14 nm in size and evenly spread throughout the GO nanosheets. Shen *et al.* (2010) described GO-magnetic nanoparticles composites synthesized through a high temperature reaction of ferric triacetylacetonate with GO in 1-methyl-2-pyrrolidone. The prepared composite was confirmed by XRD, TGA and TEM analyses. Li *et al.* (2011) synthesized magnetite colloidal nanocrystals coated GO by functionalizing the GO with Cl groups by first treating with $SOCl_2$, then compositing the resultant GO-Cl with magnetic nanoparticles. The hybrid material was characterized using XRD, XPS and EDX to confirm the attachment of iron oxide nanoparticles onto GO sheets.

Numerous studies on the applications of magnetic GO nanocomposites have been carried out. He *et al.* (2010) reported that their Fe_3O_4-GO composite have good adsorption capacities as high as 190.14 and 140.79 mg g^{-1} for methylene blue and neutral red cationic dyes, respectively. Sheng *et al.* (2012) used magnetic Fe_3O_4 nanoparticles composited with GO for the excellent removal of As(V) from aqueous solutions. It becomes clear

University of Malaya

from these studies that magnetic GO nanocomposites are effective pollutant adsorbents in water and can be easily recollected using a magnet.

All the studies regarding the applications of the magnetic GO nanocomposites toward toxic and hazardous pollutants demonstrate that the composites are effective adsorbents for remediation and detection of these contaminants. This is due to its graphitized basal plane structure which allow it to have strong hydrophobic and π–π stacking interactions with the aromatic moieties present in many persistent organic pollutants. Therefore, this unique properties allows GO as a platform for modifications of magnetic iron oxides surface as a new adsorbent for pollutants decontamination.

University of Malaya

2.4 Applications of functionalized magnetic nanoparticles as adsorbent

In recent years, functionalized magnetic nanoparticles have been extensively studied for various applications in the analytical and environmental fields. Modified magnetic materials have been successfully used for the preconcentration of contaminants such as phenolic compounds (Zhao *et al*., 2008), metals ion (Ge *et al*., 2012) and sulphonamides (Font *et al*., 2008).

An adsorbent is a solid substance that collects solutes on its surface and can be classified as either synthetic or natural. The adsorption process is when atoms, ions, or molecules, (the adsorbate) is chemically or physically adhered to a surface of the adsorbent (Figure 2.7). This technique has been found to be superior to other techniques for removing pollutants from water systems in terms of initial cost, flexibility, simplicity of design, ease of operation, insensitivity to toxic pollutants (Moazed & Viraraghavan, 2005) and efficiency (Senturk *et al*., 2009).

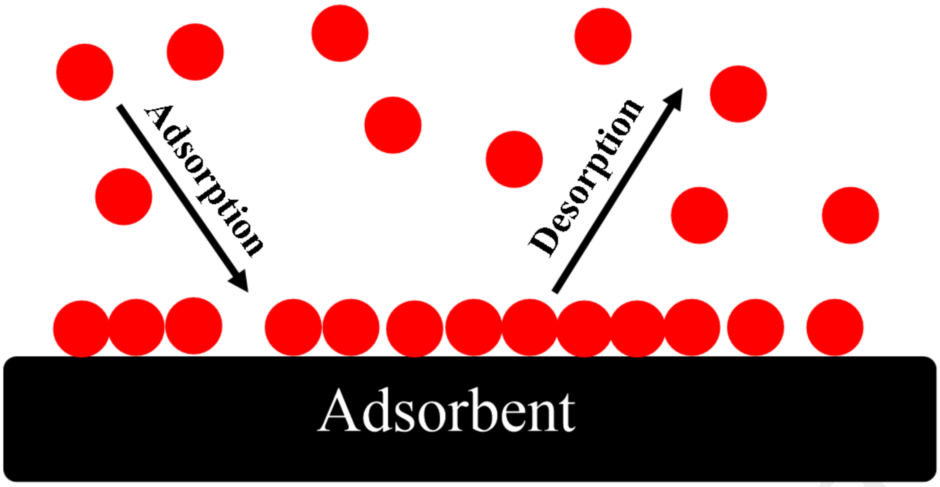

Figure 2.7: Schematic illustration of the adsorption-desorption process

2.4.1 Magnetic solid phase extraction (MSPE) application

A sample must be pretreated before it can be subjected to chromatographic analysis to improve sensitivity and selectivity of the detection (Bai *et al*., 2010). A simple, rapid and effective sample pre-treatment method is preferred to ease labor cost. The MSPE technique is based on the use of a magnetic adsorbent to preconcentrate the target analytes and remove possible matrix interferences in the analysis of pollutants (Liu *et al*., 2009; Li *et al*., 2017). It offers advantages such as good selectivity, low cost, high extraction efficiency, short extraction time and high preconcentration factor (Yang *et al*., 2014). In the MSPE method, modified magnetic adsorbents are dispersed in the sample to adsorb target compounds. Then the adsorbents are collected using an external magnet and the adsorbed analytes are eluted with appropriate solvents (Figure 2.8). Some pioneering works on MSPE have shown the importance of magnetic materials as solid sorbents for the efficient extraction and preconcentration of trace organic compounds such as PAHs and PAEs in environmental matrices.

University of Malaya

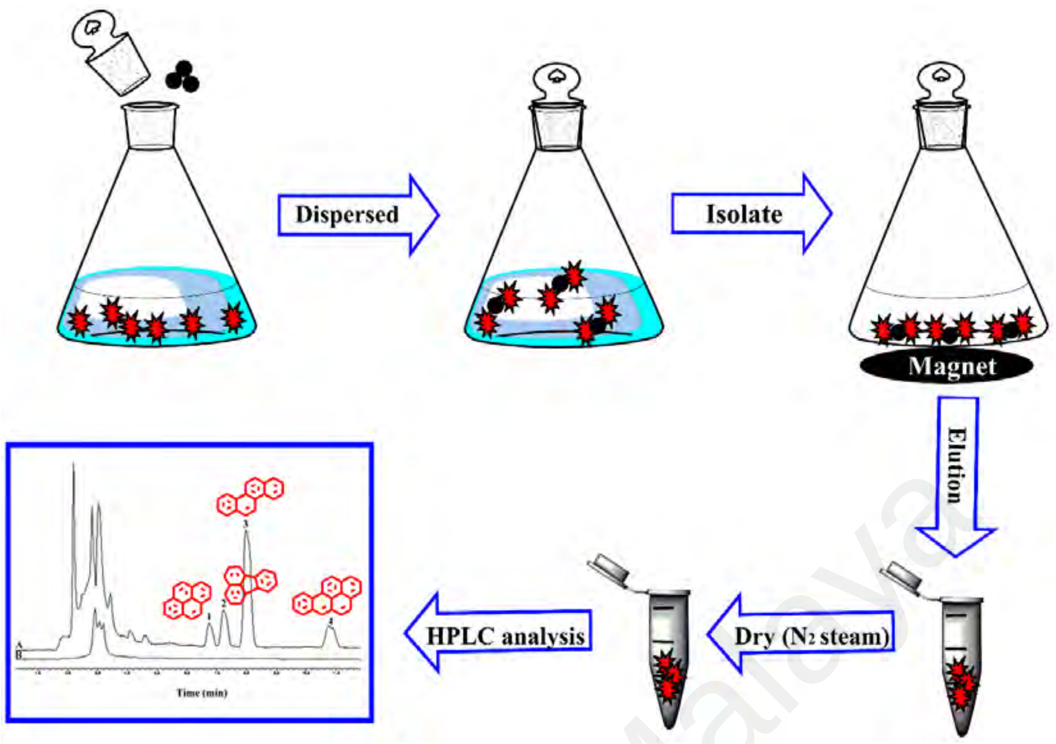

Figure 2.8: The schematic procedure of MSPE for different analyte preconcentration from aqueous media

2.4.1.1 Polycyclic aromatic hydrocarbons (PAHs)

PAHs are a major group of ubiquitous and persistent environmental pollutants. They consist of two or more fused aromatic rings of carbon and hydrogen (Liu *et al*., 2009). They are well known environmental contaminants, having toxic, mutagenic, teratogenic and carcinogenic properties (Wang *et al*., 2013; Zhou *et al*., 2017). They are classified as priority pollutants by the United States Environmental Protection Agency (EPA) (Wise *et al*., 2015; Zhou *et al*., 2014). Among these, the EPA had listed benzo(a)pyrene, benz(a)anthracene, chrysene, benzo(b)fluoranthene, benzo(k)fluoranthene, dibenz(a,h)anthracene and indeno(1,2,3-cd)pyrene as particularly hazardous, belonging to the group B2, due to their high probability to cause danger to the environment and living beings (Peters *et al*., 1999). PAHs are usually produced when organic matter such as garbage, fossil fuels and oil are incompletely combusted (Kim *et al*., 2013; Ricardo *et al*., 2017). Typically, they are spread in the environment through industrial emissions

University of Malaya

and vehicular and geochemical processes (Nurerk *et al*., 2017). They are highly mobile in the environment, spreading quickly through air, soil and water.

Kazerouni *et al*. (2001) had reported the presence of benzo(a)pyrene in 200 different meat dishes, of which very well grilled or barbecued meat had the highest concentrations of PAH, ranging from 0.40 to 1.15 ng g^{-1}. Janoszka *et al*. (2004) reported that fluoranthene and benzo(a)pyrene to be found at a concentration of 0.57 ng g^{-1} and 0.15 ng g^{-1}, respectively in chicken breast grilled on charcoal.

PAHs have been frequently detected in landfill leachates with concentrations of up to 7966 μg L^{-1} depending on its content and contribution from industrial waste (Długosz, 2013). Due to their hydrophobic properties, they are usually adsorbed onto atmospheric particles and deposited on plants, sediments and soils (Yan *et al*., 2013). It has been reported that the particle-bound PAHs accounted for 23.1 $\pm$ 3.4% of total PAHs in Dalian pine needles (Yang *et al*., 2007). Zakaria *et al*. (2002) have reported PAHs (3-7 rings) concentrations ranging from 4 to 924 ng g^{-1} in twenty-nine Malaysian riverine and coastal sediments. Ju *et al*. (2009) found PAHs ranging from 1.24 to 44.9 mg kg^{-1} in wastewater sludge samples collected from different wastewater treatment plants located along the Nakdong River in Korea.

These studies showed that PAHs (Table 2.2) are ubiquitous organic contaminants in various matrices. To measure the level of PAHs in complex samples, the sample must first be prepared. The MSPE technique which is based on the use of a magnetizable adsorbent is popular in removing possible interferences and to enrich trace PAHs in samples prior to analysis.

University of Malaya

Table 2.2: Structure and properties of PAHs investigated in this work

Compound name	Formula	Molecular weight (g mol^{-1})	Structure
Fluorene	$C_{13}H_{10}$	166	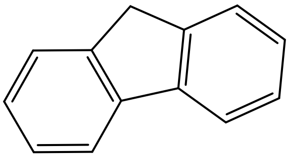
Fluoranthene	$C_{16}H_{10}$	202	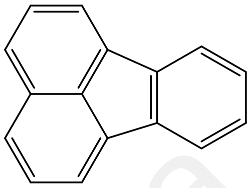
Pyrene	$C_{16}H_{10}$	202	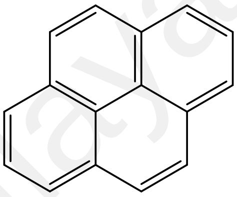
Chrysene	$C_{18}H_{12}$	228	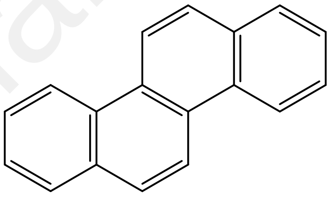
Benzo(a)pyrene	$C_{20}H_{12}$	252	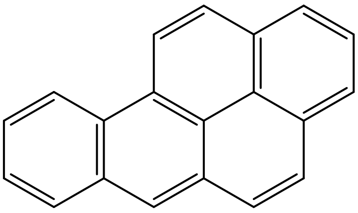

Many research groups have developed various types of magnetic adsorbents (Table 2.3) for the preconcentration of toxic and carcinogenic PAHs from various real samples. In this context, a large number of carbon based nanoparticles have been investigated in developing new hydrophobic magnetic adsorbents suitable for fast and efficient extraction of PAHs.

Liu *et al*. (2009) used magnetic C_{18} microspheres for MSPE in the determination of PAHs in spiked tap water samples. Their material had a low LOD of 0.8–36 µg L^{-1} and PAHs recoveries ranging from 35% to 85% with the RSDs (*n*=3) being less than 10%. Zhang *et al*. (2010) prepared carbon coated Fe_3O_4 nanoparticles (Fe_3O_4/C) by a simple hydrothermal reaction and employed it to extract trace PAHs from environmental water

University of Malaya

samples such as tap water, river water, rain water and wastewater. The method provided a satisfactory LOD in the range of 0.2–0.6 ng L^{-1} and good recoveries (76–110%) with low relative standard deviations ranging from 0.8 to 9.7%.

Ding *et al*. (2010) introduced a new MSPE adsorbent, *n*-octadecylphosphonic acid modified mesoporous magnetic nanoparticles. The resultant material can be used for the rapid, convenient and efficient adsorption of PAHs from water samples with LOD and LOQ in the range of 14.1–70.0 ng L^{-1} and 46.9–233.2 ng L^{-1}, respectively. Wang and co-researchers have studied graphene based material for use as the MSPE sorbent. They synthesized magnetic microsphere-confined graphene adsorbent (Fe_3O_4@SiO_2-G) for the extraction of five PAHs, namely fluorene, anthracene, phenanthrene, fluoranthene, and pyrene from environmental water samples prior to high performance liquid chromatography (Wang *et al*., 2013). The use of graphene was advantageous as it possesses delocalized π electrons, high surface area and a hydrophobic nature which makes it ideal for the adsorption of aromatic compounds. The lipophilic PAHs can be detected with a low LOD in the range of 0.5 to 5.0 ng L^{-1}. Good recoveries were obtained for all selected PAHs (83.2–108.2%).

Ballesteros-Gómez & Rubio (2009) synthesized magnetic nanoparticles coated with hemimicelles of alkyl (C_{10}-C_{18}) carboxylates to extract PAHs from surface and ground environmental water samples collected from various places in southern Spain**.** The adsorbent, alkyl carboxylate-coated MNPs had a low LOD in the range of 0.1-0.25 ng L^{-1}. The developed method was efficient and sensitive as it can detect the presence of trace PAHs in the water sample from the Navallana reservoir at low concentrations ranging from 0.42 to 0.96 ng L^{-1}.

A sensitive and reliable method for determination of PAHs in grilled meat samples was developed and validated by Moazzen *et al*. (2013). Magnetic carbon nanotubes (MCNTs) were applied as the MSPE adsorbent for the extraction of carcinogenic

University of Malaya

pollutants from meat samples prior to gas chromatography-mass spectroscopy (GC-MS) analysis. Benz(a)anthracene, benzo(b)fluoranthene, benzo(a)pyrene, and chrysene were successfully detected in beef, lamb and chicken meat samples with the mean cumulative concentration being 4.000, 3.414 and 0.931 μg kg^{-1}, respectively. By using MCNTs, the method was simplified and time consuming procedures such as column passing and filtration steps were eliminated.

The studied hydrophobic magnetic adsorbents all have high adsorption and extraction efficiency for the targeted PAHs. However, most of the reported adsorbents for the detection of PAHs are simply too expensive. Hence, the current research is carried out to investigate alternative economical materials to overcome this problem. This study focuses on the utilization of FFAs obtained from the hydrolysis of TAG in palm cooking oil and waste palm cooking oil as the alternative low cost precursor material to develop adsorbents for detecting PAHs. To our knowledge, there have not been any studies that had investigated this idea yet.

University of Malaya

University of Malaya

Table 2.3: Modified magnetic adsorbents for the enrichment of PAHs

Adsorbent	Method	Sample	Ref.
Alkyl carboxylate-coated MNPs	MSPE/HPLC-FLD	Surface and underground water	(Ballesteros-Gómez & Rubio, 2009)
Magnetic C_{18} microspheres	MSPE/GC-MS	Tap water	(Liu *et al*., 2009)
Magnetic Carbon Nanotubes (MCNTs)	MSPE/GC-MS	Grilled beef, lamb, chicken meats	(Moazzen *et al*., 2013)
Fe_3O_4/C	MSPE/HPLC-FLD	Tap/rain/river/wastewater	(Zhang *et al*., 2010)
Fe_3O_4 diphenyl nanoparticles	MSPE/GC-MS	Urine	(Bianchi *et al*., 2012)
Carbon-ferromagnetic nanocomposites	MSPE/GC-MS	Lake water	(Bai *et al*., 2010)
Fe_3O_4@SiO_2-G	MSPE/HPLC-FLD	Reservoir/river/tap/sea water	(Wang *et al*., 2013)

2.4.1.2 Phthalate esters (PAEs)

PAEs are a group of diesters of ortho-phthalic acid (dialkyl or alkyl aryl esters of 1,2-benzenedicarboxylic acid). The widespread presence of PAEs in daily life products have attracted considerable public attention because of their suspected carcinogenic and estrogenic content (Yan *et al*., 2017; Wu *et al*., 2017). PAEs have been found in many consumable products such as cosmetics, fragrances, lubricants, paints, and adhesives (Feás *et al*., 2008). The United States Environmental Protection Agency (EPA) and several agencies have listed PAEs as priority pollutants. In Europe, the New EU Regulation (EU) no.10/2011 on plastic materials had fix the specific migration limits (SML) for benzyl butyl phthalate and diethyl-hexyl-phthalate at 30 mg kg^{-1} and 1.5 mg kg^{-1}, respectively and a generic specific migration limit of 60 mg kg^{-1} when there are no SMLs or other restrictions (Wang *et al*., 2013).

As PAEs are only physically bound to the polymer chains of the polluting material, they can leach into the environment. They will then contaminate food, soil, water, and air that come into contact. Numerous studies have revealed the presence of phthalates in food or drink packaging or processing. In 1999, the use of disposable PVC gloves during meal preparation caused diethylhexyl phthalate contamination in the range of 10 to 4400 ng g^{-1} (Tsumura†* *et al*., 2003). Dibutyl phthalate has also been found at a concentration of 3 ng mL^{-1} in drinking water (Luo *et al*., 2014). Other studies reported the presence of PAEs in river water at concentrations ranging from 0.1 to 300 µg L^{-1} (Sung *et al*., 2003). Zeng *et al*. (2008) reported concentrations of PAEs ranging from 0.195 to 33.6 µg g^{-1} dry weight in agricultural soils from peri-urban areas of Guangzhou. These studies tell us that the presence PAEs typically found in environmental samples are at trace level. Therefore, sample preparation is necessary for establishing a reliable determination method for the analysis of PAEs prior to chromatographic separation.

University of Malaya

Carbonaceous nanomaterials have attracted great attention in recent years in developing MSPE adsorbents due to their strong hydrophobic and π-π stacking interaction with aromatic compounds such as phthalates (Table 2.4).

Table 2.4: Structure and properties of PAEs investigated in this work

Compound name	Formula	Molecular weight (g mol^{-1})	Structure
Dipropyl phthalate	$C_{14}H_{18}O_4$	250	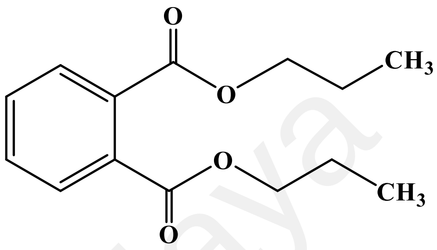
Benzyl butyl phthalate	$C_{19}H_{20}O_4$	312	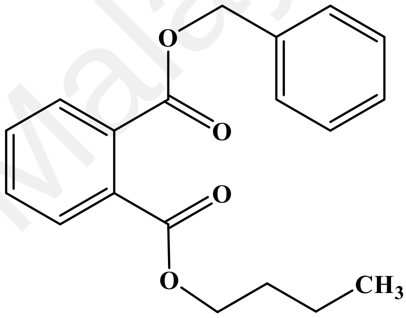
Dicyclohexyl phthalate	$C_{20}H_{26}O_4$	330	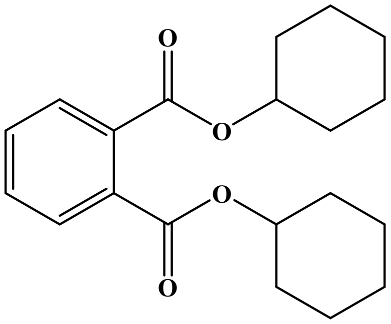

Recently, various modified magnetic adsorbents (Table 2.5) including magnetic graphene nanocomposites have been designed for the extraction of PAEs from various matrices. Wang *et al*. (2013) fabricated a magnetic microsphere confined graphene (Fe_3O_4@SiO_2-G) for the extraction of some PAEs from environmental water and soybean milk samples prior to high performance liquid chromatography analysis. They found that the prepared Fe_3O_4@SiO_2-G nanocomposites have great extraction capability toward the targeted analytes with LOD in the range of 0.07 to 0.10 ng mL^{-1} for water samples and 0.15 to 0.30 ng mL^{-1} for soybean milk samples. Wu *et al*. (2012) investigated the

University of Malaya

performance of magnetic graphene nanocomposites as MSPE adsorbent for the extraction of some PAEs including diethyl phthalate, di-*n*-propylphthalate, di-*n*-butylphthalate, dicyclohexylphthalate and diethylhexylphthalate prior to their determination by HPLC. Their proposed method had high enrichment factors ranging from 1574 to 2880 and low LOD ranging from 0.01 to 0.04 ng mL^{-1}. Three dimensional graphene based magnetic nanocomposite (3D-G-Fe_3O_4) was used as MSPE adsorbent for the determination of PAEs from fruit juice (Hao *et al*., 2014). They found that their 3D-G-Fe_3O_4 had an excellent adsorption capacity for specific analytes because of its high specific surface area allowed by the 3D porous structure. The proposed method showed good recoveries in the range of from 87.0% to 97.8% for all selected PAEs. Magnetic carbon nanotubes (CNTs) also have strong adsorption capabilities towards hydrophobic organic compounds and have been proven to possess great potential in serving as a MSPE adsorbent for the analysis of various organic compounds, mainly PAEs. Luo *et al*. (2012) prepared magnetic carbon nanotubes (CNTs) to extract carcinogenic PAEs from bottled beverages, tap water, and perfume samples. They established a rapid, sensitive, and cost-effective method for the analysis of PAEs from various consumable products with LODs ranging from 4.9 to 38 ng L^{-1}. Jiao *et al*. (2012) also used a multi-walled carbon nanotubes based adsorbent for the determination of trace levels of PAEs in drinking water. The recoveries and LODs were in the range of 86.6-100.2% and 0.009-0.032 μg L^{-1}, respectively.

These studies have demonstrated the potential applications of carbon based magnetic iron oxide materials in sample preparation and enrichment of PAEs. In this study, waste palm fatty acid is investigated as the carbonaceous starting material in developing a low cost magnetic adsorbent suitable for the adsorption of PAEs in real matrices. GO is introduced on the surface of waste palm fatty acid based magnetic adsorbent to enhance the adsorption of pollutant through mechanisms such as hydrogen bonding, hydrophobic and π-π interactions.

University of Malaya

2.4.2 Remediation of oil

Oil is a water pollutant which is introduced to water bodies in the form of cutting liquids, lubricants, fats, and heavy hydrocarbons. Oil spills lead to severe economic, social, and environmental related issues which are still a present-day problem (Saleem *et al.*, 2018). It is nearly impossible to completely avoid oil discharge into water bodies and therefore there is an immense need for technology to properly remove oil from water surfaces.

Oil usually enters water bodies through industrial discharge such as food processing waste, oil refinery byproducts and municipal waste (Ahmad *et al.*, 2005; Srinivasan & Viraraghavan, 2010). The concentration of oil in effluents from industrial sources has been found to reach as high as 40,000 mg L^{-1}. It has also been reported that 1 ton of spilled oil can contaminate up to 12 km^2 of water surface (Zhu *et al.*, 2010). Oil upon contacting the water surface, forms a thick layer of sludge covering the surface of water bodies. As a consequence, the passage of light is blocked which severely affects the photosynthesis of aquatic plants causing ecological imbalance (Mirshahghassemi *et al.*, 2017). Furthermore, these oils spills are toxic to aquatic animals, as the hydrocarbons present in oils can enter their body through ingestion and inhalation causing fatality in most cases. Additionally, oily waste on water increases treatment cost for wastewater treatment plants and may damage their machinery (Rajakovic *et al.*, 2007; Zhou *et al.*, 2008). In order to combat oil spills, the development of efficient adsorbent materials to separate and remove oils from water must be expedited.

Recently, there has been enormous interest in the use of hydrophobic magnetic adsorbents for the remediation, removal and clean-up of oil contaminants (Wattie *et al.*, 2018). They are selective, and can be quickly and easily separated from the treated water by a magnet (Figure 2.9).

University of Malaya

Table 2.5: Modified magnetic adsorbents for enrichment of PAEs

Adsorbent	Method	Sample	Ref.
3D-G-Fe_3O_4	MSPE/HPLC-DAD	Fruit juice	(Hao *et al*., 2014)
Magnetic graphene nanocomposite	MSPE/HPLC-UV	Bottled water/river water/coca cola/green tea	(Wu *et al*., 2012)
$Fe_3O_4@SiO_2$-G	MSPE/HPLC-UV	River/reservoir water/soybean milk	(Wang *et al*., 2013)
Magnetic carbon nanotubes	MSPE/GC-MS	Bottled beverages, tap water and perfume samples.	(Luo *et al*., 2012)
Magnetic multi-walled carbon nanotubes	MSPE/GC-MS	Drinking water	(Jiao *et al*., 2012)

University of Malaya

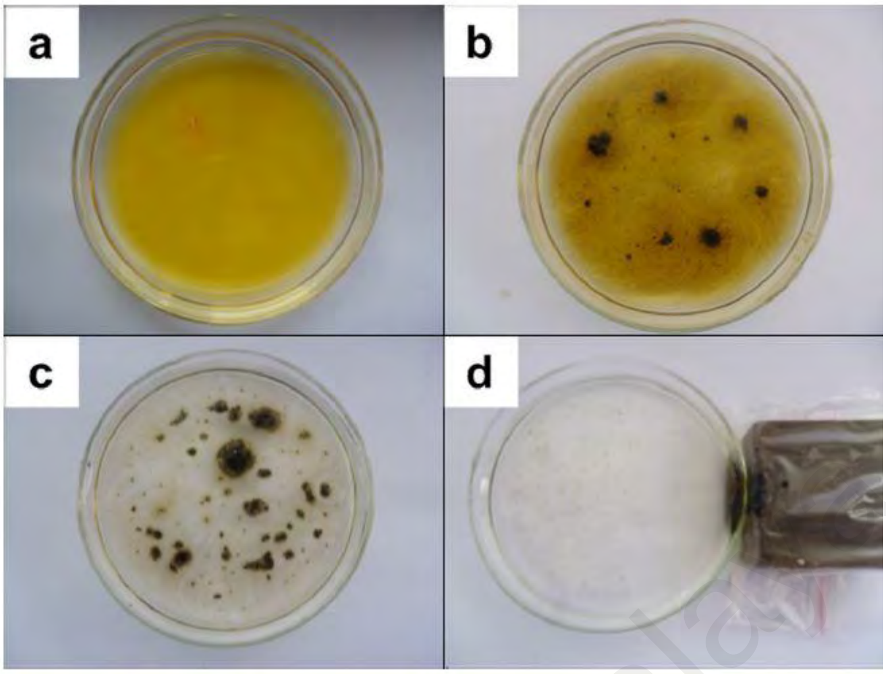

Figure 2.9: Digital photograph images of removal of lubricating oil from water surface by magnetic nanocomposites under magnetic field (a-d) (adapted from Chen *et al*., 2013)

To address the oil spillage problem, the surface of magnetic adsorbents can be coated with materials that have highly hydrophobic properties (Table 2.6) for selective adsorption and rapid separation of oil from aqueous solution.

Magnetic carbon composites are one of the viable solutions that exist. Zhu *et al*. (2010) reported the fast and selective removal of oils from water surface through superhydrophobic core–shell Fe_2O_3@C nanoparticles. The adsorbent could selectively absorb lubricating oil up to 3.8 times its own weight while completely repelling water. The oil-absorbed nanoparticles can then be quickly collected in seconds by applying an appropriate external magnetic field. More importantly, the superhydrophobic Fe_2O_3@C nanoparticles can be reused in water-oil separation several times as the adsorbed oil could be readily removed from the surfaces of nanoparticles by a simple ultrasonic treatment and still maintain its highly hydrophobic and superoleophilic characteristics.

Chu & Pan (2012) fabricated three-dimensional macroporous Fe/C nanocomposites for use as highly selective oil-adsorption materials. The reported macroporous

University of Malaya

nanocomposites exhibited fast and selective adsorption of a wide range of oils and hydrophobic organic solvents from the surface of water. Moreover, the nanocomposites could maintain its hydrophobicity even after repeated usage. However, a drawback to their method is that it requires a multistep synthesis procedure and the nanocomposites only exhibited a limited thermal stability.

A magnetic superhydrophobic bulk material with good reusability for the facile removal of oil was synthesized by Ge *et al*. (2013) to overcome the limitations mentioned above. The strongly oleophilic magnetic bulk material was demonstrated to be a reusable oil sorbent that can be recollected using a magnetic bar. The adsorbed oil could be then removed just by burning in air. Banerjee and co-workers introduced a new high performance Fe_3O_4–carbon composite system made by pyrolyzing iron containing metal organic framework (MOF) MIL-53 with some mixture of the polymorph MIL-88B (Banerjee *et al*., 2012). The synthesized composite possesses highly hydrophobic properties and shows potential for removal and recovery of oil pollutants from aqueous media.

In the present study, we focus on the use of palm fatty acid as a precursor material to develop hydrophobic adsorbents due to their cost effectiveness and local availability.

University of Malaya

Table 2.6: Modified magnetic adsorbents for removal of oil

Adsorbent	Experimental oil	Sorption capacity (g/g)	Ref.
Epoxidized natural rubber–magnetite nanocomposites	Petrol oil	7.00	(Venkatanarasimhan & Raghavachari, 2013)
Polystyrene coated magnetic nanocomposites	Lubricating oil	3.00	(Chen *et al*., 2013)
Hydrophobic organoclay-iron oxide hybrids	Crude oil	4.00	(Hsu *et al*., 2010)
Fe_2O_3@C nanoparticles	Lubricating oil	3.80	(Zhu *et al*., 2010)

CHAPTER 3: METHODOLOGY

3.1 Chemicals, materials and reagents

Iron(II) chloride tetrahydrate and iron(III) chloride hexahydrate were purchased from Sigma Aldrich (Missouri, MO, USA). N,N-dimetylformamide (DMF), (3-aminopropyl) triethoxysilane (APTES), aqueous ammonia, ethanol, ethyl acetate, acetonitrile, hydrochloric acid (HCl), potassium hydroxide (KOH), anhydrous sodium sulphate, methanol, graphite powder, sulphuric acid, potassium permanganate, hydrogen peroxide and *n*-hexane were purchased from Merck (Darmstadt, Germany). Domestic and commercial oil (including corn oil and lubricating oil) were bought from Ngo Chew Hong Oils and Fats (M) Sdn. Bhd. (Selangor, Malaysia). Palm cooking oil was purchased from a supermarket in Bangsar, Kuala Lumpur. The collected waste palm cooking oil had been used in a restaurant for frying purposes. Before use, the waste palm cooking oil samples were filtered in order to eliminate the particulate materials and other impurities in the process.

The gas-liquid chromatography reference standard for fatty acid methyl esters and polycyclic aromatic hydrocarbons (PAHs) standards, fluorene (Flu), fluoranthene (FLT), pyrene (Pyr), chrysene (Cry) and benzo(a)pyrene (BaP) were obtained from Supelco (Bellefonte, USA). Analytical standards of phthalate esters (PAEs) including dipropyl phthalate (DPP), benzyl butyl phthalate (BBP) and dicyclohexyl phthalate (DCHP) were supplied by Acros Organics (New Jersey, USA). All stock solutions were prepared in methanol at a concentration of 100 mg L^{-1} and stored in a dark amber glass at 4 °C.

3.2 Instruments

The functional groups of the nanoparticles were first characterized using a FT-IR spectrometer (Spectrum 400 Perkin Elmer, Waltham, MA, USA) with a diamond ATR

University of Malaya

accessory, using absorption mode with 4 scans at a resolution of $\pm$ 4 cm^{-1}, and a wavenumber range of 4000 to 450 cm^{-1}. Wettability analyses were performed using the Theta Lite 100 and Theta Lite 101 contact angle measurement instruments (Attension, Espoo, Finland). TEM images of the adsorbents were obtained using a transmission electron microscope (TEM) instrument (JEOL JEM-2100F, MA, USA). A thermogravimetric analyzer (Perkin Elmer, TGA 4000, Waltham, MA, USA) was used to study the thermal behavior of the prepared adsorbents from 30 to 900 °C with a heating rate at 20 °C min^{-1} under nitrogen flow to study the thermal behaviour of the prepared nanoparticles. The SEM images and elemental analysis of the prepared nano-sorbents were investigated by field emission scanning electron microscopy (SEM HITACHI SU8220, Tokyo, Japan) equipped with energy dispersive X-ray spectrometry (XMX1011, OXFORD Instruments). The crystal phase of the prepared adsorbents was determined using a PANanalytical EMPYREAN X-ray powder diffraction (XRD) diffractometer (CuK, radiation, λ=1.541874 nm), at a scanning speed of 0.07° / min from 15° to 75° (2θ) (Siemens, Frimley, UK). The magnetic properties was analyzed by using vibrating sample magnetometer (VSM LakeShore 7400 series, Tokyo, Japan). The surface area and pore size were measured using Brunauer-Emmett-Teller (BET) by nitrogen adsorption-desorption isotherms at 77.350 K in Micromeritics (ASAP2020, Georgia, USA).

3.2.1 GC conditions

The fatty acids composition was analyzed using a Shimadzu 2010 gas chromatograph (Shimadzu, Kyoto, Japan) equipped with a split/splitless injector and a flame ionization detector (FID). A BPX50 capillary column (SGE Analytical Science, Australia) (30 m x 0.25 mm i.d. 0.25 µm film thickness) was used for the separation of fatty acids. Helium (with 99.999% purity) was the carrier gas and is fed at a constant flow rate of 59.2 mL min^{-1}. The injection port was operated using split mode. The detector

University of Malaya

temperature was set at 260 °C, injector temperature was set at 139 °C. The oven temperature was initially set at 139 °C for 2 min, then ramped by 8 °C min^{-1} up to 165 °C, then 3 °C min^{-1} up to 192 °C, 13.7 °C min^{-1} up to 240 °C and finally 11 °C min^{-1} at 240 °C.

3.2.2 HPLC conditions

Separation and detection of target analytes were achieved using a HPLC system (Shimadzu, Tokyo, Japan) consisting of a LC-20AT pump, SPD-M20A diode array detector, SIL-20A HT auto sampler, and CTO-10AS VP column oven. Separation was conducted using a C-18 reverse phase column (250 mm x 4.6 mm; particle size 5 μm) hypersil gold (Thermo science, USA). There are two chromatographic conditions for separation of PAHs (including Flu, FLT, Pyr, Cry and BaP) and simultaneous separation of PAHs and PAEs (including Flu, FLT, Cry, DPP, BBP and DCHP).

3.2.2.1 Liquid chromatographic conditions for separation of PAHs

The mobile phase was acetonitrile-water (80:20, v/v) at a flow rate of 1.0 mL min^{-1}. The injection volume was 10 μL. The detections were set as follows: 5.54 min, 254 nm (for Flu); 6.77 min, 284 nm (for FLT); 7.22 min, 270 nm (for Pyr); 8.03 min, 266 nm (for Cry); and 10.82 min, 266 nm (for BaP).

3.2.2.2 Liquid chromatographic conditions for simultaneous separation of PAHs and PAEs

Separation and quantification of the selected PAEs and PAHs was performed using a mobile phase of methanol-water (80:20, v/v) at a flow rate of 0.6 mL min^{-1}. The injection volume was 10 μL. DPP was eluted after 8.68 min at 243 nm, BPP, 11.62 min at 280 nm,

University of Malaya

DCHP, 19.71 min at 243 nm, Flu, 13.21 min at 254 nm, FLT, 17.15 min at 284 nm and Cry, after 23.16 min at 266 nm.

3.3 Preparation of new adsorbents

In this study, we developed three new adsorbents namely MNP@FFAs-PCO, MNP@FFAs-WPCO and MNP@FFAs-WPCO-GO. The preparation procedures are described below:

3.3.1 Synthesis of MNP@FFAs-PCO

Synthesis of MNP@FFAs-PCO involves four steps, hydrolysis of triacylglycerol of palm cooking oil, preparation of MNPs through chemical co-precipitation, preparation of MNP-APTES and preparation of MNP@FFAs-PCO.

3.3.1.1 Hydrolysis of triacylglycerol of palm cooking oil

The procedure for the hydrolysis of triacylglycerol of palm cooking oil to obtain free fatty acids (Figure 3.1(A)) was adapted from a reported work (Salimon *et al*., 2011). Typically, 50 g of palm cooking oil and 300 mL of 1.75 M of ethanolic KOH was heated at 65 °C for 2 hours. The unsaponifiable products were extracted using 100 mL of *n*-hexane and then discarded. The obtained mixture was mixed with deionized water and acidified with 100 mL 6 N hydrochloric acid until the solution turned reaches pH 1. The extraction of fatty acids was repeated three times by using 100 mL of *n*-hexane for each extraction. The extraction product, a fatty acids-hexane mixture was washed with deionized water and dried with anhydrous sodium sulphate. The solvent was removed by rotary evaporator at 35 °C to obtain the free fatty acids.

University of Malaya

3.3.1.2 Preparation of MNPs

The procedure for the preparation of the MNPs is shown in Figure 3.1(B). The MNPs were synthesized using a chemical co-precipitation method (Can *et al*., 2009). Briefly, 3.1736 g of $FeCl_2.4H_2O$ and 7.5709 g $FeCl_3.6H_2O$ was dissolved in 320 mL deionized water. The mixed solution was then stirred under nitrogen at 80 °C for 1 hour. Then, 40 mL of aqueous ammonia was added into the reaction mixture rapidly. The resulting mixture was stirred under nitrogen for another 1 hour and then cooled to room temperature. The precipitated magnetic particles was washed five times with hot water until the filtrate becomes neutral and then it is separated by magnetic decantation.

3.3.1.3 Preparation of MNP-APTES

MNP-APTES was prepared according to method by Feng *et al*. (2008). Briefly, 10 mL of hydrolyzed APTES was added to 100 mL magnetite fluid in round bottom flask. The mixture was stirred for 5 hours at 60 °C under nitrogen protection. After the solution was cooled to room temperature, the resulting brownish product was separated by an external magnet and washed with ethanol and deionized water several times. The final product was then dried in a vacuum at 70 °C for 24 hours (Figure 3.1(C)).

3.3.1.4 Preparation of MNP@FFAs-PCO

Figure 3.1(D) illustrates the preparation route of MNP@FFAs-PCO. Freshly prepared 1.000 g MNP-APTES was dispersed in 10 mL of DMF, followed by the addition of 2.000 g free fatty acids. The reaction mixture was stirred overnight at 60 °C under nitrogen. Then, the solution was cooled to room temperature and the obtained brownish product (MNP@FFAs-PCO) was magnetically collected. The obtained MNP@FFAs-PCO was washed repeatedly with excess ethanol and deionized water, respectively and then finally vacuum dried at 70 °C for 24 hours.

University of Malaya

3.3.2 Synthesis of MNP@FFAs-WPCO

Figure 3.1 (B-D) depicts the procedure for the preparation of the MNP@FFAs-WPCO. Synthesis of MNP@FFAs-WPCO does not involve the hydrolysis of triacylglycerol of palm cooking oil. To prepare MNP@FFAs-WPCO, 1.000 g of MNP-APTES was dispersed in 10 mL of DMF, followed by the direct addition of 2.000 g of waste palm cooking oil to the solution and the mixture was stirred overnight at 60 °C, under nitrogen protection. After the solution was cooled at room temperature, the resulting brownish product was washed with ethanol and deionized water several times and collected by magnetic decantation. Then, the final product was dried in the vacuum at 70 °C for 24 hours.

University of Malaya

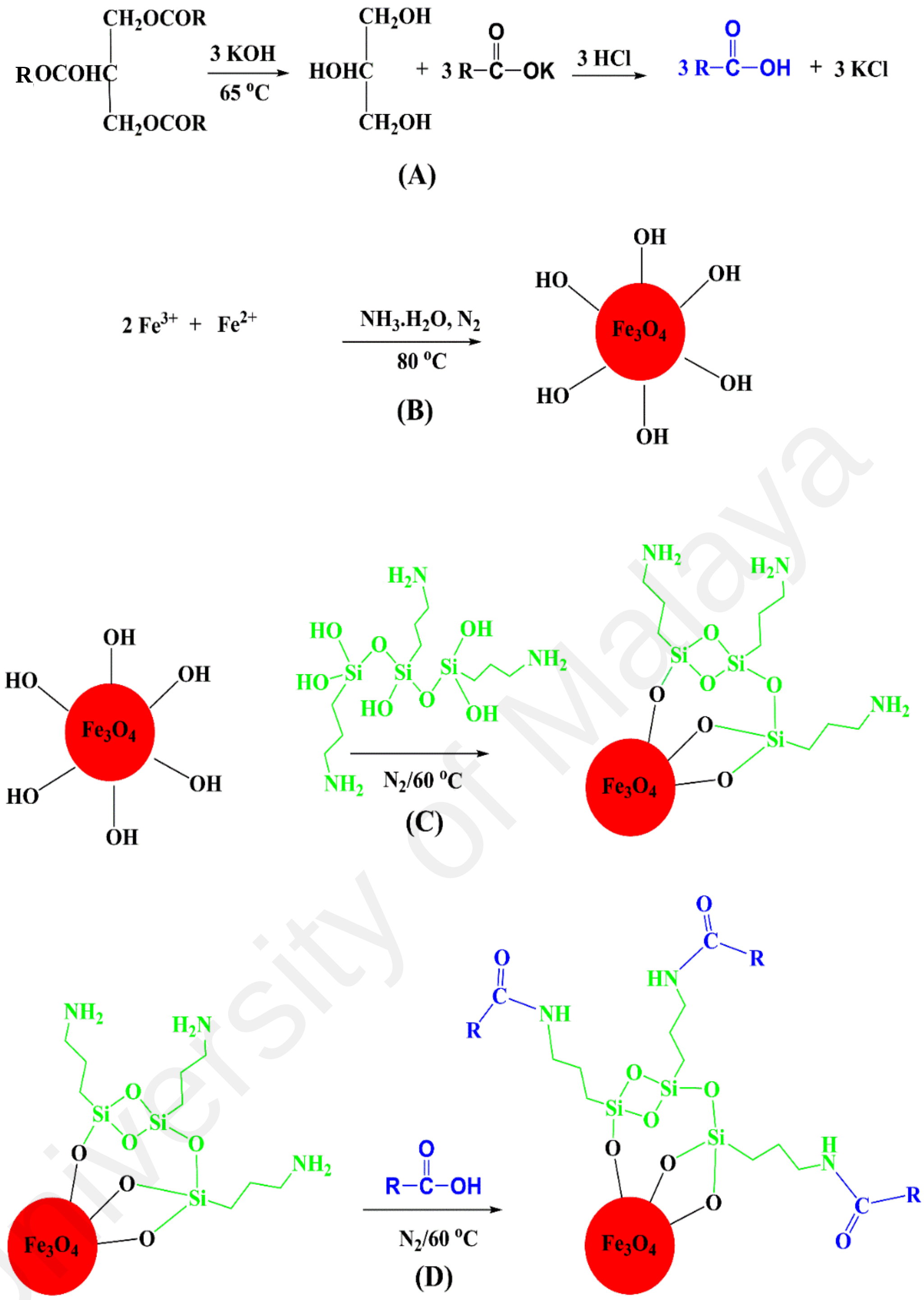

Figure 3.1: The preparation scheme of (A) Free fatty acids (B) MNPs (C) MNP-APTES and (D) MNP@FFAs-PCO or MNP@FFAs-WPCO (R = the alkyl chain of the free fatty acids)

University of Malaya

3.3.3 Synthesis of MNP@FFAs-WPCO-GO

3.3.3.1 Preparation of Graphene oxide (GO)

Before synthesis of MNP@FFAs-WPCO-GO is proceed, GO was obtained first from the simple oxidation of natural graphite powders. The procedure used is a slightly modified version of a previously reported work (Nodeh *et al.*, 2016). About 1.00 g of graphite powder was dispersed in 20 mL of distilled water and 100 mL of sulphuric acid. The mixed solution was stirred for 2 hours to form a homogeneous solution. Then, 7.00 g of potassium permanganate was added slowly to the solution under continuous magnetic stirring for 24 hours at room temperature. Then, the solution was placed in an ice bath and hydrogen peroxide was added until the solution turns yellow. The resulting mixture was diluted with deionized water and left overnight to settle. The product obtained was then washed extensively using water until a neutral pH was obtained.

3.3.3.2 Preparation of MNP@FFAs-WPCO-GO

The schematic diagram for the synthesis path of MNP@FFAs-WPCO-GO is shown in Figure 3.2. 2.00 g of MNP@FFAs-WPCO was mixed with 1.00 g of GO and dispersed in 20 mL of deionized water. The mixed solution was stirred for 5 hours at room temperature. MNP@FFAs-WPCO-GO with different ratios of MNP@FFAs-WPCO and GO (1:1, 1:2, 1:3, 1:4, 2:1, 3:1 and 4:1) were obtained after being washed with water and dried in vacuum for 24 hours at 70 °C.

University of Malaya

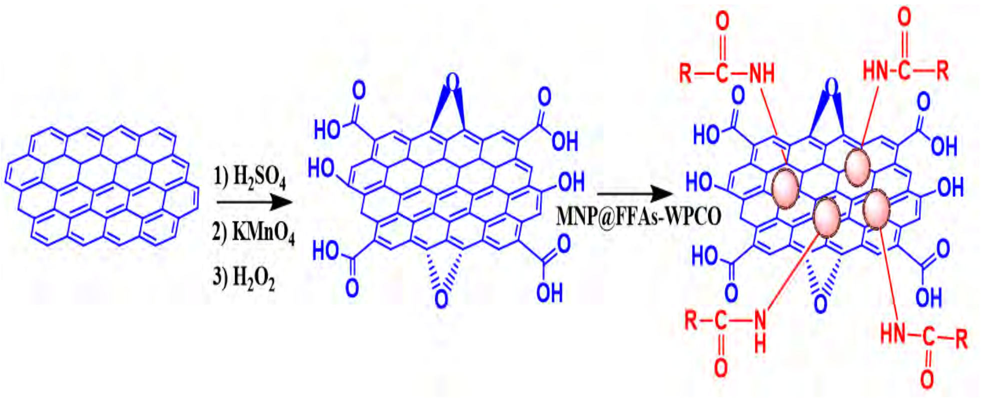

Figure 3.2: The preparation scheme of MNP@FFAs-WPCO-GO

3.4 The applications of new adsorbents

These new materials were used as adsorbents for magnetic solid phase extraction (MSPE) and oil removal studies.

3.4.1 MSPE study

In this section, MNP@FFAs-PCO and MNP@FFAs-WPCO were applied as adsorbents for MSPE of PAHs from landfill leachate and sludge samples. The third adsorbent, MNP@FFAs-WPCO-GO was applied as a MSPE adsorbent for simultaneous determination of PAHs and PAEs from landfill sludge, cabbage and apple samples.

3.4.1.1 Optimization of MSPE procedure

Several factors that affect extraction efficiency such as adsorbent dosage, type of organic eluent, volume of organic eluent, extraction time, desorption time, pH of the solution and sample volume were studied.

University of Malaya

3.4.1.2 Adopted extraction conditions

(i) MSPE extraction conditions using MNP@FFAs-PCO adsorbent

15 mg of MNP@FFAs-PCO was placed in a vial. Then, 30 mL of the prepared spiked PAHs solution was transferred into the same vial. The solution was shaken for 15 min. The adsorbent was isolated from the sample solution using an external magnet and the sample solution was then decanted. The adsorbed PAHs on MNP@FFAs-PCO was eluted by shaking with 2.0 mL of desorption solvent (*n*-hexane) for 10 min. The collected eluate was dried under a flow of nitrogen gas and the residue was dissolved in 0.5 mL acetonitrile. Finally, 10 µL of the eluate was injected into the HPLC system for analysis.

(ii) MSPE extraction conditions using MNP@FFAs-WPCO adsorbent

25 mg of the MNP@FFAs-WPCO was added into 150 mL of water samples containing trace level of PAHs. The extraction time used to facilitate the adsorption of PAHs on MNP@FFAs-WPCO was 25 min. For desorption condition, The PAHs adsorbed on MNP@FFAs-WPCO was eluted with 2.5 mL of ethyl acetate by shaking for 25 min. The collected eluate was dried under a stream of N_2 and the residue was dissolved in 0.5 mL of acetonitrile. Finally, 10 µL of the eluate was injected into the HPLC system for analysis.

(iii) MSPE extraction conditions using MNP@FFAs-WPCO-GO adsorbent

20 mg of MNP@FFAs-WPCO-GO was placed in a 200 mL of sample solution containing spiked of mixture PAEs and PAHs. The extraction time used to facilitate the adsorption of PAHs on MNP@FFAs-WPCO-GO was 10 min. For desorption condition, the adsorbed analytes on MNP@FFAs-WPCO-GO were desorbed using 2.0 mL of acetone by shaking for 10 min. The collected acetone was then evaporated to dryness

University of Malaya

under a stream of nitrogen and then the residue was dissolved in 0.5 mL of methanol. Finally, 10 µL of aliquots was injected into the HPLC system for analysis.

3.4.1.3 Reusability study

The adsorption-desorption experiment was conducted five times in succession to determine its reusability. The conditions used are described as follows.

(i) Reusability condition of MNP@FFAs-PCO

The spent MNP@FFAs-PCO was washed with *n*-hexane several times and then dried before being reused.

(ii) Reusability condition of MNP@FFAs-WPCO

The used MNP@FFAs-WPCO was washed with ethyl acetate several times and then dried before being reused.

(iii) Reusability condition of MNP@FFAs-WPCO-GO

The used magnetic adsorbent, MNP@FFAs-WPCO-GO was washed with acetone several times and then dried before being reused.

3.4.1.4 Method validation

(i) Linearity, precision and accuracy

The linearity of the adsorption process was determined using seven different concentration levels. The precision of the proposed method was measured in term of relative standard deviation (%RSD) and was evaluated using 7 variances with spiking

University of Malaya

levels of 10 ng mL^{-1} of PAHs mixture and 7 variances with spiking levels of 100 ng mL^{-1} of PAEs-PAHs mixture in ultra-purified water. Standard deviation (SD) and RSD were determined using the following equations:

$$SD = \sqrt{\frac{\sum(x-\bar{x})^2}{n-1}} \tag{3.1}$$

$$RSD = \frac{SD}{\bar{x}} \times 100\% \tag{3.2}$$

Where $\bar{x}$ represents the mean value, x is the result of each individual runs, and n is the number of measurements (Patnaik, 2010). Recovery is the quantitative measure of accuracy. The percentage of recovery (%R) was calculated by using the following equation:

$$\%R = \frac{Concentration\ of\ spike\ sample - Concentration\ of\ unspike\ sample}{Concentration\ of\ spike\ added} \times 100\% \tag{3.3}$$

(ii) Limit of detection (LOD) and limit of quantification (LOQ)

The limit of detection (LOD) and the limit of quantification (LOQ) are two main parameters evaluated in method validation. The limits of detection and quantification were determined from the standard deviation of the blank (σ) and slope of calibration curve (S) using the following equations (Konieczka & Namiesnik, 2016):

$$LOD = 3\left(\frac{\sigma}{S}\right) \tag{3.4}$$

$$LOQ = 10\left(\frac{\sigma}{S}\right) \tag{3.5}$$

3.4.1.5 Real samples application

(i) Real samples analysis using MNP@FFAs-PCO adsorbent

To investigate the matrix effect of the optimized method, three level concentrations of PAHs including 5, 10 and 100 ng mL^{-1} were spiked in the leachate and sludge from landfill site, Jeram, Kuala Selangor. The leachate samples were then filtered through a

University of Malaya

0.22 μm membrane and stored at 4 °C prior to use. 30 mL of the filtered leachate were used in each MSPE run.

The sludge samples were dried at room temperature, pulverized and passed through a 1 mm sieve. Then, ultrasound-assisted extractions (UAE) of the sludge samples was carried out. Briefly, 1.00 g of the sludge sample was mixed with 3 mL of methanol in a 50 mL centrifuge tube and then sonicated for 10 min. The mixed sludge solution was centrifuged at 3500 rpm for 5 min and the supernatant was filtered through a PTFE syringe filter (13 mm, 0.22 μm pore size) into a sample vial (Tahmasebi & Yamini, 2012). The total volume of sample in the vial was then made up to 30 mL with distilled water and then the magnetic solid phase extraction procedure was carried out as discussed in Section 3.4.1.2 (i). The percent recovery (%R) was determined from the equation (3.3).

University of Malaya

(ii) Real samples analysis using MNP@FFAs-WPCO adsorbent

To investigate the matrix effect of the optimized method, the analysis was performed by spiking leachate and sludge from a landfill site, Jeram, Kuala Selangor at three concentrations levels (0.5, 50 and 50 ng mL^{-1}) of PAHs. The samples were pre-treated as described previously in Section 3.4.1.5 (i). Then, the total volume was made up to 150 mL with distilled water and MSPE was carried out as described previously in Section 3.4.1.2 (ii). The percent recovery (%R) was determined from the equation (3.3).

(iii) Real samples analysis using MNP@FFAs-WPCO-GO adsorbent

To investigate the matrix effect of the optimized method, the real sample analysis was performed by spiking landfill sludge collected from landfill site, Jeram, Kuala Selangor, cabbage and apple samples obtained from a local supermarket in Bangsar, Kuala Lumpur at three concentrations levels (50, 100 and 1000 ng mL^{-1}) of DPP, BBP, DCHP and Flu and (1, 10 and 100 ng mL^{-1}) of FLT and Cry. The sample pre-treatment of landfill sludge samples was mentioned earlier in Section 3.4.1.5 (i). The fruit and vegetable samples were cut and homogenized using a laboratory homogenizer. Subsequently, 20.00 g of the samples were accurately weighed and put into a 50 mL centrifugal tube, followed by the addition of a 10 mL of water-methanol mixture (1:10). The mixture was vortexed for 2 min and centrifuged at 4000 rpm for 5 min. The supernatant was then filtered through a 0.45 mm filter paper and transferred into sample glass bottles (Mahpishanian *et al*., 2015). After the total volume of cabbage, apple and landfill sludge samples were made up to 200 mL with distilled water. Then, they were analyzed using the MSPE procedure described in Section 3.4.1.2 (iii). The percent recovery (%R) was determined from the equation (3.3).

3.4.2 Oil removal procedure

In this section, MNP@FFAs-PCO and MNP@FFAs-WPCO were applied as the adsorbents for remediation of oil from aqueous samples.

3.4.2.1 Optimization of oil adsorption procedure

Several factors that affect the oil adsorption efficiency such as weight of adsorbent, contact time and pH of the solution were studied.

3.4.2.2 Adopted removal conditions

(i) Oil removal conditions using MNP@FFAs-PCO adsorbent

The batch adsorption studies were carried out by mixing 10 mg of adsorbent MNP@FFAs-PCO with 3 mL lubricating oil in 20 mL of water (pH 7) at 25 °C for 30 min. After 30 min, the MNP@FFAs-PCO adsorbent was then separated from the water using an external magnet. Here, the gravimetric analysis was used to determine the oil

University of Malaya

adsorbing capacity of the adsorbent (Chen *et al.*, 2013). The weight of the adsorbent before and after oil adsorbance was measured as $m1$ and $m2$ using a weighing balance. The difference between $m1$ and $m2$ represented the weight of adsorbed oil. The oil adsorption capacity, k was calculated using the following equation.

$$k = \frac{(m2 - m1)}{m1} \tag{3.6}$$

Where k is the oil adsorption capacity (g/g), $m1$ and $m2$ are the weight of the adsorbent before and after oil adsorption, respectively.

(ii) Oil removal conditions using MNP@FFAs-WPCO adsorbent

12 mg of MNP@FFAs-WPCO was placed in 20 mL of water at pH 7 containing 3 mL of lubricating oil. The contact time used to facilitate the adsorption of oil on MNP@FFAs-WPCO was 50 min and after that, the adsorbent was separated from the water using an external magnet. The oil adsorption capacity, k of the nanoparticles was determined from equation (3.6).

3.4.2.3 Reusability study

The used adsorbents (*i.e.*, MNP@FFAs-PCO and MNP@FFAs-WPCO) were washed with *n*-hexane ultrasonically to remove adsorbed oil. Then, they were dried in an oven at 90 °C for 24 hours. The regenerated adsorbents were reused and the sorption efficacy was calculated.

University of Malaya

CHAPTER 4: RESULTS AND DISCUSSION

4.1 Introduction

This chapter is divided into three sections. Section 4.2 discusses about the characterization and applications of new adsorbent, free fatty acids which obtained from hydrolysis of triacylglycerol (TAG) of palm cooking oil functionalized magnetic nanoparticles (MNP@FFAs-PCO) while Section 4.3 describes about the properties and utilizations of designed adsorbent based free fatty acids which directly obtained from waste palm cooking oil functionalized magnetic nanoparticles (MNP@ FFAs-WPCO). Section 4.4 presents the characterization and application of free fatty acids from waste palm cooking oil functionalized magnetic nanoparticles immobilized on the surface of the graphene oxide (MNP@FFAs-WPCO-GO).

In section 4.2, the new adsorbent, free fatty acids which obtained from hydrolysis of TAG of palm cooking oil functionalized magnetic nanoparticles (MNP@FFAs-PCO) was fabricated. Palmitic and oleic acid are the major free fatty acids obtained after hydrolysis TAG of palm cooking oil. They are interesting and economical precursor to a novel adsorbent system for remediation and detection of toxic pollutants. This is due to their long alkyl chains which can strongly interact with hydrophobic contaminants, mainly PAHs and oil pollutants, thus enabling their extraction and removal.

The proposed adsorbent, MNP@FFAs-PCO has been effectively applied for the extraction of the selected four polycyclic aromatic hydrocarbons (PAHs), namely fluoranthene (FLT), pyrene (Pyr), chrysene (Cry) and benzo(a)pyrene (BaP) from the environmental samples and decontaminated oil from aqueous media. The fabricated MNP@FFAs-PCO is found to be effective in extracting all the chosen PAHs from complex matrices and could selectively adsorb oil from aqueous samples.

University of Malaya

Inspired from the performance of MNP@FFAs-PCO based free fatty acids obtained from hydrolysis of TAG of palm cooking oil as an adsorbent, therefore the selection of free fatty acids from waste palm cooking oil is an innovative idea. Conveniently, waste palm-based cooking oil already contain high amounts of free fatty acids as they are produced through a hydrolytic process that occurs during cooking (Sharma *et al*., 2011). This means that spent cooking oil can directly be used as a source of free fatty acids without the need of the chemically and environmentally expensive TAG hydrolysis process. Since waste palm cooking oil is typically considered a waste, using this as a precursor material offer numerous advantages, including cost-effective and remove waste that would otherwise need to be disposed of.

In section 4.3, we thus introduce a new low-cost adsorbent, MNP@FFAs-WPCO with the aim of exploring its feasibility as an adsorbent for the extraction of fluorene (Flu) in addition to the selected PAHs mentioned in Section 4.2 and for the removal of oil from contaminated aqueous systems. We then compare the performance of the MNP@FFAs-WPCO in terms of PAHs extraction efficacy and oil adsorption to that for MNP@FFAs-PCO.

It is already proven in Section 4.3 that MNP@FFAs-WPCO has good hydrophobic interaction with hydrophobic contaminants in real samples. Due to its excellent performance for adsorption of these pollutants, its application is further extended to the simultaneous determination of various organic contaminants in real samples. Organic pollutants in real samples have a wide range of polarities which require hydrogen bonding, hydrophobic and π–π interactions to ensure their proper adsorption. Thus, to have sufficient adsorption of these pollutants, the structure of MNP@FFAs-WPCO was integrated by graphene oxide (GO) moieties that containing carboxylic, epoxy and hydroxyl groups. GO contains hydrophobic carbon framework and could be well dispersed in aqueous media due to the presence of its oxygen functional groups.

University of Malaya

The synergistic association between GO and free fatty acid chains enhances the dispersion of the fabricated adsorbent, MNP@FFAs-WPCO-GO and allows it to make interactions with selected PAHs and PAEs that can be found in food, polluted waters and sediments due to their widespread use over the last 100 years (Cortazar *et al*., 2002). Based on the structure of MNP@FFAs-WPCO-GO, we can expect that three kinds of adsorbent-adsorbate interactions might be responsible for the adsorption of PAHs and PAEs toward its framework. One of main interaction was π–π interaction between benzene rings of PAEs and PAHs. The other was hydrogen bonding between the oxygen-containing groups contained in PAEs and GO. The third interaction was hydrophobic interaction between carbon surface of MNP@FFAs-WPCO-GO and aromatic moieties of PAHs and PAEs.

In Section 4.4, we introduce a new adsorbent based free fatty acids from waste palm cooking oil functionalized magnetic nanoparticles immobilized on the surface of GO, MNP@FFAs-WPCO-GO for the simultaneous determination PAHs (*i.e.*, fluorene (Flu), fluoranthene (FLT) and chrysene (Cry)) and PAEs (*i.e.*, dipropyl phthalate (DPP), benzyl butyl phthalate (BBP), and dicyclohexyl phthalate (DCHP)) in apple, cabbage and landfill sludge samples. The extraction performance of this adsorbent will be discussed in this section.

University of Malaya

4.2 Free fatty acids from palm cooking oil functionalized magnetic nanoparticles (MNP@FFAs-PCO) and its applications

4.2.1 Physicochemical properties of MNP@FFAs-PCO

The compositions of the fatty acids obtained from hydrolysis TAG of palm cooking oil are first measured and tabulated in Table 4.1. The major free fatty acids present are palmitic, stearic and oleic acids.

Table 4.1: The composition of fatty acids obtained from hydrolysis of triacylglycerol palm cooking oil

Fatty acid		Fatty acid composition (%)
Lauric	(C12:0)	0.40
Myristic	(C14:0)	1.35
Palmitic	(C16:0)	59.64
Palmitoleic	(C16:1)	1.15
Stearic	(C18:0)	6.09
Oleic	(C18:1)	28.55
Arachidic	(C20:0)	0.78
Eicosenic	(C20:1)	2.03

The structure and composition of the prepared MNP@FFAs-PCO was characterized using various instruments to prove the attachment of free fatty acids on MNPs. To confirm chemical bond formation, the structures of the synthesized materials, including MNPs, MNP-APTES and MNP@FFAs-PCO were characterized by FT-IR. The FT-IR spectra of all prepared materials are shown in Figure 4.1(A-C). For the FT-IR spectrum of MNPs, the peak at 537 cm^{-1} represents the vibration of the Fe-O band (Zhang *et al*., 2010). The two absorption peaks at 3400 and 1604 cm^{-1} correspond to the stretching and bending of

University of Malaya

the O-H group on the surface of MNPs (Mahmoud *et al*., 2015). After modification with (3-aminopropyl)triethoxysilane (APTES), the new peak appears at 981 cm^{-1} which corresponds to the Si-O group from APTES confirming the presence of silane on the surface of MNP-APTES. The bands at 3411 cm^{-1} and 1603 cm^{-1} are attributed to N-H stretching vibration and the NH_2 group, respectively (Wang *et al*., 2013). The intense peak at 1626 cm^{-1} is associated with C=O stretching. In addition, new bands appeared at 2921 and 2853 cm^{-1} for MNP@FFAs-PCO are assigned to the asymmetric and symmetric CH_2 stretching, respectively. The new bands indicated that free fatty acids have been successfully functionalized onto the surface of MNP-APTES.

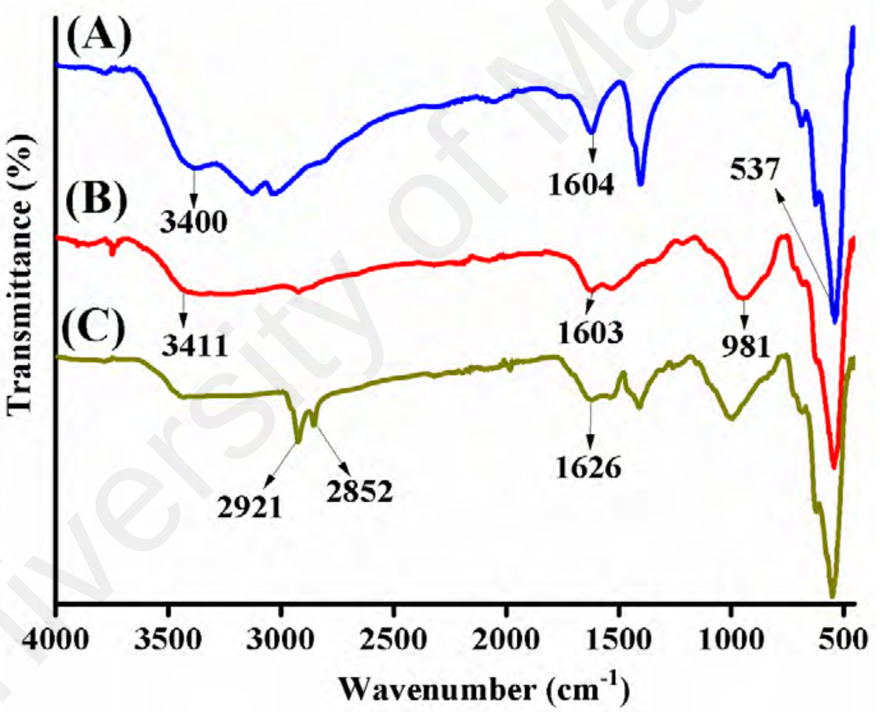

Figure 4.1: FT-IR spectra of (A) MNPs (B) MNP-APTES and (C) MNP@FFAs-PCO

In order to study the crystallinity of the synthesized MNPs, MNP-APTES and MNP@FFAs-PCO, the crystal phase of the prepared adsorbents was analyzed using XRD (Figure 4.2(A-C)). The spectrum of MNPs showed the presence of diffraction peaks at 2θ = 30.42°, 35.59°, 43.42°, 53.63°, 57.35° and 63.02°, respectively which are assigned to the (220), (311), (400), (422), (511) and (440) planes of Fe_3O_4 (JCPDS 88-0866). These

University of Malaya

indicate that the Fe_3O_4 nanoparticles has a cubic spinel structure (Marquez *et al.*, 2009). Similar diffraction peaks are also observed in the MNP-APTES and MNP@FFAs-PCO spectra revealing that the cubic spinel structure of Fe_3O_4 nanoparticles were not altered during the functionalization process. However, the intensity of the signals decreased for MNP-APTES and MNP@FFAs-PCO, suggesting the presence of APTES and free fatty acids on the MNPs after modification.

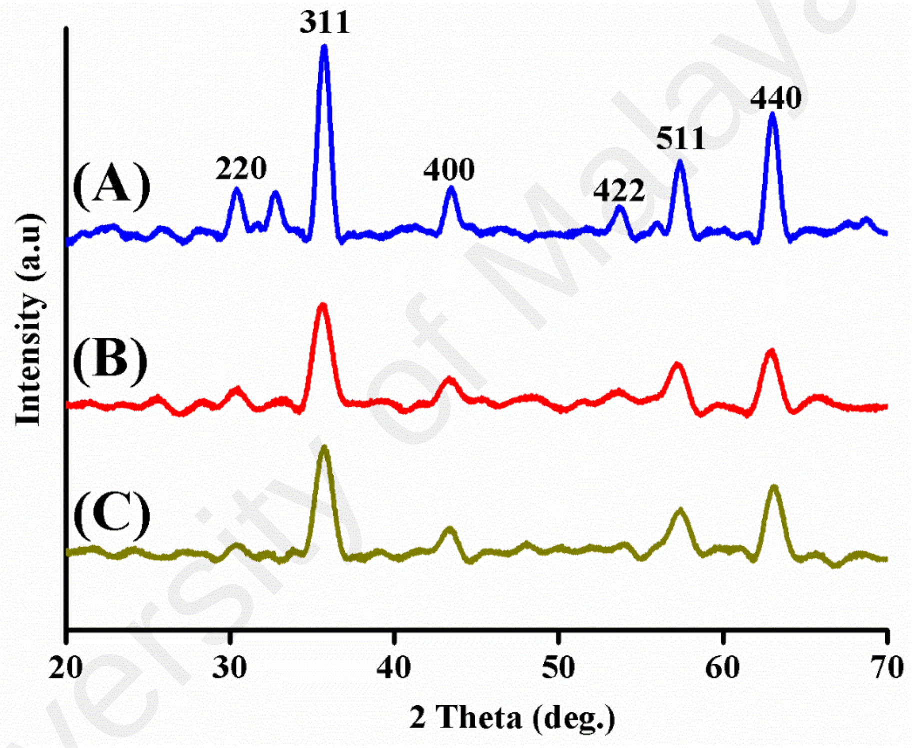

Figure 4.2: XRD patterns of (A) MNPs (B) MNP-APTES and (C) MNP@FFAs-PCO

University of Malaya

Elemental analysis was employed to confirm the presence of elements of interests in MNPs, MNP-APTES and MNP@FFAs-PCO (Figure 4.3(A-C)). It was found that the composition of MNPs are 75.5% Fe and 24.5% O. This indicates that the magnetite (Fe_3O_4) nanoparticles have been successfully synthesized. For MNP-APTES, APTES is confirmed to have coated the MNPs surface due to the presence of 5.0% C, 1.3% Si and 0.9% N in MNP-APTES. The high percentage of C (9.7%) and O (37.6%) in

MNP@FFAs-PCO, proved that free fatty acids have been successfully functionalized on MNP-APTES.

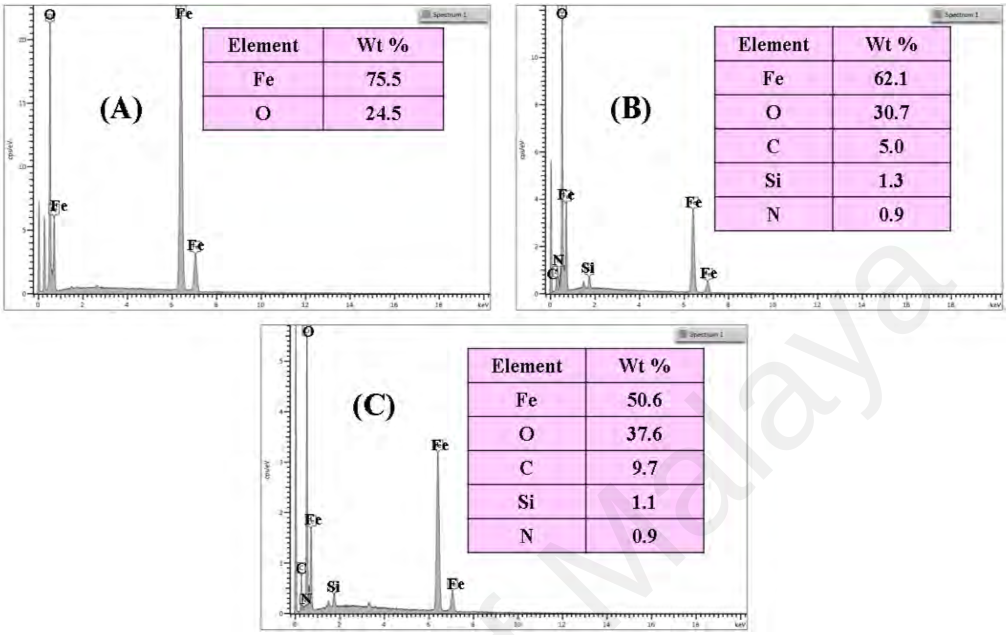

Element	Wt %
Fe	75.5
O	24.5

Element	Wt %
Fe	62.1
O	30.7
C	5.0
Si	1.3
N	0.9

Element	Wt %
Fe	50.6
O	37.6
C	9.7
Si	1.1
N	0.9

Figure 4.3: EDX spectra of (A) MNPs (B) MNP-APTES and (C) MNP@FFAs-PCO

TGA was employed to assess the thermal stability over the surface of the synthesized compounds. The TGA results of MNPs, MNP-APTES and MNP@FFAs-PCO are shown in Figure 4.4(A-C) and Table 4.2. The initial weight loss from the MNPs at temperature 35 to 129 °C due to loss of adsorbed water and hydroxyl group (6.25%). At temperature 260 to 540 °C, the weight loss of about 2.09% is recorded and attributed to crystal phase transformation from magnetite (Fe_3O_4) to maghemite (γ-Fe_2O_3). For MNP-APTES, it shows weight loss of 3-aminopropyl groups about 2.65% occurred between 250 °C to 420 °C while MNP@FFAs-PCO experienced a weight loss about 4.86% due to the breakdown of 3-aminopropyl and free fatty acids moieties from the surface of MNPs at temperature of 200 to 440 °C.

University of Malaya

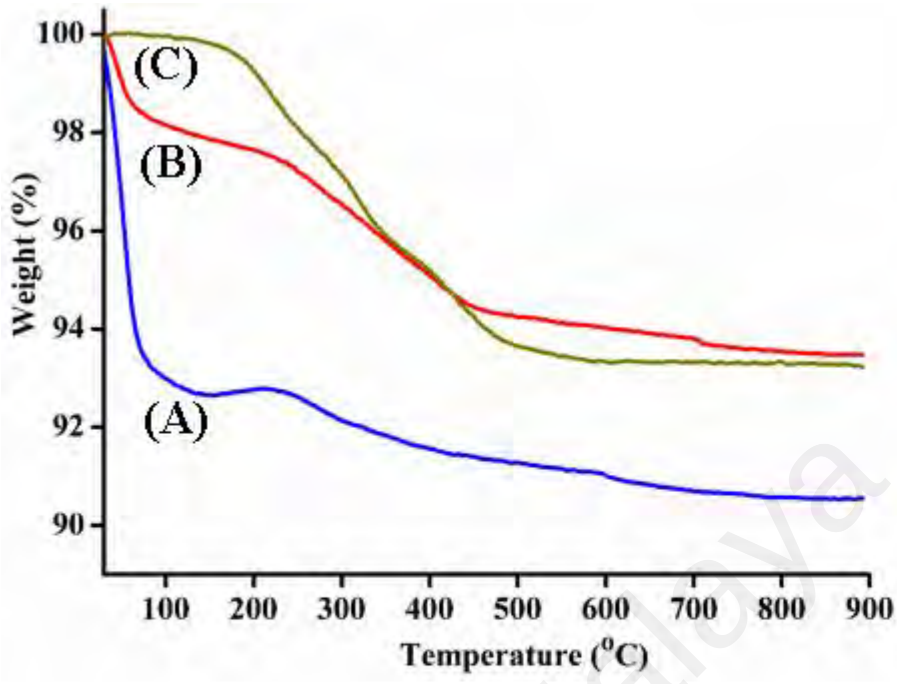

Figure 4.4: TGA thermograms of (A) MNPs (B) MNP-APTES and (C) MNP@FFAs-PCO

Table 4.2: TGA analysis of MNPs, MNP-APTES and MNP@FFAs-PCO

Sample	Region (°C)	Weight loss (%)	Assignment
MNPs	(35 – 129) (260 – 540)	6.25 2.09	Water loss/ hydroxyl group Crystal phase transformation from Fe_3O_4 to γ-Fe_2O_3
MNP-APTES	(250 – 420)	2.65	3-aminopropyl groups
MNP@FFAs-PCO	(200 – 400)	4.86	3-aminopropyl & free fatty acids moieties

The particle size and morphology of the prepared materials were studied using transmission electron microscopy (TEM) and field emission scanning electron microscopy (FESEM). It was clearly observed that all the particles are nano-sized, spherical in shape and have a uniform size distribution (Figure 4.5(A-F)). The TEM results (Figure(A-C) show that the MNPs are strongly aggregated due to dipole-dipole interaction (Jadhav *et al.*, 2013). After surface modification of MNPs with APTES, an improvement in dispersibility was observed as the APTES prevent dipole-dipole interaction between MNPs (Jadhav *et al.*, 2013). However, after being coated with free

University of Malaya

fatty acids, MNP@FFAs-PCO show fewer aggregates compared to MNP-APTES. It is possible that this result is due to the increase in particles size after the introduction of free fatty acids layer onto the surface of MNP-APTES. The diameter distribution graphs shown in Figure 4.5(G-I) shows the average diameters of MNPs, MNP-APTES and MNP@FFAs-PCO are 4.90 ± 2.34 nm, 6.90 ± 2.51 nm and 6.99 ± 2.81 nm, respectively. The increase in particle size after the functionalization process is due to the layers of APTES and free fatty acids on the surface of the MNPs.

.

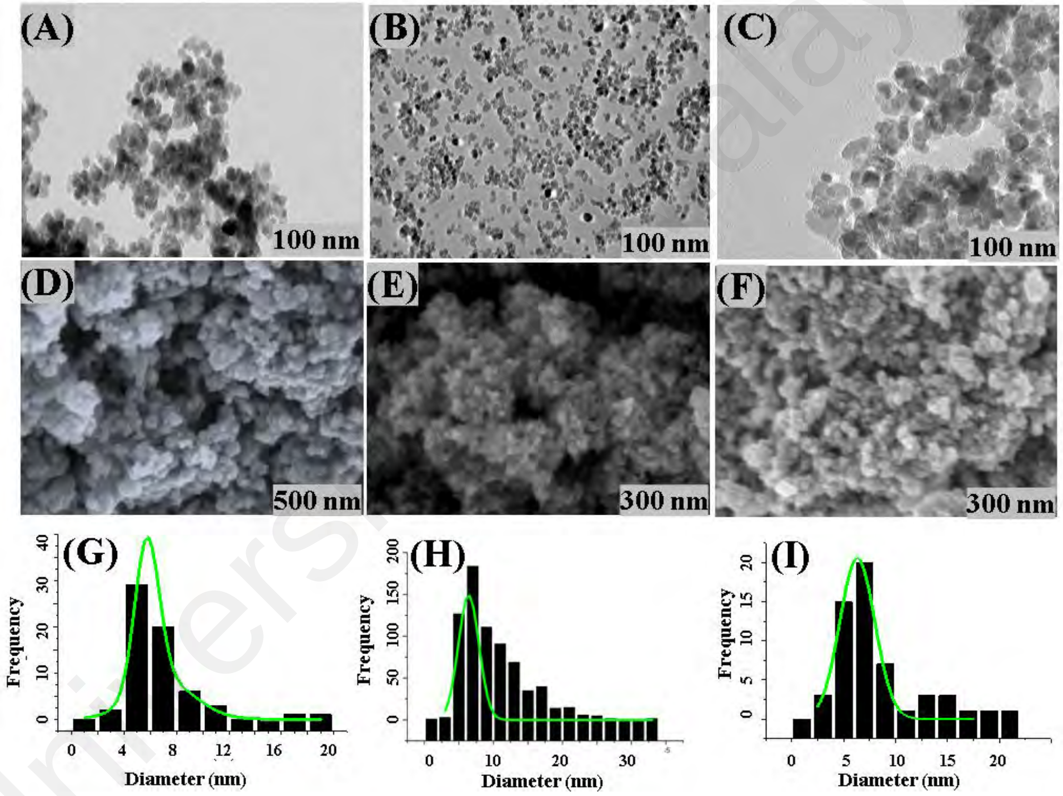

Figure 4.5: TEM images of (A) MNPs (B) MNP-APTES and (C) MNP@FFAs-PCO; FESEM images of (D) MNPs (E) MNP-APTES and (F) MNP@FFAs-PCO; and diameter distributions of (G) MNPs (H) MNP-APTES and (I) MNP@FFAs-PCO

In order to examine the porous structure of MNPs, MNP-APTES and MNP@FFAs-PCO, they were characterized using a gas sorption analyzer. Figure 4.6(A-C) shows the specific surface area of MNPs, MNP-APTES and MNP@FFAs-PCO are 123.5, 106.6 and 9.3 m^2 g^{-1}, respectively. The decrease in specific surface area may have resulted from

Universiti Malaya

the increase in particle diameter due to the encapsulation by APTES and free fatty acids during the functionalization process. The result obtained in this study agrees well with other reported works (Zhang *et al*., 2010; Wang *et al*., 2013).

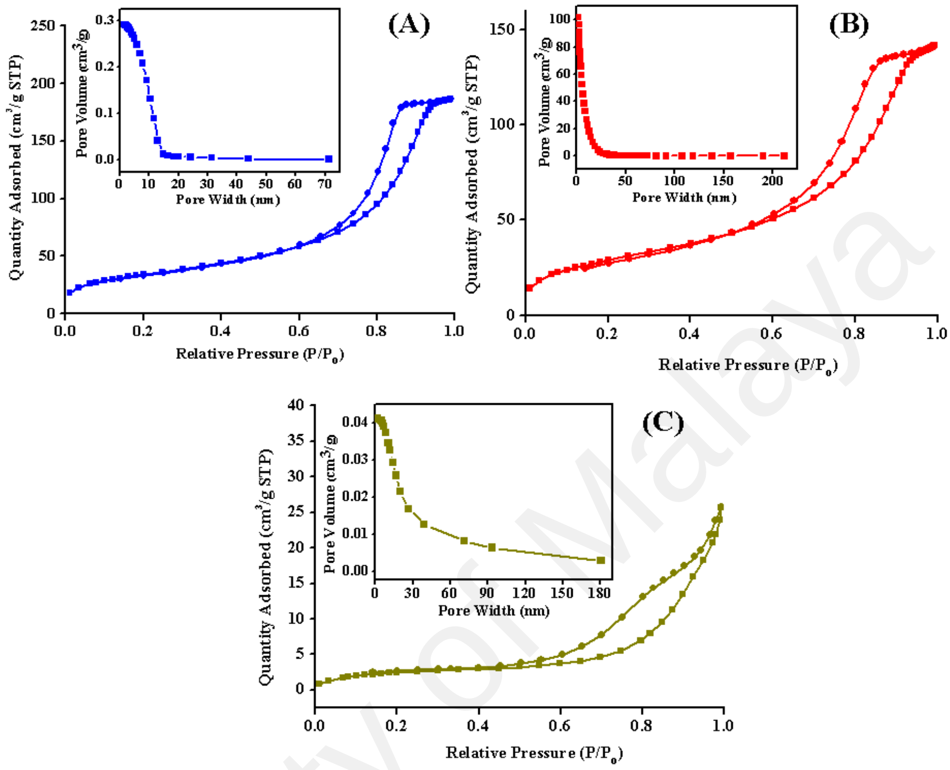

Figure 4.6: N_2 adsorption-desorption isotherms of (A) MNPs; (B) MNP-APTES and (C) MNP@FFAs-PCO

The magnetic behaviour of all fabricated materials was assessed using a vibrating sample magnetometer. This analysis is important to confirm that the prepared magnetic adsorbents are sufficiently magnetic to allow for rapid separation from the water being treated. The magnetization curves of MNPs, MNP-APTES and MNP@FFAs-PCO at room temperature are shown in Figure 4.7. All samples exhibited superparamagnetic behaviour as the remanence and coercivity are close to zero. VSM results show the saturation magnetization (Ms) for MNPs, MNP-APTES and MNP@FFAs-PCO are 63.30 emu g^{-1}, 58.23 emu g^{-1} and 56.17 emu g^{-1}, respectively. The results imply that the prepared magnetic nanoparticles can be readily dispersed in an aqueous solution and then easily collected using an external magnet (see photos inset of Figure 4.7). In addition, the

University of Malaya

magnetization values of MNP-APTES and MNP@FFAs-PCO are lower compared to that for bare MNPs due to APTES and free fatty acids layers shielding the MNPs, thereby reducing magnetic interaction.

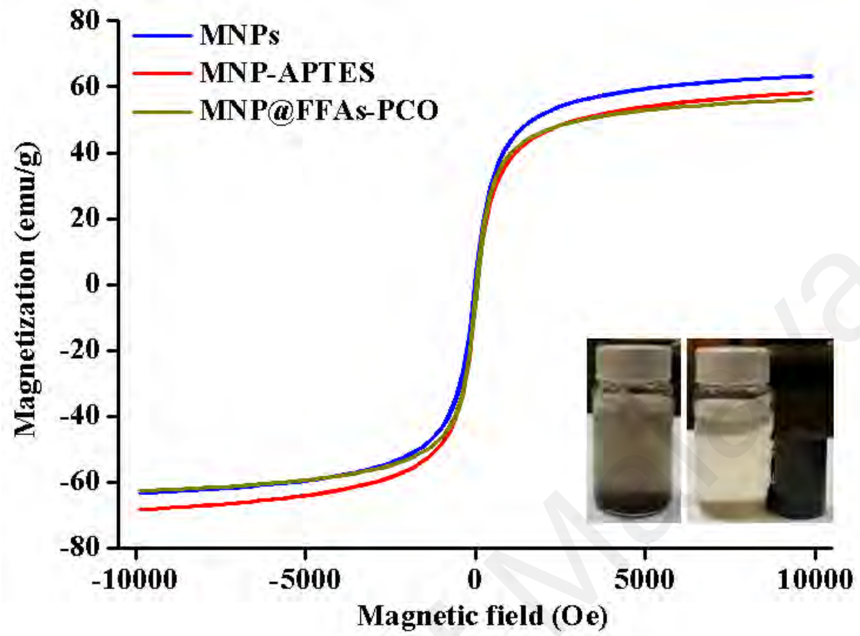

Figure 4.7: The magnetization hysteresis loops of MNPs, MNP-APTES and MNP@FFAs-PCO. The inset shows photographs of magnetic nanoparticles dispersed in solution (left) and separated from water solution under an external magnetic field (right)

In order to properly interact with hydrophobic organic pollutants, the designed adsorbents must also be hydrophobic. To confirm the hydrophobicity of the synthesized materials, water contact angle (WCA) analysis was carried out. Figure 4.8(A) shows a water droplet had spread on the surface of MNPs substrate. This means that the MNPs are highly hydrophilic. In contrast, MNP@FFAs-PCO exhibited highly hydrophobic behaviour as the water droplet deposited on MNP@FFAs-PCO surface was nearly spherical. The contact angle (CA) was measured to be 123.6° (Figure 4.8(B)). This confirmed that the hydrophobizing agent, free fatty acids are coated onto the surface of MNPs.

University of Malaya

For use in real applications, the stability of the synthesized MNP@FFAs-PCO must first be examined. It was found that, the WCA on MNP@FFAs-PCO remain higher than 120° (Figure 4.8(C)) even after 72 hours heat treatment at 70 and 90 °C and storage for 30 days at ambient temperature. This is indicative of good thermal and long term stability of synthesized MNP@FFAs-PCO. The relationship between pH and WCA of MNP@FFAs-PCO is shown in Figure 4.8(D). The WCA values always remained higher than 110° when the pH of water droplet was varied from 2.0 to 14.0. This suggests that the pH of the aqueous solution has little effect on the wettability of the MNP@FFAs-PCO surface.

University of Malaya

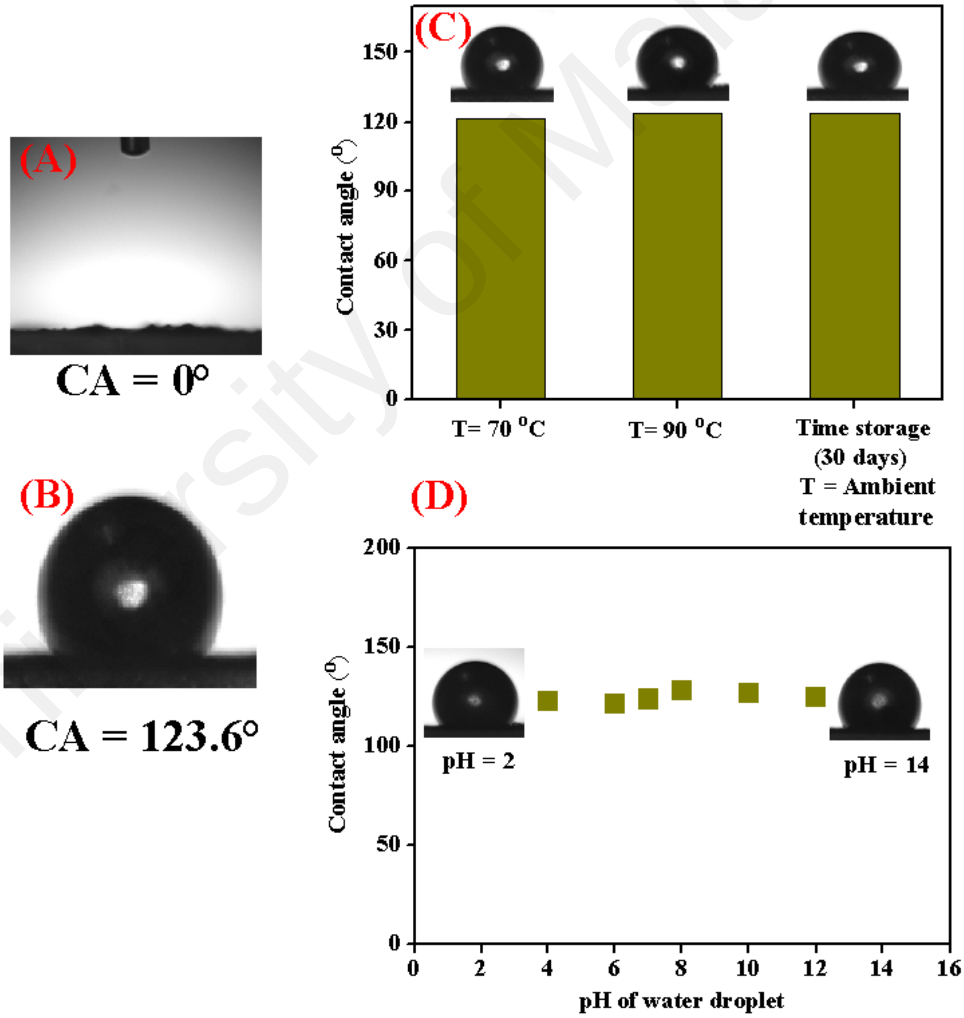

Figure 4.8: Optical image of a water droplet placed on (A) MNPs and (B) MNP@FFAs-PCO (C); the water contact angle on MNP@FFAs-PCO after corrosion/heat treatment (70 °C & 90 °C) and time storage (30 days) at ambient temperature and (D) Relationship between pH of water droplet on water CA on the MNP@FFAs-PCO surface

Buoyancy can be used to assess the hydrophobicity of the designed adsorbent. The buoyant properties of MNP@FFAs-PCO was studied by dispersing the adsorbent on the surface of the water under constant mechanical stirring. MNP@FFAs-PCO remained floating on the surface of water even when agitated (Figure 4.9(A-B)). It was also found to remain on the surface of water even after being kept overnight (Figure 4.9(C-D)). This is because of the high hydrophobicity and low density of MNP@FFAs-PCO prevent it from sinking (Zhu *et al*., 2010). The buoyant character of MNP@FFAs-PCO makes it very useful for oil adsorption from oil spills and extraction of PAHs as it facilitates collection of the spent absorbent collection avoiding secondary environment pollution.

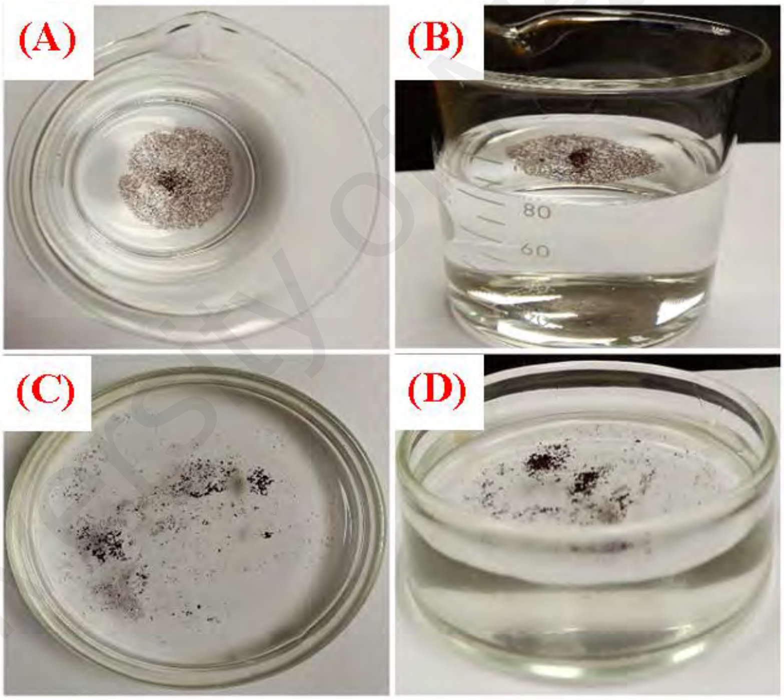

Figure 4.9: Top and side view for situation of MNP@FFAs-PCO particles (A-B) floating under mechanical stirring, and (C-D) static on water surface after one night

University of Malaya

4.2.2 Applications of the MNP@FFAs-PCO

The characterization results confirm the structure and composition of the prepared adsorbent. The synthesized adsorbent was used as the adsorbent for magnetic solid phase extraction of selected PAHs and remediation of oil from aqueous solution to study the feasibility of the designed adsorbent.

4.2.2.1 MSPE performance

The batch sorption experiment was conducted to investigate the performance of MNP@FFAs-PCO on the extraction of several PAHs. As comparison, the sorption experiment was also conducted on MNPs and MNP-APTES. Figure 4.10 shows the extraction efficiencies of bare MNPs, MNP-APTES and MNP@FFAs-PCO. It was found that MNP@FFAs-PCO is the best adsorbent for the extraction of PAHs as it has the highest extraction efficacies for all targeted PAHs. This result can be explained by considering that the long alkyl chains of the free fatty acids form a hydrophobic framework which facilitates the adsorption of PAHs through hydrophobic interaction as shown in Figure 4.11. The lower extraction capabilities when using bare MNPs and MNP-APTES mean that MNP@FFAs-PCO is the most suitable adsorbent to use in subsequent experiments.

University of Malaya

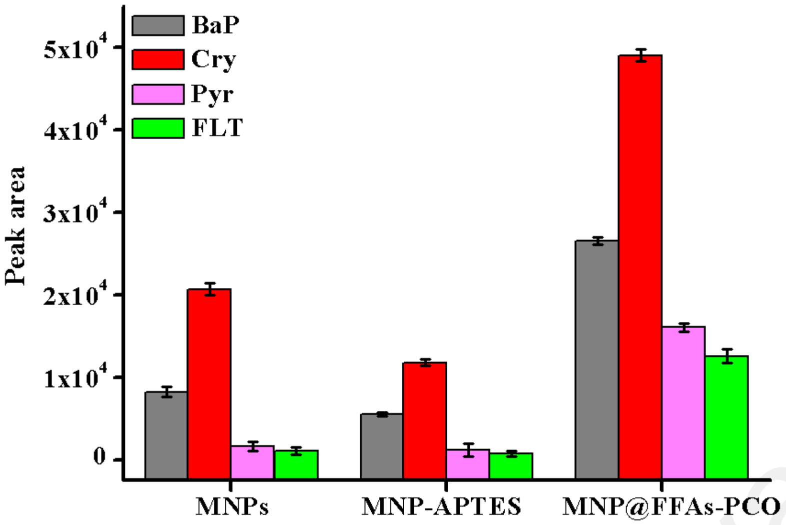

Figure 4.10: Comparison of the extraction efficiencies of PAHs between MNPs, MNP-APTES and MNP@FFAs-PCO. (Amount of the adsorbents (*i.e.*, MNPs, MNP-APTES and MNP@FFAs-PCO) = 10 mg, desorption solvent = *n*-hexane, volume of desorption solvent = 2.0 mL, extraction time = 10 min, desorption time = 5 min, sample pH = 6.5 and sample volume = 15 mL)

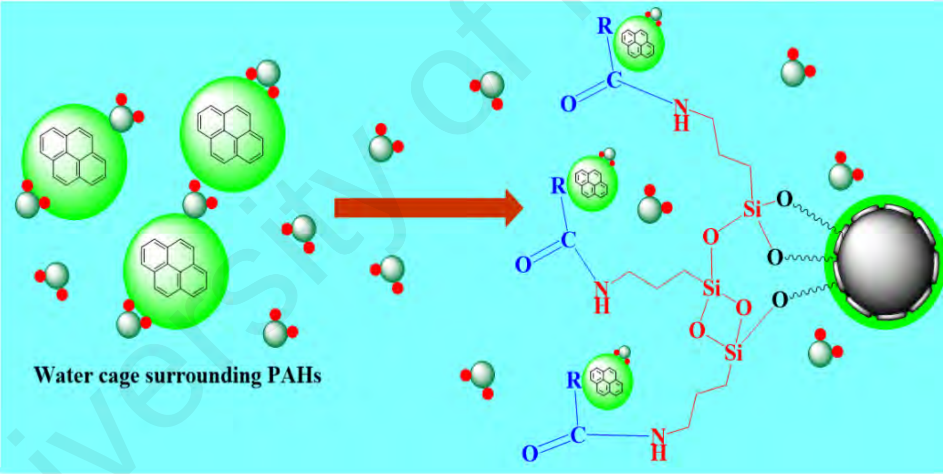

Figure 4.11: The illustration of the adsorption of targeted PAHs toward hydrophobic frameworks of MNP@FFAs-PCO during MSPE procedure (R = the alkyl chain of the free fatty acid)

The surface characteristics of the adsorbent surface and its interaction with the adsorbate are mainly controlled by several parameters such as adsorbent dosage, desorption solvent types, desorption solvent volume, extraction time, desorption time, pH, and sample volume. A batch adsorption study was carried out on MNP@FFAs-PCO to study the effect of these environmental parameters. Each experiment was performed in triplicate. The optimization experiments were conducted using spiked standard aqueous

University of Malaya

solutions containing 100 ng mL^{-1} of PAHs each. HPLC chromatography was used to evaluate the influence of these factors on the efficacy PAHs extraction. The amount of adsorbent used is crucial in any extraction procedure. Thus, various amounts of MNP@FFAs-PCO ranging from 3–25 mg sorbent were tested. As shown in Figure 4.12, the recoveries of PAHs increases when the adsorbent amount is increased from 3 mg to 15 mg. PAHs recovery plateaus after 15 mg due to the active sites on the PAHs being saturated after the 15 mg point. Hence, 15 mg of MNP@FFAs-PCO appears to be the optimal amount for MSPE of PAHs and is set as the amount to use in further experiments.

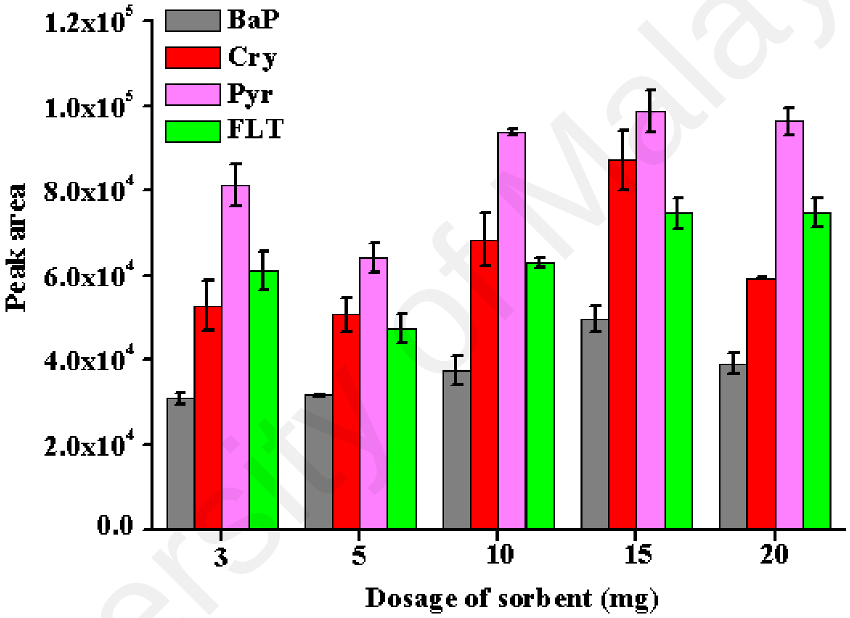

Figure 4.12: The effect amount of sorbent on the extraction efficiency of PAHs. (Desorption solvent = *n*-hexane, volume of desorption solvent = 2.0 mL, extraction time = 10 min, desorption time = 5 min, sample pH = 6.5 and sample volume = 15 mL)

University of Malaya

To recover the sorbent after extraction, the PAHs must be desorbed from the sorbents. Therefore, an ideal elution solvent should be strong enough to elute all the targeted PAHs. In this study, four different common organic solvents (acetonitrile, toluene, *n*-hexane and ethyl acetate) were investigated as eluents. The desorption capabilities of these eluents are compared in Figure 4.13(A). As shown in the figure, *n*-hexane had a higher desorption capacity compared to other eluents. This fact can be attributed to the high solubility of the target analytes in this solvent. Thus, *n*-hexane is selected as the desorption solvent. Additionally, the effect of the volume of desorption solvent on the desorption efficacy was studied from 1.0 to 3.0 mL (Figure 4.13(B)). It was found that the analytes could be completely desorbed from the sorbent by rinsing the sorbent with 2.0 mL of desorption solvent. When the volume of desorption solvent is increased from 2.5 to 3.0 mL, the peak areas decreases due to decrease enrichment factors (EFs) (Yusoff *et al.*, 2017).

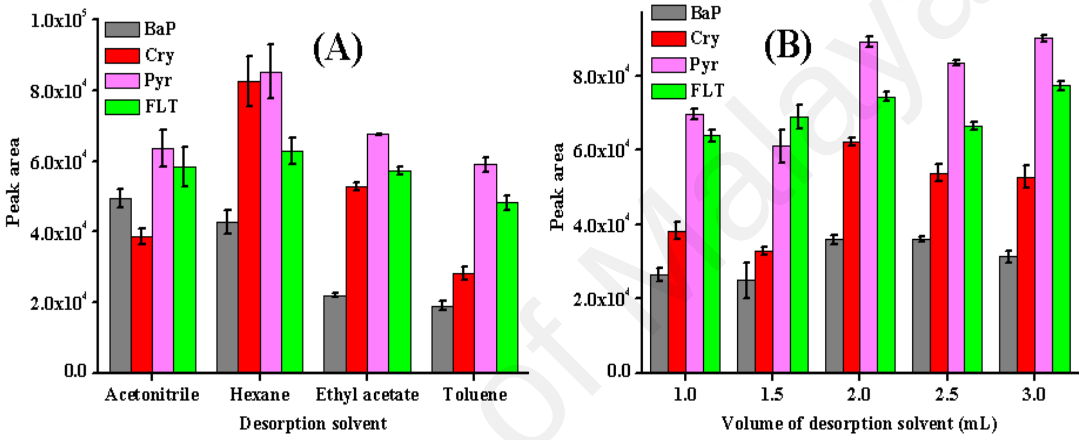

Figure 4.13: The effect of (A) desorption solvent. (Amount of MNP@FFAs-PCO = 15 mg, volume of desorption solvent = 2.0 mL, extraction time = 10 min, desorption time = 5 min, sample pH = 6.5 and sample volume = 15 mL) and (B) volume of desorption solvent (Amount of MNP@FFAs-PCO = 15 mg, desorption solvent = *n*-hexane, extraction time = 10 min, desorption time = 5 min, sample pH = 6.5 and sample volume = 15 mL) on the extraction efficiency of PAHs.

A sufficient contact time is needed to attain maximum PAHs. Thus, the extraction time profiles are studied by varying the extraction time between 5 and 25 min. As shown in Figure 4.14(A), the extraction recoveries of all PAHs increased with extraction time up to 15 min, then plateaus after. This phenomenon is due to the fact that a large number of vacant surface sites are available for adsorption during the initial stage (Sokker *et al.*, 2011), but they became saturated after 15 min. Similarly, the desorption time profiles were studied by varying the desorption time from 1 to 20 min. As shown in Figure 4.14(B), a desorption time of 10 min is sufficient to completely desorb PAHs from the

University of Malaya

sorbent. Hence, 15 min and 10 min are respectively selected as the best extraction and desorption times.

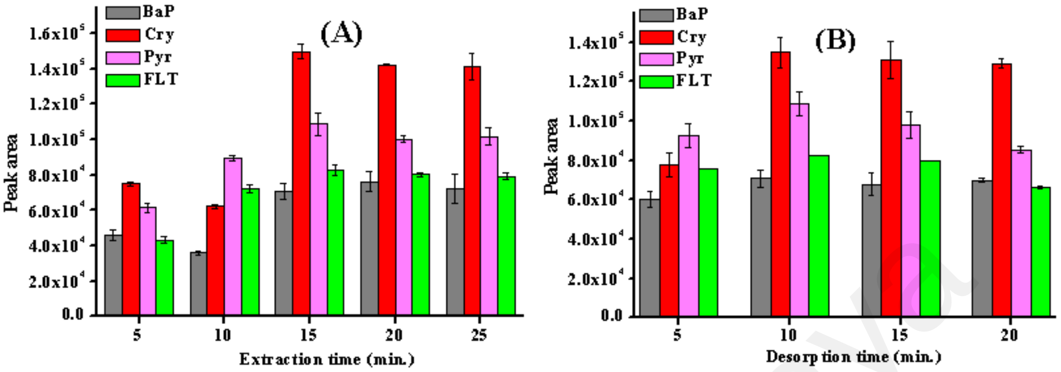

Figure 4.14: The effect of (A) extraction time (Amount of MNP@FFAs-PCO = 15 mg, desorption solvent = *n*-hexane, volume of desorption solvent = 2.0 mL, desorption time = 5 min, sample pH = 6.5 and sample volume = 15 mL) and (B) desorption time (Amount of MNP@FFAs-PCO = 15 mg, desorption solvent = *n*-hexane, volume of desorption solvent = 2.0 mL, extraction time = 15 min, sample pH = 6.5 and sample volume = 15 mL) on the extraction efficiency of PAHs

One of the chief features in extraction studies, as stated by various researchers, is the effect of pH on adsorption/desorption efficiency. pH plays an important role on the adsorption efficacy of the adsorbent seemingly owing to its impact on the surface charge of the adsorbent material, the degree of ionization of the target analytes and the ionization/dissociation of the of functional groups of the adsorbate molecules (Shahabuddin *et al.*, 2016). In this experiment, the effect of sample solution pH was studied in the range of 2.0 to 10.0. The sample solution pH was adjusted using volumes of 0.1 M HCl or NaOH. In Figure 4.15, it is observed that high recoveries of all selected PAHs are obtained at pH 6.5. Low recoveries are observed when the pH is higher or lower. This phenomenon can be explained by considering the charged species and charge density on the surface of the sorbent (MNP@FFAs-PCO). Under acidic conditions, large amounts of protons are available, therefore increasing the protonation of the hydroxyl groups on the MNPs surface. The sorbent sites get saturated and the sorbent becomes

University of Malaya

more cationic. Under basic conditions, the hydroxyl groups from MNPs deprotonates, causing the surface of the adsorbent to become more anionic. This reduces the hydrophobicity of MNP@FFAs-PCO, therefore affecting interaction with PAHs. In contrast, in term of adsorbate, PAHs exist as neutral molecules under ordinary conditions, and their formation was maintained invariably when pH of its environment is changed (Han *et al*., 2012). Thus, pH 6.5, the natural pH of the sample is selected as the best pH to use.

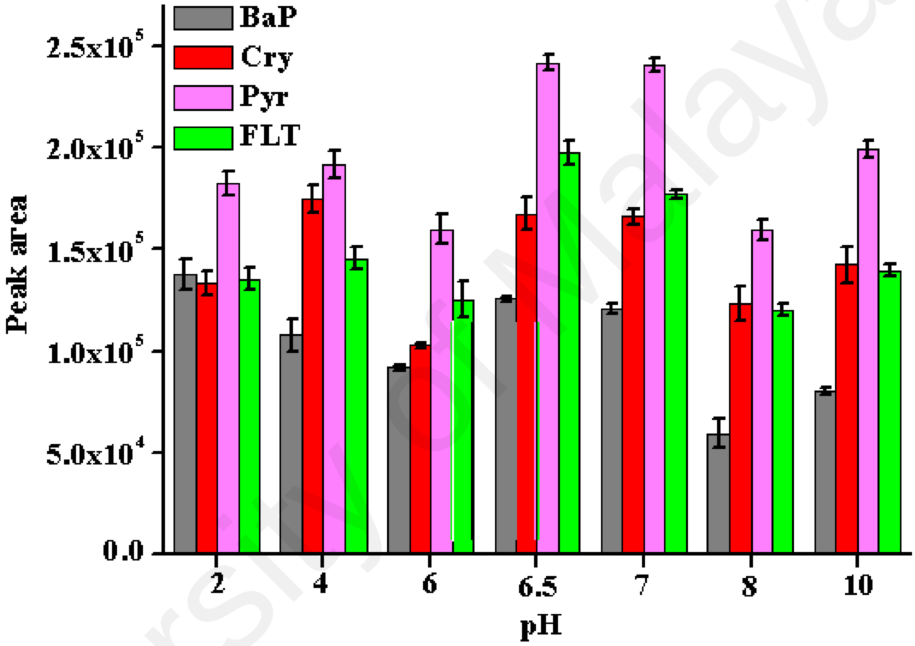

Figure 4.15: The effect of pH of the sample on the extraction efficiency of PAHs. (Amount of MNP@FFAs-PCO = 15 mg, desorption solvent = *n*-hexane, volume of desorption solvent = 2.0 mL, extraction time = 15 min, desorption time = 10 min and sample volume = 15 mL)

In real samples, the concentrations of target analytes are usually much lower than the detection limit of analytical instruments. It becomes necessary to preconcentrate the target analytes from large volume of water samples to get high preconcentration factor. The effect of the sample volume was examined by varying the sample solution volume between 15 mL to 100 mL. As shown in Figure 4.16, the extraction efficiency increased

University of Malaya

when the sample volume increases with sample volume up to 30 mL and then plateaus above 30 mL. Hence, 30 mL of sample volume is selected as the best volume to use.

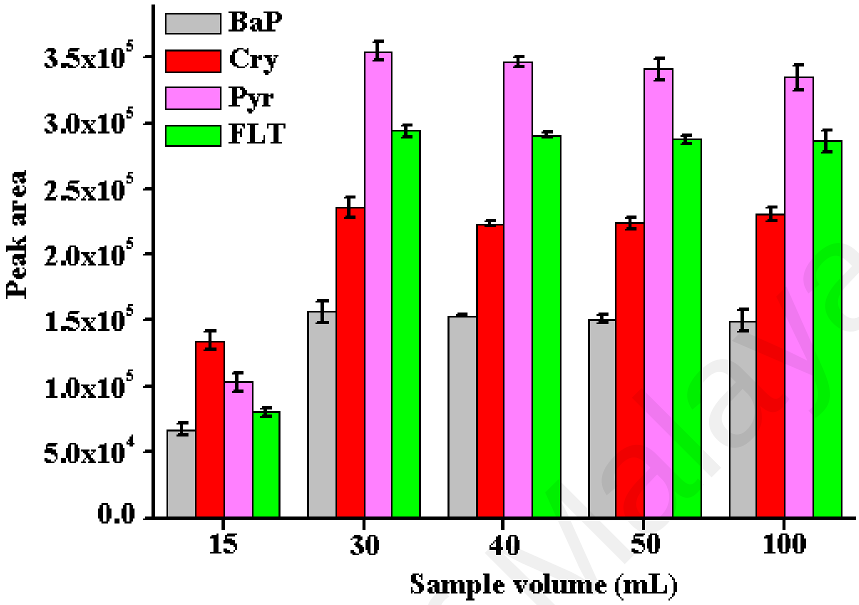

Figure 4.16: The effect of sample volume on the extraction efficiency of PAHs. (Amount of MNP@FFAs-PCO = 15 mg, desorption solvent = *n*-hexane, volume of desorption solvent = 2.0 mL, extraction time = 15 min, desorption time = 10 min and sample pH = 6.5)

The reusability of MNP@FFAs-PCO was investigated by measuring its adsorption efficacy for five cycles. The recoveries of PAHs are shown in Figure 4.17. The sorbent can be reused at least five times without significant loss in the recoveries of all analytes. MNP@FFAs-PCO demonstrates good reusability and stability in the MSPE procedure.

University of Malaya

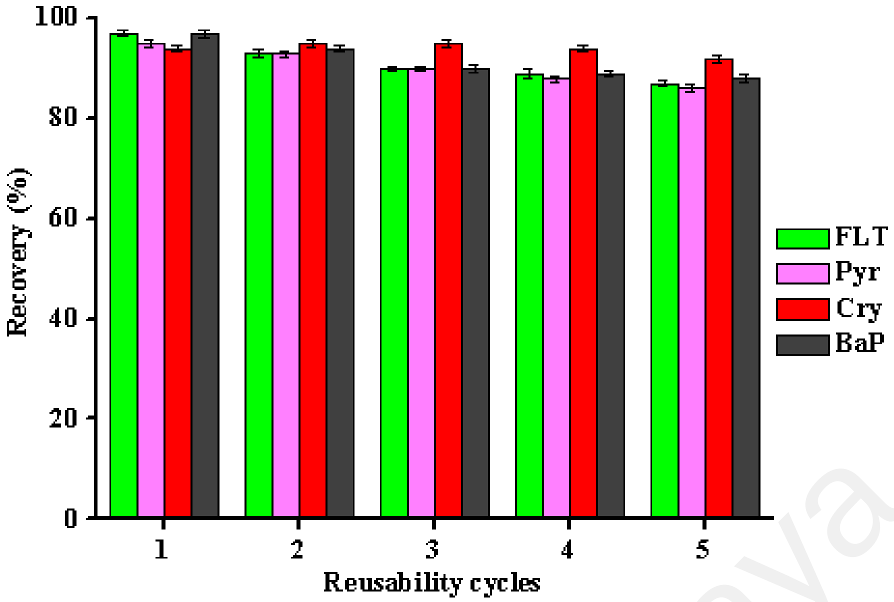

Figure 4.17: Reusability cycles of MNP@FFAs-PCO for extraction of PAHs

Based on the above discussion, the optimal extraction conditions for the extraction of studied PAHs are 10 mg of MNP@FFAs-PCO, 2.0 mL of *n*-hexane as desorption solvent, 15 min as the extraction time, 10 min as desorption time, pH 6.5 for the sample solution and 30 mL of sample volume. A series of experiments with regard to the linearity, limit of detection (LOD), limit of quantification (LOQ) and precision were carried out to validate the proposed MSPE method performance. The results are tabulated in Table 4.3. The calibration curves are linear over a wide range of 0.1-100 ng mL^{-1} with a coefficient of determination correlation of 0.9998. Based on the results obtained, the LOD and LOQ values of the targeted PAHs ranged from 0.01 to 0.05 ng mL^{-1} and 0.03 to 0.16 ng mL^{-1}, respectively. Intra- and inter-day relative standard deviations (RSDs) were assessed to evaluate the precision of the developed method. Satisfactory results were achieved with the intra-day RSD% being between 3.9% and 5.8% and inter-day RSD% being between 1.1 to 3.1%. This demonstrates the good reproducibility of the current method.

University of Malaya

Table 4.3: Analytical performance for HPLC-DAD determination of PAHs using MNP@FFAs-PCO

Analyte	Linearity	R^2	LOD	LOQ	Precision	
	LDR(ng mL^{-1})		(ng mL^{-1})	(ng mL^{-1})	Intra-day (RSD% *n* = 7)	Inter-day (RSD% *n* = 3)
FLT	0.1-100	0.9998	0.05	0.16	5.8	2.3
Pyr	0.1-100	0.9998	0.03	0.08	3.8	3.1
Cry	0.1-100	0.9998	0.02	0.07	4.2	1.6
BaP	0.1-100	0.9998	0.01	0.03	3.9	1.1

Next, we assessed the applicability of the developed method in real samples by using environmental samples including leachate and sludge collected from Jeram Landfill, Kuala Selangor. No PAHs were detected in these real samples. In this study, the recoveries of the PAHs from landfill leachate and sludge were measured at spiking levels of 100, 10 and 5 ng mL^{-1}. The results obtained are shown in Table 4.4. The PAHs recoveries from spiked leachate samples ranged from 98.5% to 113.8% with the RSDs (*n* = 5) ranging from 3.5% to 12.2% and PAHs recoveries from spiked sludge samples ranged from 81.1% to 119.3% with the RSDs (*n* = 5) ranging from 3.1% to 13.6%. The results demonstrate the potential of MNP@FFAs-PCO in the application of environmental sample analysis. Figure 4.18 shows a typical HPLC-DAD chromatograms of the PAHs samples extracted from leachate samples using the developed method before and after spiking with 100 ng mL^{-1} of each PAHs.

The proposed method was successfully applied for the determination of PAHs in the landfill leachate and sludge samples. The simple and low-cost method provides an alternative method for analysis of non-polar compounds in complex environmental samples.

University of Malaya

Table 4.4: The recoveries and standard deviations of PAHs in real environmental samples with a spiked concentration of 5 ng mL^{-1}, 10 ng mL^{-1} and 100 ng mL^{-1} for each analyte

Analyte	Spiked (ng mL^{-1})	Leachate (n = 5)		Sludge (n = 5)	
		Recovery (%)	RSD (%)	Recovery (%)	RSD (%)
FLT	5	103.5	9.7	103.0	8.4
	10	109.1	9.6	89.2	3.1
	100	98.5	5.8	99.4	13.6
Pyr	5	105.2	7.7	107.0	6.0
	10	109.1	11.9	81.1	8.7
	100	100.3	3.5	109.1	8.7
Cry	5	98.9	8.6	84.6	9.5
	10	108.9	12.2	108.1	10.1
	100	113.8	9.4	119.3	3.5
BaP	5	113.6	8.8	92.6	6.5
	10	107.5	8.6	103.5	11.1
	100	110.6	5.2	107.7	8.2

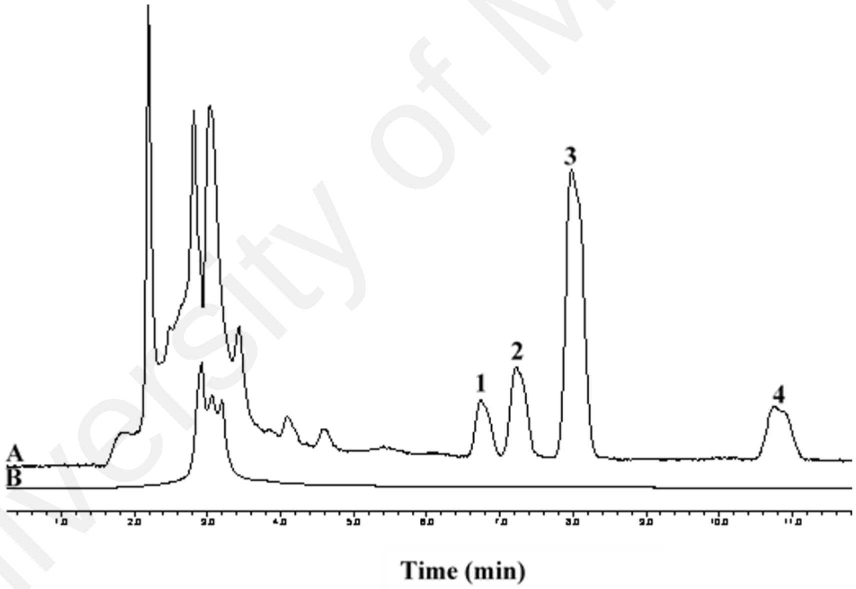

Figure 4.18: HPLC-DAD chromatograms of the PAHs after extraction using proposed MSPE: Non-spiked (A); and 100 ng mL^{-1}of each PAHs spiked leachate sample (B) (1) FLT, (2) Pyr, (3) Cry, and (4) BaP

University of Malaya

4.2.2.2 Oil removal efficiency

A preliminary batch adsorption experiment was conducted to determine the suitability of the as-prepared adsorbents for the removal of oil from aqueous solution. The oil adsorption capacity of bare MNPs, MNP-APTES and MNP@FFAs-PCO are compared in Figure 4.19. Evidently, the oil adsorption capacity of MNP@FFAs-PCO is higher compared to MNPs and MNP-APTES. This is consistent with our findings that MNP@FFAs-PCO can interact with selected PAHs through hydrophobic interaction. This result justifies the use of MNP@FFAs-PCO as an effective adsorbent for subsequent experiment.

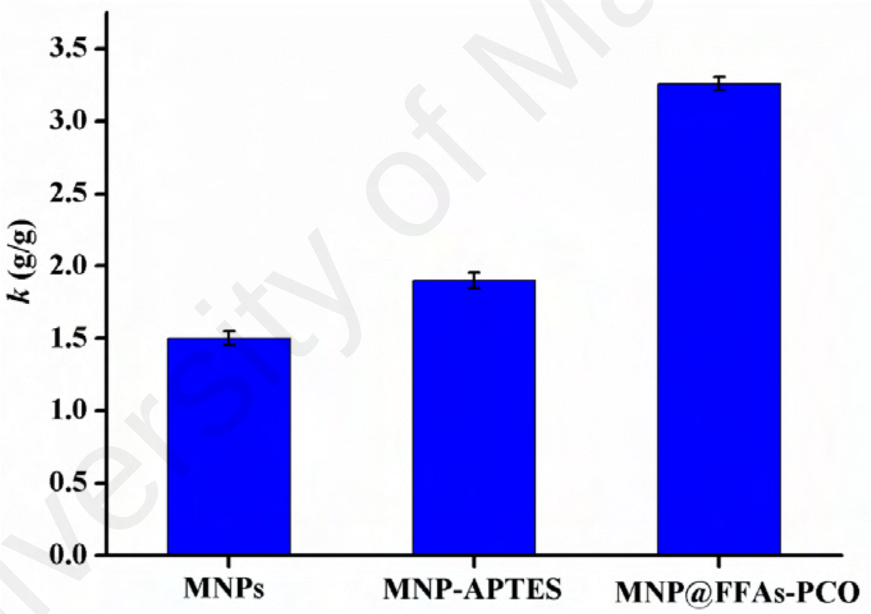

Figure 4.19: Comparison of the adsorption capacity of MNPs, MNP-APTES and MNP@FFAs-PCO. (Amount of the adsorbents (*i.e.*, MNPs, MNP-APTES and MNP@FFAs-PCO) = 15 mg, contact time = 60 min and pH of the aqueous solution = 7)

University of Malaya

In this study, the amount of oil adsorbed on the synthesized magnetic adsorbent was found to depend mainly on the weight of adsorbent, pH of the solution and contact time. These factors were studied and optimized in this order. The oil adsorbent capacity, k is used to evaluate the influence of these factors on the oil removal efficacy. All experiments were carried out in triplicate.

The amount of adsorbent used determines the adsorption capacity of an adsorbent for a given initial concentration of the adsorbate. The effect of adsorbent dosage on sorption efficacy of lubricating oil was examined by taking different quantities of MNP@FFAs-PCO adsorbent ranging from 2 to 20 mg. As evident from Figure 4.20, the adsorption efficacy of the oil increases with increase in amount of adsorbent from 2 mg to 10 mg. Any further increase in dosage of MNP@FFAs-PCO does not change the adsorption efficacy due to the saturation of the sites for oil adsorption. It was found that 10 mg MNP@FFAs-PCO is the best dosage to use as it has the highest adsorption efficacy for lubricating oil. This dosing amount is used in subsequent experiments.

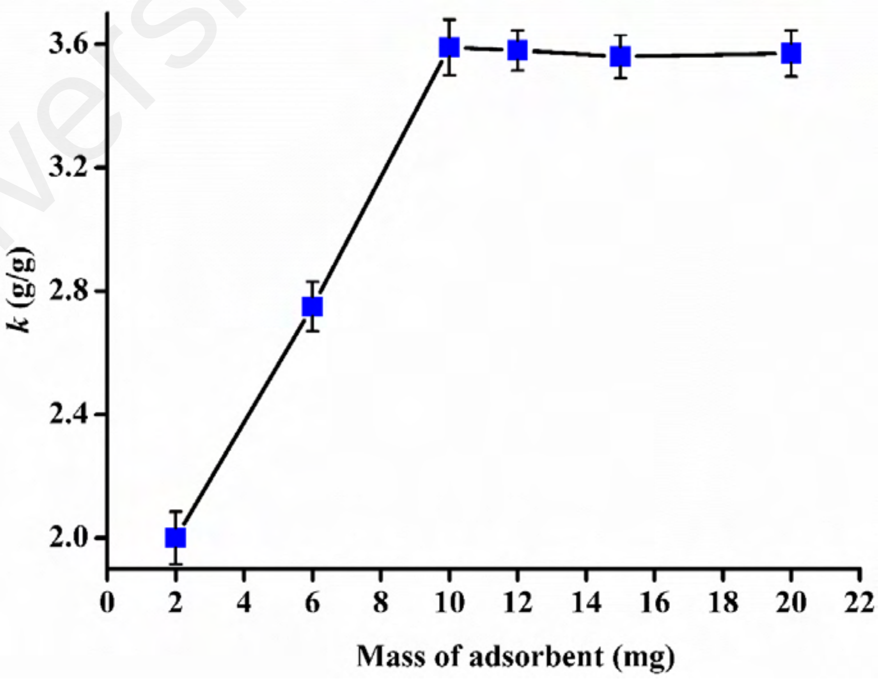

Figure 4.20: The effect of adsorbent dosage on the adsorption capacity of oil. (Contact time = 60 min and pH of the aqueous solution = 7)

University of Malaya

The optimum contact time is the minimum amount of time the adsorbent must be in contact with the adsorbate to attain the maximum oil adsorption. A specified dose of MNP@FFAs-PCO was allowed to contact lubricating oil for a time period ranging from 10 to 60 min (Figure 4.21). At the end of the time period, the adsorption of the oil was measured. It was found that the adsorption for the oil increased with contact time up to 30 min and then did not change after that. At lower contact times, the adsorption of the oil is low simply because the contact time provided for oil adsorption is insufficient (Ahmad *et al*., 2005). As the contact time is increased, the oil tends to break into smaller droplets as it contacts the long alkyl chain of the MNP@FFAs-PCO increasing the interfacial area for oil adsorption to happen (Ahmad *et al*., 2005). Additionally, oil adsorption efficacy did not change after 30 min as the adsorption sites were saturated with oil (Bhattacharyya & Gupta, 2006). Hence, 30 min contact time is selected as the optimum time for further studies.

University of Malaya

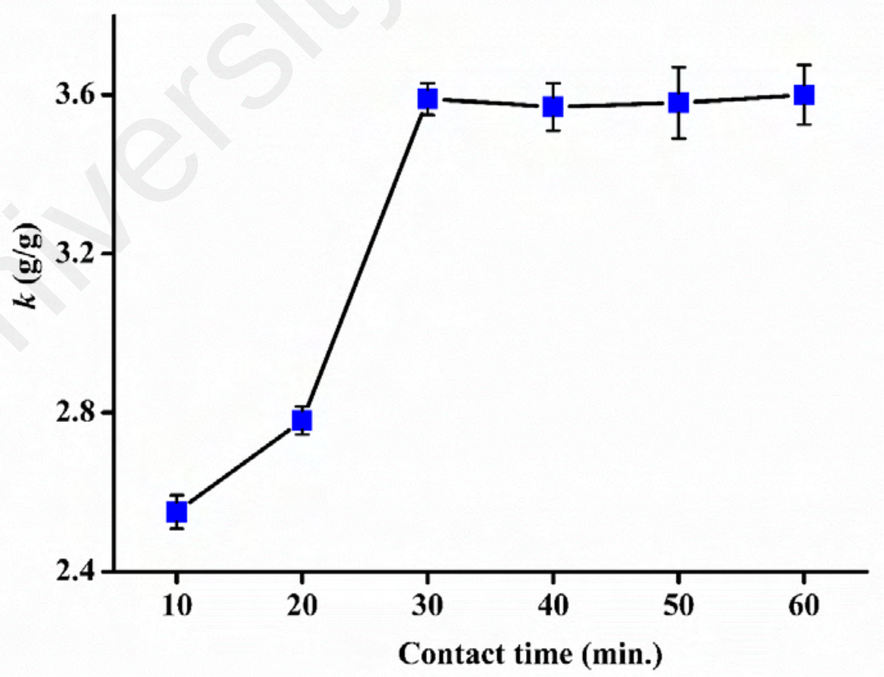

Figure 4.21: The effect of contact time on the adsorption capacity of oil. (Amount of MNP@FFAs-PCO = 10 mg, and pH of the aqueous solution = 7)

The pH of the solution is an important factor to consider in the adsorption process as it affects the binding sites of the adsorbents (Farah *et al*., 2007; Ngah & Hanafiah, 2008) and the stability of the oil emulsion (Srinivasan & Viraraghavan, 2010). In this study, the solution's pH was varied between 3 and 8 to see its effects on oil adsorption. From Figure 4.22, the best oil adsorption efficacy is recorded at pH 7. A lower oil adsorption efficacy is observed when the pH is lower or higher than 7. This phenomenon can be explained by the alteration of the amount of protons available in the solution and the stability of the oil emulsion. Under acidic conditions, the abundant protons available protonates remaining hydroxyl groups on the surface of MNPs, causing the MNP@FFAs-PCO to become more cationic (Ngah & Hanafiah, 2008). This greatly enhances the hydrophilicity of the adsorbent. Moreover, the acidity of the media destabilizes the oil emulsion to coalesce into flocs (Ahmad *et al*., 2005), which reduces the interfacial area for oil adsorption. In alkaline solutions, the hydroxyl groups on the MNPs deprotonates to cause the surface of the adsorbent to be more anionic, therefore reducing the hydrophobic property of MNP@FFAs-PCO. Thus, the neutral pH 7 is chosen as the optimum pH to use.

University of Malaya

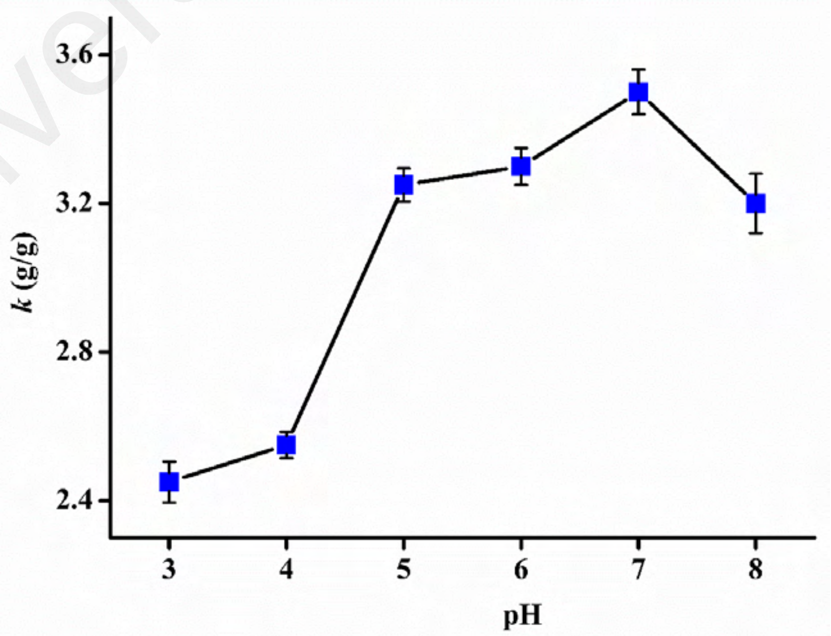

Figure 4.22: The effect of pH on the adsorption capacity of oil. (Amount of MNP@FFAs-PCO = 10 mg and contact time = 30 min)

An advantage our adsorbent possess is reusability, which may significantly reduce material waste and operation cost. Figure 4.23 shows the reusability of MNP@FFAs-PCO as an adsorbent for lubricating oil sorption. It is evident from the result that the regenerated MNP@FFAs-PCO can be reused at least 6 times and still maintain its ability to adsorb oil 2.3 times its own weight.

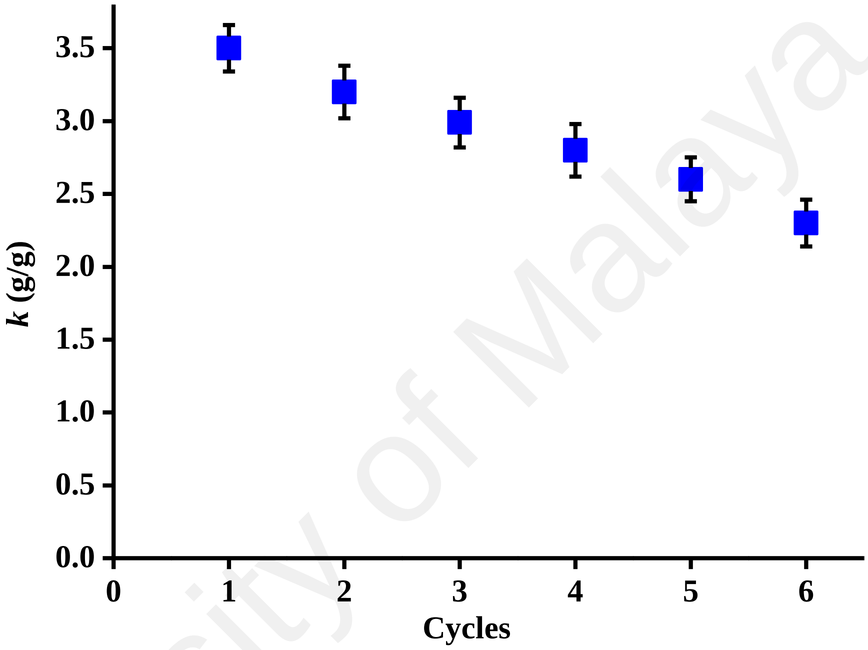

Figure 4.23: Oil-adsorption capacity of MNP@FFAs-PCO after different oil-adsorption cycles

The oil loaded MNP@FFAs-PCO and unloaded MNP@FFAs-PCO were then analyzed through EDX and compared to prove oil adsorption had taken place. The EDX spectra in Figure 4.24(A-B) show that the mass content of C in the oil loaded MNP@FFAs-PCO (42.73%) is much higher than the content of C in unloaded MNP@FFAs-PO (9.7%). FT-IR analysis (Figure 4.24(C)) showed that the alkane bands at wavelength 2853.91 and 2923.27 cm^{-1} are more intense for the oil loaded MNP@FFAs-PCO. These results suggest the adsorption of oil onto the hydrophobic alkyl chain layer at the MNP@FFAs-PCO surface. In addition, the TGA thermogram for the oil loaded MNP@FFAs-PCO shown in Figure 4.24(D) indicates that there is no weight loss

University of Malaya

associated with water loss at 100 °C. This implies that the oil loaded MNP@FFAs-PCO only adsorbed oil and not water. Thus, it is reinforced that MNP@FFAs-PCO is a highly hydrophobic adsorbent which selectively adsorb oil while completely repelling water and this is in agreement with the results of the water contact angle test.

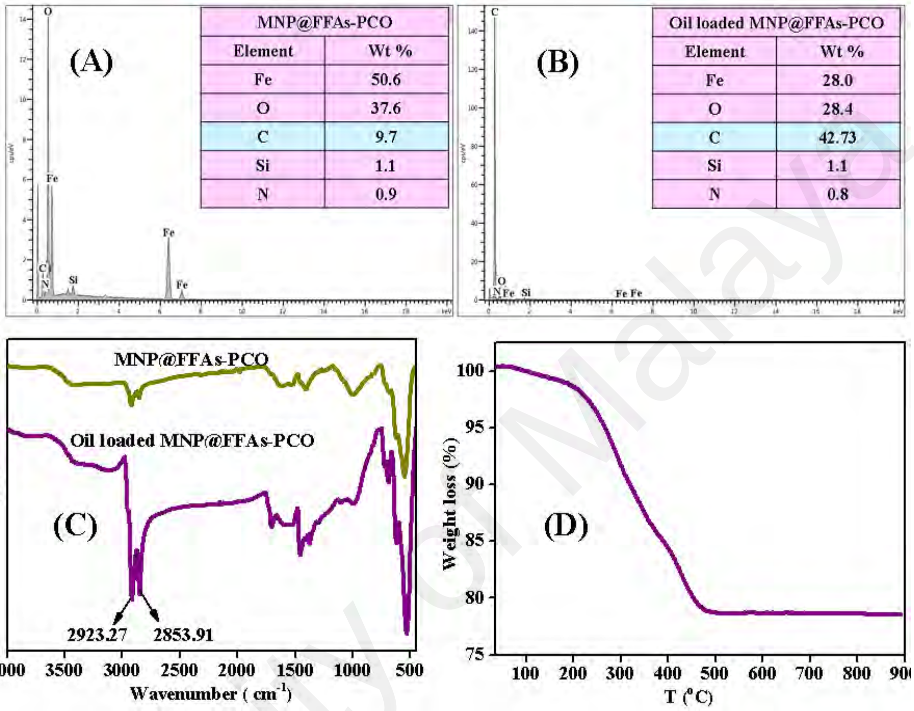

MNP@FFAs-PCO

Element	Wt %
Fe	50.6
O	37.6
C	9.7
Si	1.1
N	0.9

Oil loaded MNP@FFAs-PCO

Element	Wt %
Fe	28.0
O	28.4
C	42.73
Si	1.1
N	0.8

Figure 4.24: EDX spectra of (A) MNP@FFAs-PCO and (B) oil loaded MNP@FFAs-PCO; (C) FT-IR spectra of MNP@FFAs-PCO and oil loaded MNP@FFAs-PCO and (D) TGA thermogram of oil loaded MNP@FFAs-PCO

The chemical stability, environmental durability and highly hydrophobic nature of MNP@FFAs-PCO suggest that it could be developed for the use in oily wastewater treatment. Thus, the application of MNP@FFAs-PCO in the removal of a wide range of oils from water was studied. Figure 4.25 shows the adsorption capacity of MNP@FFAs-PCO for selected oils at ambient temperature. The MNP@FFAs-PCO oil adsorption capacity for lubricating oil, corn oil and palm oil was found to be 3.50, 2.66 and 2.80 g/g, respectively. The higher oil adsorption capacity for lubricating oil is due to its higher viscosity (Chu & Pan, 2012). The physical properties of studied oil based on viscosity

University of Malaya

and density is shown in Table 4.5. The adherence of oils on the surface of MNP@FFAs-PCO is better for more viscous oils and therefore oil uptake capacity is enhanced.

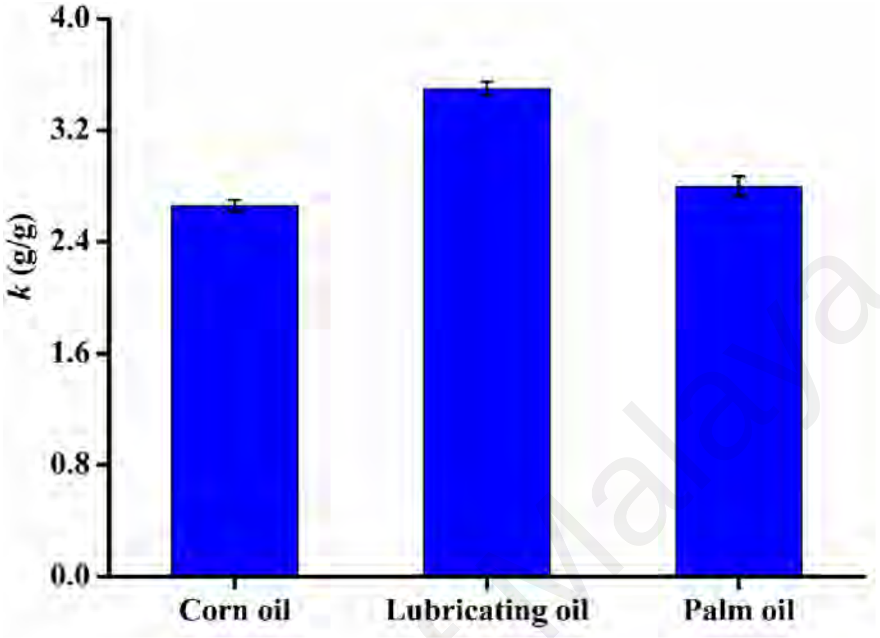

Figure 4.25: Adsorption capacity of the MNP@FFAs-PCO for the adsorption of selected oil. (Amount of MNP@FFAs-PCO = 10 mg, contact time = 30 min and pH of the aqueous solution = 7)

Table 4.5: The physical properties of experimental oils

Types of oil	Density at 25 °C (g/cm^3)	Viscosity at 25 °C (cP)
Lubricating oil	0.8896	135.22
Corn oil	0.9119	52.30
Palm oil	0.9188	77.19

From performance MSPE of PAHs and oil removal analysis, it was revealed that MNP@FFAs-PCO showed good adsorptions towards these hydrophobic organic compounds. Inspired from the performance of MNP@FFAs-PCO based free fatty acids obtained from hydrolysis TAG of palm cooking oil as an adsorbent, there is an idea worth exploring is the direct utilization of free fatty acids from waste palm cooking oil as the

University of Malaya

precursor material to develop new hydrophobic adsorbent namely MNP@FFAs-WPCO. This newly MNP@FFAs-WPCO is applied as adsorbent for enrichment of PAHs and oil removal to determine the feasibility of this adsorbent. The characterization and applications of MNP@FFAs-WPCO is discussed in the next section. A comparison study in terms of properties and adsorption performances between MNP@FFAs-WPCO and MNP@FFAs-PCO is also presented.

4.3 Free fatty acids from waste palm cooking oil functionalized magnetic nanoparticles (MNP@FFAs-WPCO) and its applications

4.3.1 Physicochemical properties of MNP@FFAs-WPCO

A comparison between fatty acids compositions after hydrolysis TAG of palm cooking oil (PCO) and that already present in waste palm cooking oil is shown in Table 4.6. The major of free fatty acids, mainly palmitic (59.64%) and oleic (28.55%) acids, while waste palm cooking oil (WPCO) consists mainly of 41.73% oleic acid and 40.56% of palmitic acid. This finding is in agreement with work by Taufiqurrahmi *et al*. (2011) who found that the WPCO in his study contained mainly 28% oleic acid and 21.47% palmitic acid. Knothe & Steidley (2009) also reported an increase in oleic acid concentration in palm cooking oil after it had been used for frying. Due to abundance of long chain free fatty acids present in WPCO, it was expected the newly fabricated adsorbent based free fatty acids from WPCO will exhibits highly hydrophobic.

University of Malaya

Table 4.6: Fatty acids compositions obtained from hydrolysis of triacylglycerol palm cooking oil and waste palm cooking oil

Fatty acid		Fatty acid composition (%) of palm cooking oil	Fatty acid composition (%) of waste palm cooking oil
Lauric	(C12:0)	0.40	-
Myristic	(C14:0)	1.35	-
Palmitic	(C16:0)	59.64	40.56
Palmitoleic	(C16:1)	1.15	-
Stearic	(C18:0)	6.09	5.46
Oleic	(C18:1)	28.55	41.76
Linoleic	(C18:2)	-	12.26
Arachidic	(C20:0)	0.78	-
Eicosenic	(C20:1)	2.03	-

University of Malaya

The structure and composition of the designed MNP@FFAs-WPCO were analyzed using various instruments to confirm its successful synthesis. FT-IR spectrometry was carried out to confirm the presence of characteristic functional groups in the prepared MNP@FFAs-WPCO and the result is shown in Figure 4.26. The presence of free fatty acids on MNP@FFAs-WPCO is verified by the presence of new characteristic absorptions peaks being the C=O group at ~1712 cm^{-1} and NHCO group at ~1405 cm^{-1}. The appearance of new peaks at ~2925 and ~2860 cm^{-1} can be related to the asymmetric and symmetric methylene and methyl vibrations, respectively. This result is similar to the FT-IR result obtained for MNP@FFAs-PCO in Section 4.2.1.

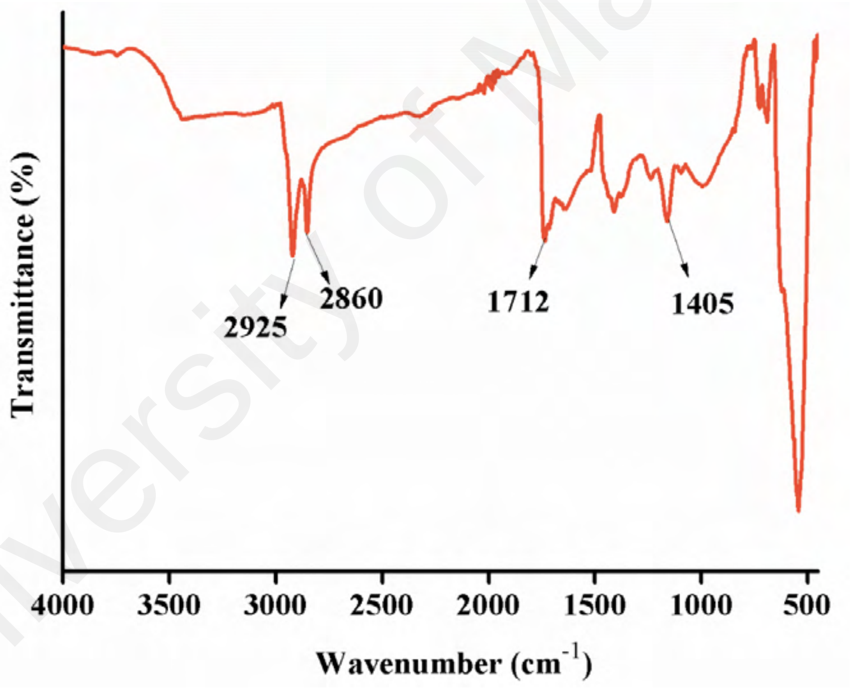

Figure 4.26: FT-IR spectrum of MNP@FFAs-WPCO

The crystallinity of MNP@FFAs-WPCO was analyzed by XRD. As seen in Figure 4.27, MNP@FFAs-WPCO showed approximately identical characteristic diffraction peaks at 2θ value of 30.42°, 35.59°, 43.42°, 53.63°, 57.35° and 63.02° which can be assigned to (220), (311), (400), (422), (511) and (440). This reveals that the surface

University of Malaya

modification of MNPs does not alter its phase. The XRD result is similar to that for MNP@FFAs-PCO discussed in Section 4.2.1.

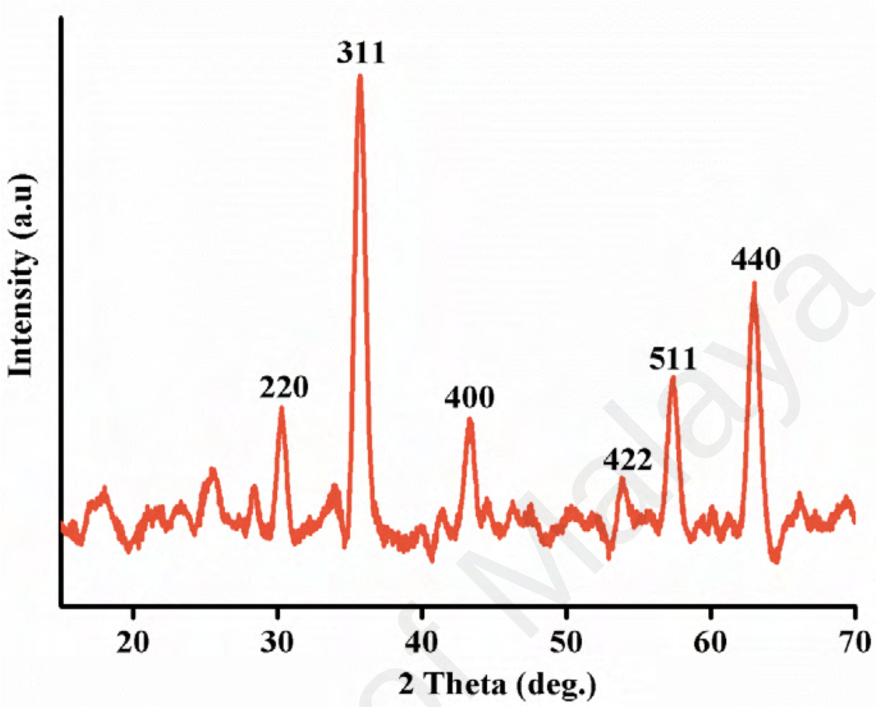

Figure 4.27: XRD pattern of MNP@FFAs-WPCO

Elemental analysis was performed to confirm the presence of elements such as Fe, Si, N, O and C in the prepared adsorbents (Figure 4.28(A-B)). The result reveals that MNP@FFAs-WPCO contains 39.0% Fe, 1.2% Si, 0.8% N, 26.3% C and 33.0% O, where the increased percentage of C and O is due to the presence of free fatty acids on the surface of MNP@FFAs-WPCO. This result is again similar to the EDX result obtained for MNP@FFAs-PCO described in Section 4.2.1. Because the percentage of C in MNP@FFAs-WPCO is higher than in MNP@FFAs-PCO, MNP@FFAs-WPCO is more hydrophobic and therefore has a higher affinity towards hydrophobic organic pollutants.

University of Malaya

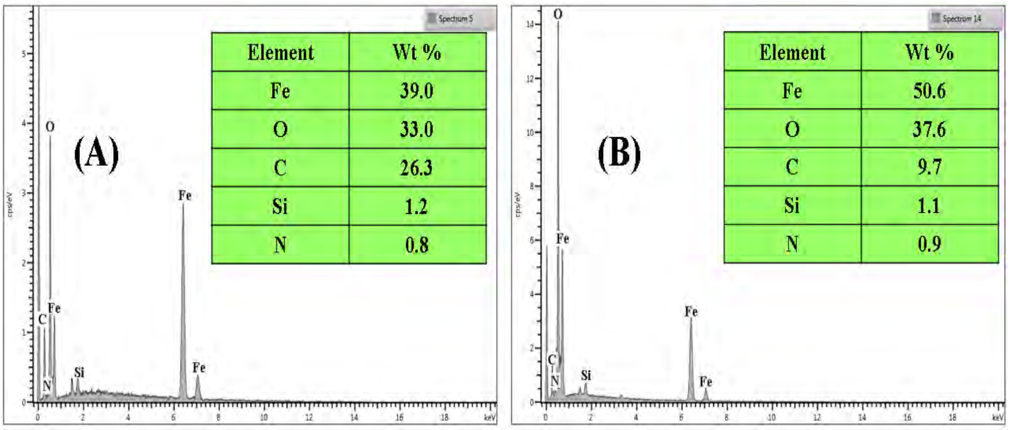

Element	Wt %
Fe	39.0
O	33.0
C	26.3
Si	1.2
N	0.8

Element	Wt %
Fe	50.6
O	37.6
C	9.7
Si	1.1
N	0.9

Figure 4.28: EDX spectra of (A) MNP@FFAs-WPCO and (B) MNP@FFAs-PCO

The thermal stability of the adsorbents was studied using TGA analysis (Figure 4.29(A-B)) and Table 4.7. TGA thermograms of MNP@FFAs-WPCO and MNP@FFAs-PCO show a weight loss of about 5.82% and 4.86%, respectively due to decomposition of organic moieties which are 3-aminopropyl and free fatty acids groups from the surface of MNPs at temperature 200 °C to 440 °C.

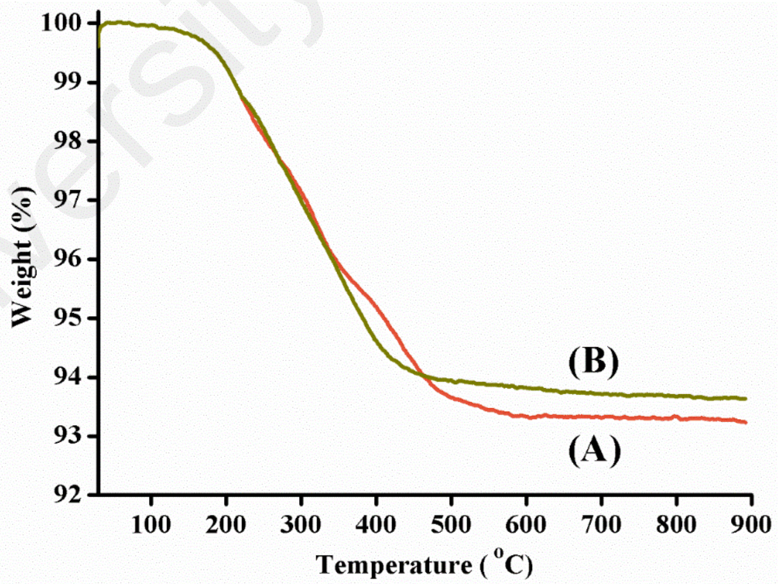

Figure 4.29: TGA thermograms of (A) MNP@FFAs-WPCO and (B) MNP@FFAs-PCO

University of Malaya

Table 4.7: TGA analysis of MNP@FFAs-WPCO and MNP@FFAs-PCO

Sample	Region (°C)	Weight loss (%)	Assignment
MNP@FFAs-WPCO	(200– 400)	5.82	3-aminopropyl & free fatty acids groups
MNP@FFAs-PCO	(200 – 400)	4.86	3-aminopropyl & free fatty acids moieties

TEM and FESEM images at two different resolutions were used to characterize the size and morphology of the fabricated adsorbents. Morphological images of MNP@FFAs-WPCO and MNP@FFAs-PCO (Figure 4.30(A-D)) show that the prepared nanoparticles are spherical in shape and have a uniform nano-size distribution. TEM analysis reveals that the distribution of MNP@FFAs-WPCO particles are well dispersed compared to that of MNP@FFAs-PCO. This is due to the high amount of free fatty acids coated on the MNPs which reduces its surface energy. The diameter distribution curves (Figure 4.30(E-F)) reveal the average size of MNP@FFAs-WPCO and MNP@FFAs-PCO as 7.23 ± 2.31 nm and 6.99 ± 2.81 nm, respectively. The higher average diameter of MNP@FFAs-WPCO is likely due to it having a thicker layer of free fatty acid.

University of Malaya

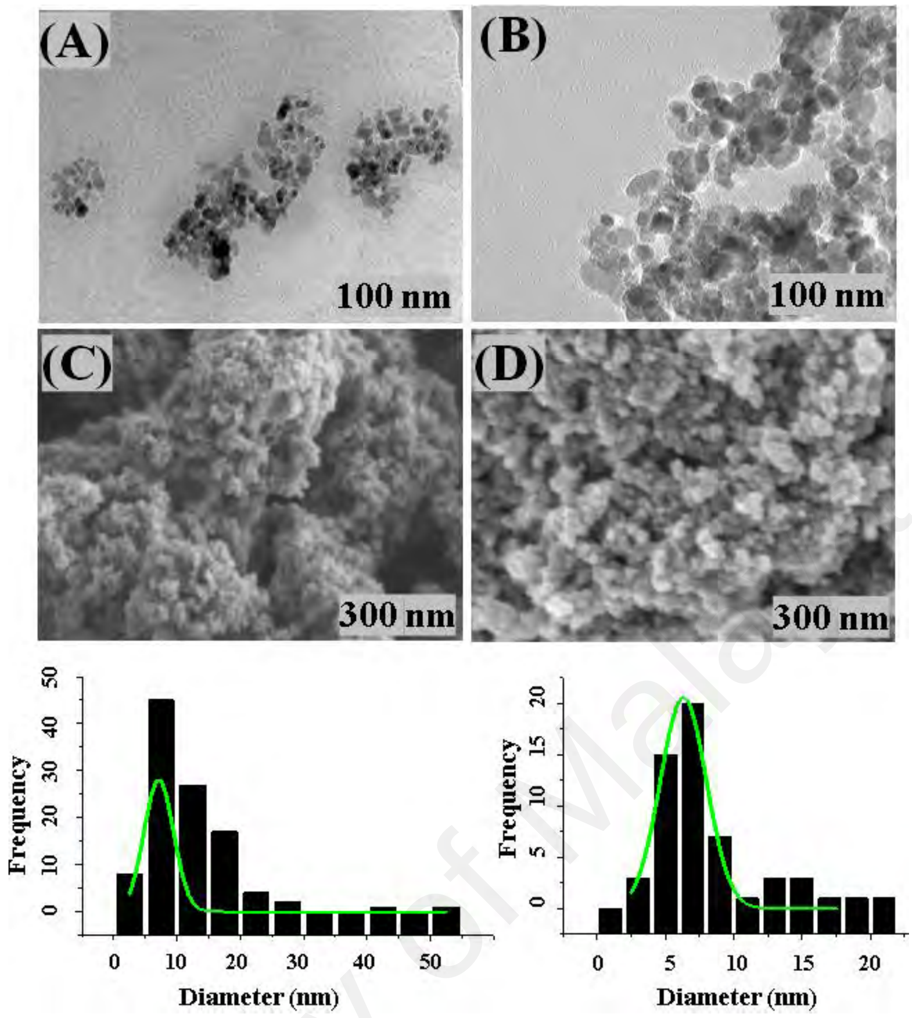

Figure 4.30: TEM images of (A) MNP@FFAs-WPCO and (B) MNP@FFAs-PCO; FESEM images of (C) MNP@FFAs-WPCO and (D) MNP@FFAs-PCO; and diameter distributions of (E) MNP@FFAs-WPCO and (F) MNP@FFAs-PCO

Nitrogen adsorption/desorption analysis was performed to investigate the porous structure of MNP@FFAs-WPCO and MNP@FFAs-PCO (Figure 4.31(A-B)). We found the surface area of MNP@FFAs-WPCO and MNP@FFAs-PCO are 55.5 and 9.3 m^2 g^{-1}, respectively. The higher surface area of MNP@FFAs-WPCO can be explained by the more even distribution of MNP@FFAs-WPCO particles compared to that of MNP@FFAs-PCO as discussed earlier in morphological analysis. It demonstrates that MNP@FFAs-WPCO is better potential adsorbent for PAHs and oil as it has higher a surface area compared to the MNP@FFAs-PCO.

University of Malaya

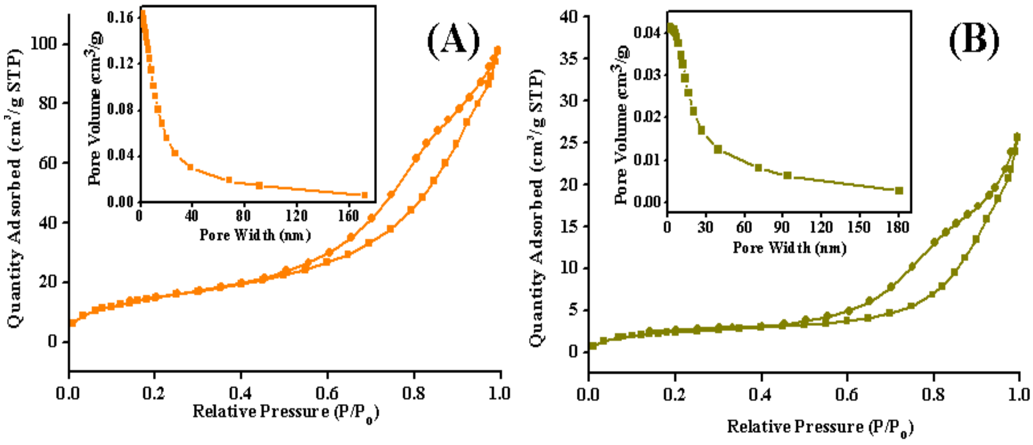

Figure 4.31: N_2 adsorption-desorption isotherms of (A) MNP@FFAs-WPCO and (B) MNP@FFAs-PCO

The magnetic behaviour of the synthesized adsorbent was analyzed using VSM. Figure 4.32(A-B) shows the VSM spectra of MNP@FFAs-WPCO and MNP@FFAs-PCO. All prepared adsorbents exhibit superparamagnetic behaviour, as their remanence and coercivity values are almost negligible. The maximal saturation magnetization of MNP@FFAs-WPCO and MNP@FFAs-PCO was found to be 53.28 emu g^{-1} and 56.17 emu g^{-1}, respectively. The lower magnetization value for MNP@FFAs-WPCO compared to MNP@FFAs-PCO suggests that there is a higher amount of non-magnetic free fatty acids layer shielding the MNPs.

University of Malaya

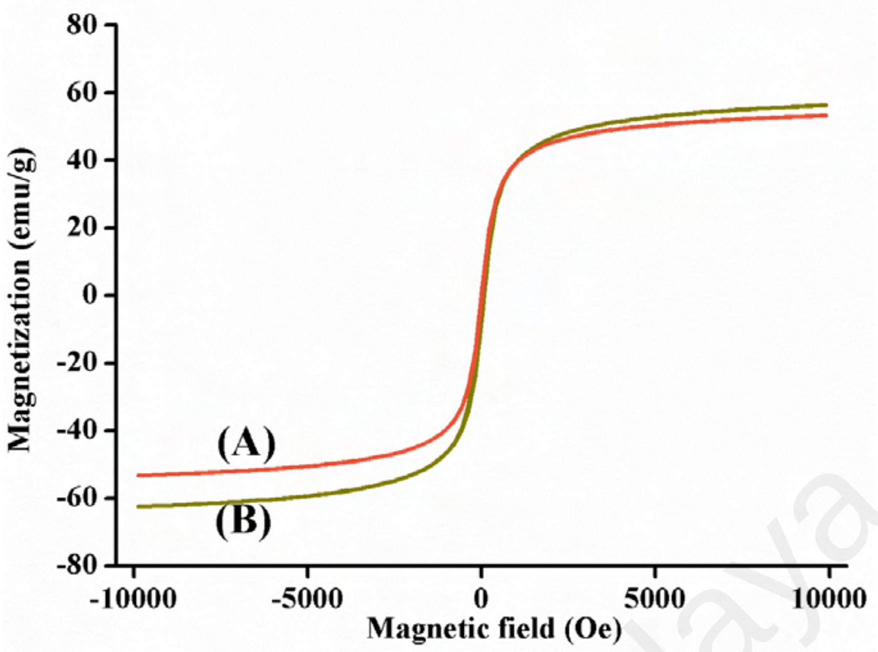

Figure 4.32: VSM magnetization curves of (A) MNP@FFAs-WPCO and (B) MNP@FFAs-PCO

The contact angle measurements of the synthesized MNP@FFAs-WPCO and MNP@FFAs-PCO are shown in Figure 4.33(A-B) as 151.12° and 123.60°, respectively. Therefore, MNP@FFAs-WPCO display superhydrophobic properties as it has a water contact angle greater than 150° (Li *et al.*, 2006) which is highly hydrophobic as compare to the MNP@FFAs-PCO. Owing to super-repellence behaviour of MNP@FFAs-WPCO for aqueous phase, the water droplet remains spherical stably on the MNP@FFAs-WPCO bed. Additionally, the superhydrophobicity of MNP@FFAs-WPCO is clearly demonstrated by the fact that it was difficult to pull down a water droplet on a syringe to the MNP@FFAs-WPCO surface in all cases, although the droplet was deformed severely (Figure 4.33(C-G)). The superhydrophobic and superoleophilic nature of MNP@FFAs-WPCO is indicative of its excellent ability for the extraction of PAHs and oil adsorption.

University of Malaya

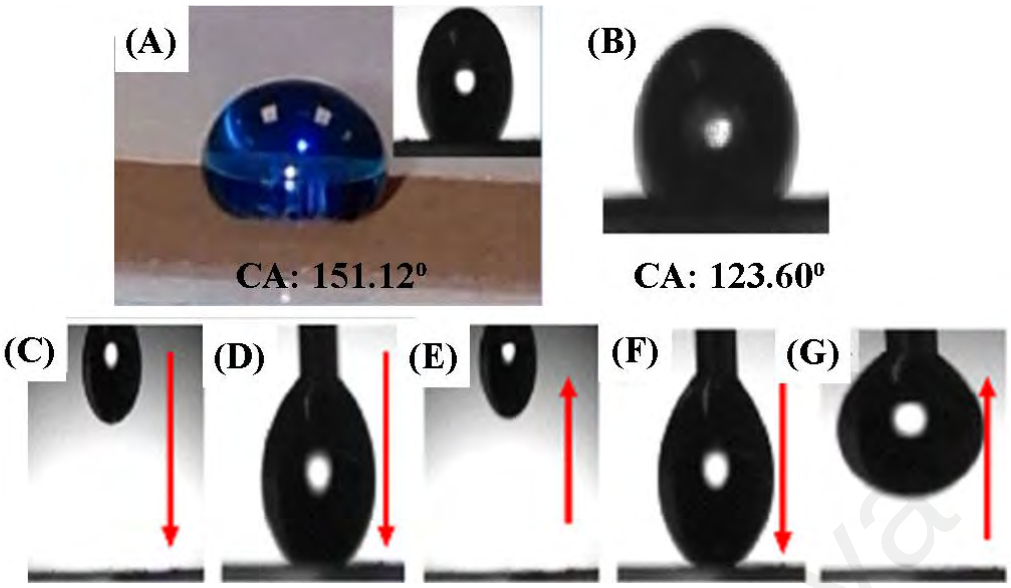

Figure 4.33: The optical image of water droplet on the prepared (A) MNP@FFAs-WPCO; (B) MNP@FFAs-PCO substrate (water was dyed with methylene blue for a clear observation) (C- G) Approach, contact, deformation, and departure process of a water droplet suspending on a syringe with respect to MNP@FFAs-WPCO surface. The arrows represent the moving direction of the substrate

The relationship between pH and CA on the surface of MNP@FFAs-WPCO was analyzed and is shown in Figure 4.34(A). It was found that MNP@FFAs-WPCO repels aqueous solutions with pH values ranging from 1 to 12. Furthermore, WCA is always higher than 110° even after the adsorbent has been exposed to elevated temperatures of 70 °C and 90 °C for 72 hours (Figure 4.34(B)). The long-time stability of the obtained MNP@FFAs-WPCO was studied by measuring the WCA after storing it for 30 days at ambient temperature, as can be seen in Figure 4.34(B), no apparent change was observed in the WCA measurement. These results reveal MNP@FFAs-WPCO as a potential adsorbent toward corrosive environmental samples. The results obtained are also similar to that obtained previously for the adsorbent MNP@FFAs-PCO.

University of Malaya

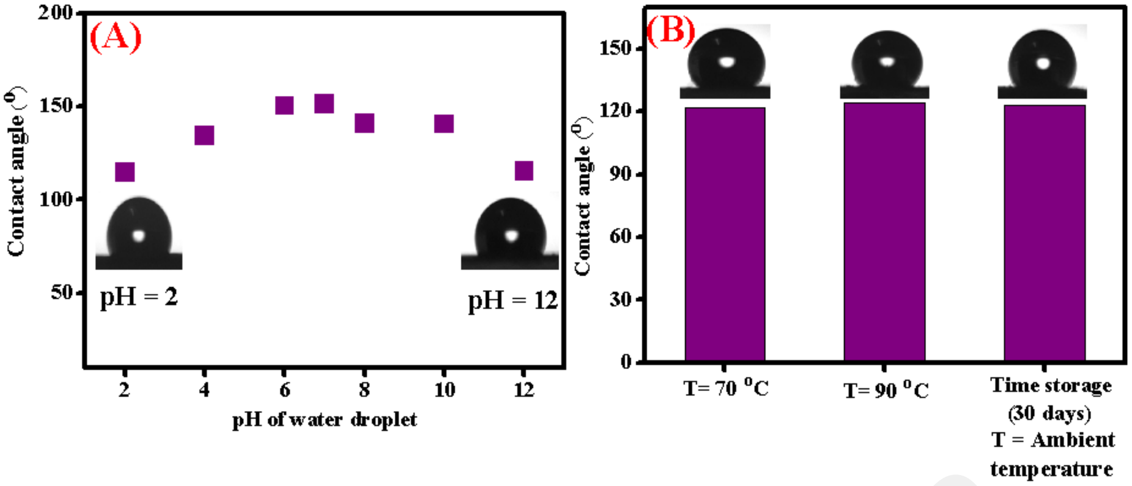

Figure 4.34: (A) The relationship between pH of water droplet and water CA on the MNP@FFAs-WPCO surface; (B) water contact angle of MNP@FFAs-WPCO after corrosion, heat treatments for 72 hours and time storage (30 days) at ambient temperature

The buoyancy of the synthesized nanosorbent was checked by placing it on a surface of water under constant stirring overnight. Remarkably, the MNP@FFAs-WPCO nanosorbent was found to float on water surface even when under constant mechanical stirring (Figure 4.35(A-B)) and remained on the surface after stirring overnight (Figure 4.35(C-D)). This finding again similar to the result obtained for MNP@FFAs-PCO. It is now proven that both synthesized adsorbents possess high buoyancy which may be exploited for the adsorption of hydrophobic organic pollutants on the surface of water.

University of Malaya

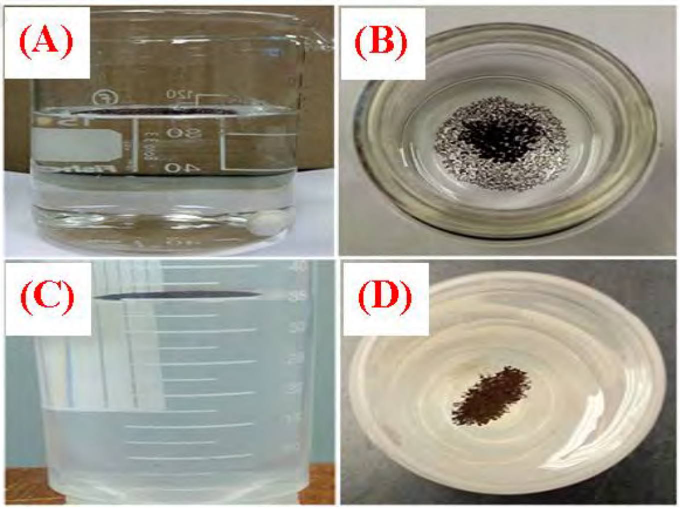

Figure 4.35: Side and top image view for situation of MNP@FFAs-WPCO particles floating while under mechanical stirring (A-B) and being left overnight (C-D)

4.3.2 Applications of the MNP@FFAs-WPCO

The successful synthesis of the designed adsorbents is proven by the analyses discussed in Section 4.3.1. MNP@FFAs-WPCO exhibits better hydrophobic property and has a higher surface area compared to MNP@FFAs-PCO. Therefore, it is expected that MNP@FFAs-WPCO is the better adsorbent for hydrophobic organic pollutants. In this section, we discuss the use of the developed adsorbent for the MSPE of selected PAHs and remediation of oil from aqueous solutions. In addition, the performance of MNP@FFAs-WPCO is compared to MNP@FFAs-PCO.

4.3.2.1 MSPE performance

Batch sorption experiments were conducted to investigate the performance of the MNP@FFAs-WPCO and MNP@FFAs-PCO on the extraction of several PAHs. Figure 4.36 shows the extraction efficacies of MNP@FFAs-WPCO and MNP@FFAs-PCO. It was found that MNP@FFAs-WPCO is the better adsorbent for the extraction of PAHs as it has the better extraction efficacies for all targeted PAHs. This is expected because the elemental and TGA analyses revealed that MNP@FFAs-WPCO is made out of many long chain free fatty acids which means more sites are accessible for the adsorption of PAHs. Apart from that, the higher surface area of MNP@FFAs-WPCO compared to the MNP@FFAs-PCO provides large active site for PAHs adsorption. The higher extraction capability on MNP@FFAs-WPCO give a good justification in using MNP-FFAs-WPCO as an adsorbent compare to MNP@FFAs-PCO.

University of Malaya

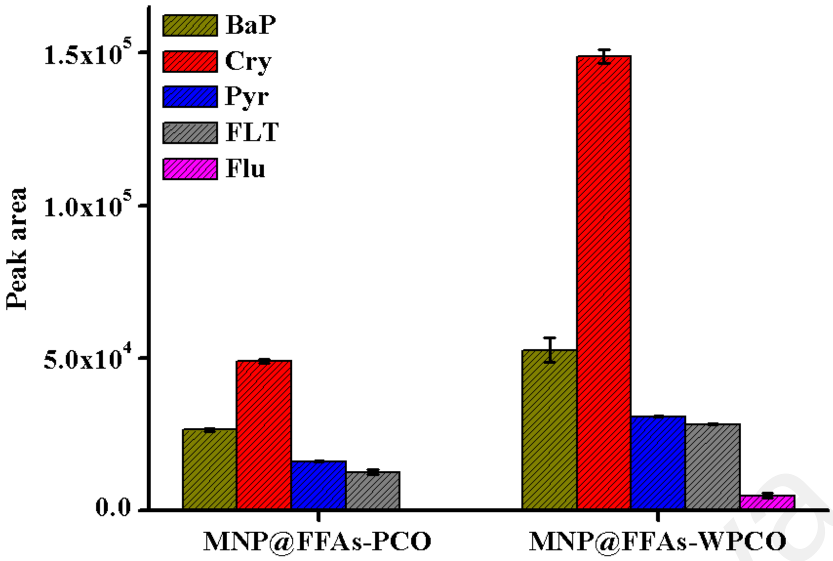

Figure 4.36: Comparison of the extraction efficiencies of PAHs between MNP@FFAs-WPCO and MNP@FFAs-PCO. (Amount of the adsorbents (*i.e.*, MNP@FFAs-PCO and MNP@FFAs-WPCO) = 10 mg, organic eluent = *n*-hexane, volume of organic eluent = 2.0 mL, extraction time = 10 min, desorption time = 5 min, sample pH = 6.5 and sample volume = 15 mL)

To attain maximum PAHs extraction efficacy using MNP@FFAs-WPCO, several parameters such as the adsorbent dosage, type of organic eluent, volume of organic eluent, extraction time, desorption time, pH of the solution and sample volume were optimized. Each experiment was performed in triplicate. The experimental parameters for MSPE were optimized using standard aqueous solution spiked with 100 ng mL^{-1} of PAHs. Chromatography of peak area was used to measure the uptake of the selected PAHs.

To optimize the first parameter, the effect of different dosages of MNP@FFAs-WPCO (5-30 mg) on PAHs extraction was investigated. Figure 4.37 shows that the recovery of all tested PAHs increases with the increase in adsorbent dosage up to 25 mg except for fluorene. Increasing the dosage to 30 mg did not manifest any significant improvement in the extraction efficacy. Therefore, 25 mg MNP@FFAs-WPCO is taken as the optimized dosage in subsequent experiments.

University of Malaya

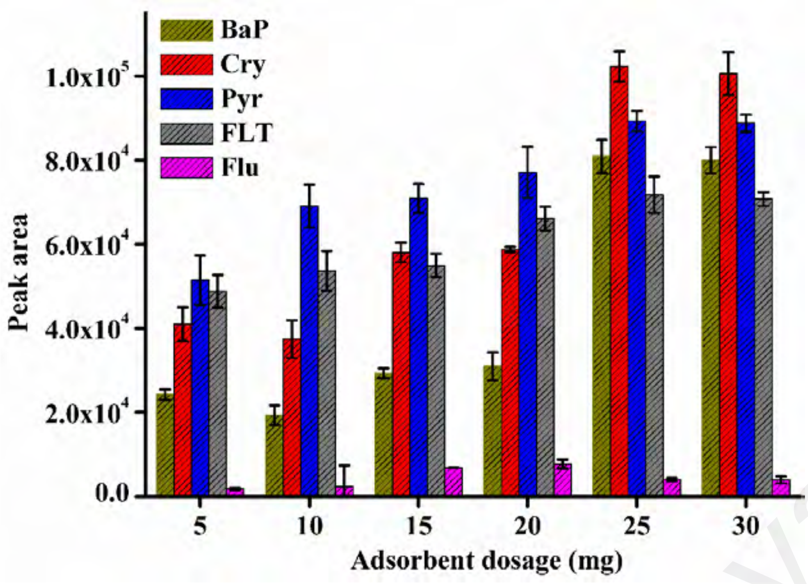

.

Figure 4.37: The effect of adsorbent dosage on the extraction efficiency of PAHs. (Organic eluent = *n*-hexane, volume of organic eluent = 2.0 mL, extraction time = 10 min, desorption time = 5 min, sample pH = 6.5 and sample volume = 15 mL)

A suitable eluting solvent is an important factor to consider in order to achieve a better extraction efficacy. Acetonitrile, *n*-hexane, ethyl acetate and toluene were investigated as potential eluents for desorption of PAHs in this experiment. As evident from Figure 4.38(A-B), 2.5 mL of ethyl acetate is the best eluting solvent as it resulted in better recoveries for almost all targeted PAHs. This result is possibly due to the presence of by-products (*i.e.*, aldehyde, ketone, and epoxy) from waste palm cooking oil (Zhang *et al*., 2012) attached on the MNP@FFAs-WPCO which contributed to PAHs extraction. Therefore, ethyl acetate, a mildly polar solvent is the most suitable organic eluent to desorb PAHs.

University of Malaya

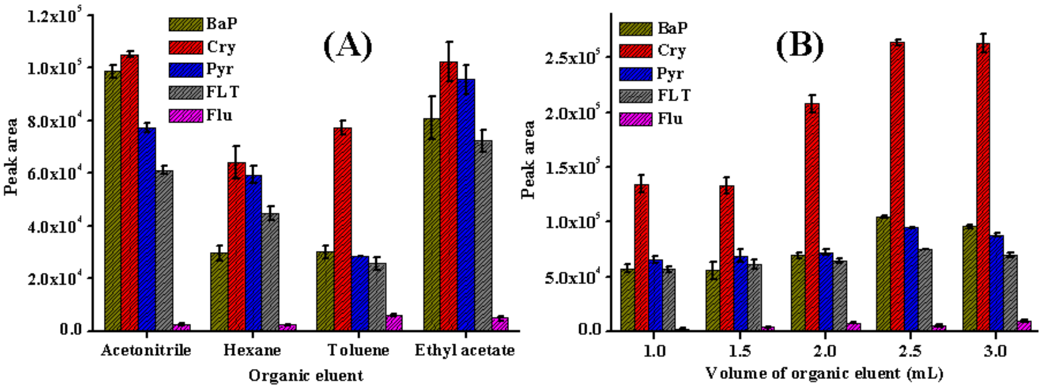

Figure 4.38: The effects of (A) organic eluent (Amount of MNP@FFAs-WPCO = 25 mg, volume of organic eluent = 2.0 mL, extraction time = 10 min, desorption time = 5 min, sample pH = 6.5 and sample volume = 15 mL) and (B) volume of organic eluent (Amount of the MNP@FFAs-WPCO = 25 mg, organic eluent = ethyl acetate, extraction time = 10 min, desorption time = 5 min, sample pH = 6.5 and sample volume = 15 mL)

The effect of extraction time ranging from 5 to 30 min on extraction efficacy was investigated (Figure 4.39(A)). As extraction time increases, response also increased significantly. All PAHs give the highest response at 25 min and prolonging the extraction time to 30 min does not alter the response. Hence, 25 min extraction time is taken as the optimum contact time for the targeted PAHs to attain maximum adsorption on the MNP@FFAs-WPCO surface. For the desorption study, 25 min desorption time was also found to be sufficient to desorb all PAHs from MNP@FFAs-WPCO (Figure 4.39(B)). Therefore, 25 min is optimum for both extraction and desorption times.

University of Malaya

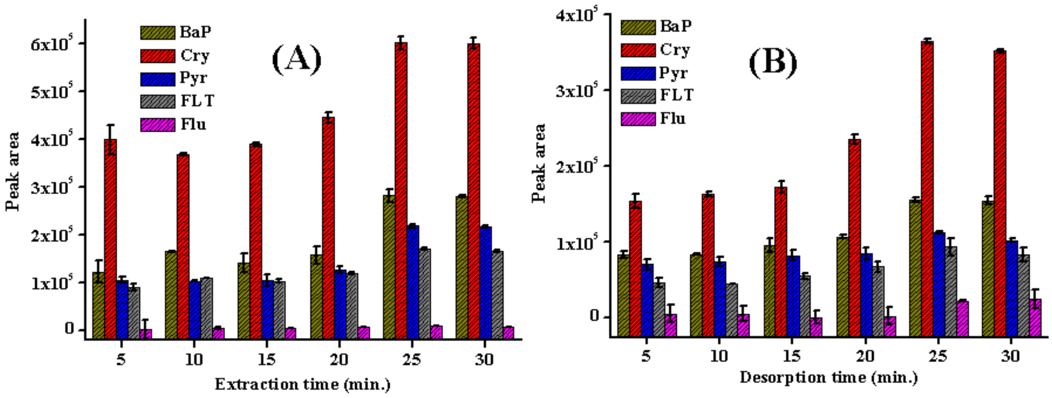

Figure 4.39: The effect of (A) extraction time (Amount of the MNP@FFAs-WPCO = 25 mg, organic eluent = ethyl acetate, volume of organic eluent = 2.5 mL, desorption time = 5 min, sample pH = 6.5 and sample volume = 15 mL) and (B) desorption time (Amount of the MNP@FFAs-WPCO = 25 mg, Organic eluent = ethyl acetate, volume of organic eluent = 2.5 mL, extraction time = 25 min, sample pH = 6.5 and sample volume = 15 mL)

The pH of the solution is an important factor in the adsorption process as it affects the surface of the adsorbent and the binding sites. In this experiment, the effect of sample solution pH on the extraction efficacy was studied at pHs (*i.e.*, 2.0, 4.0, 6.0, 6.5, 7.0, 8.0, and 10.0). It can be seen in Figure 4.40 that good recoveries for all targeted PAHs is achieved at the natural pH of sample which is pH 6.5. A similar finding is also observed when MNP@FFAs-PCO was used as the adsorbent. Therefore, pH 6.5 is taken as the optimum pH in subsequent experiments.

University of Malaya

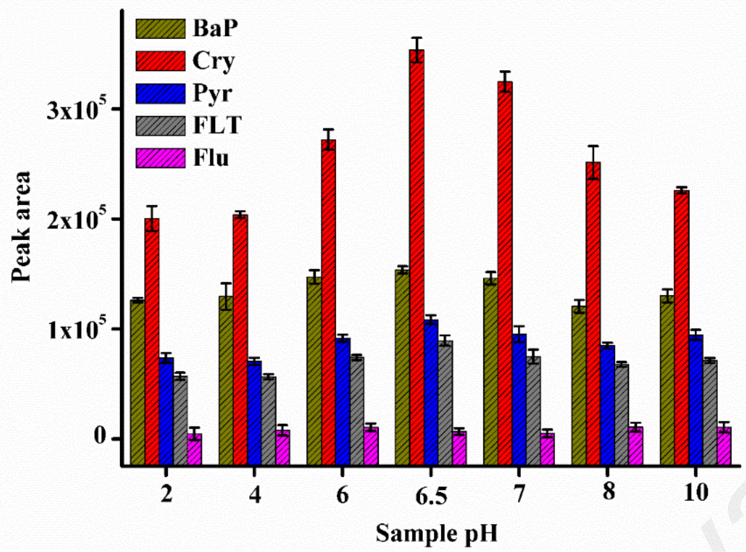

Figure 4.40: The effect of solution pH on the extraction efficiency of PAHs. (Amount of the MNP@FFAs-WPCO = 25 mg, Organic eluent = ethyl acetate, volume of organic eluent = 2.5 mL, extraction time = 25 min, desorption time = 25 min and sample volume = 15 mL)

The MNP@FFAs-WPCO sorbent possesses high extraction efficacy and great potential in pre-treatment of large volumes of water samples. The effect of sample volume (15 to 200 mL) on the PAHs extraction efficacy was studied. Figure 4.41 reveals that the recoveries for all PAHs increase when the sample volume is increased up to 150 mL and did not alter with further increase in sample volume. This might be due to the non-availability of the active sites of MNP@FFAs-WPCO which are fully occupied by the targeted PAHs. Hence, 150 mL of solution volume is selected as the optimum sample loading. This result suggests that MNP@FFAs-WPCO has a higher enrichment factor than MNP@FFAs-PCO which recorded 30 mL of sample volume as the optimum sample loading (Section 4.2.2.1).

University of Malaya

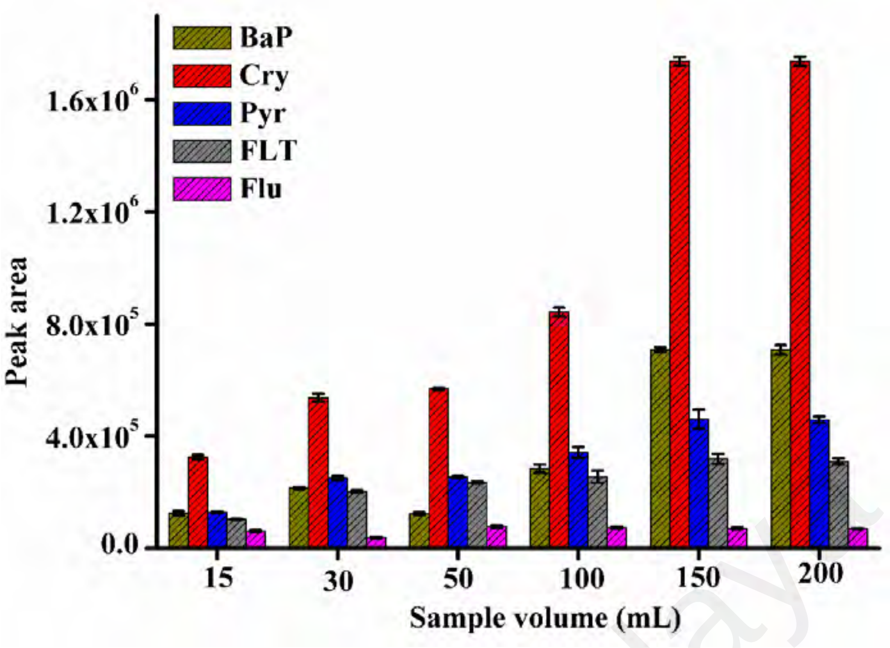

Figure 4.41: The effect of sample volume on the extraction efficiency of PAHs. (Amount of the MNP@FFAs-WPCO = 25 mg, organic eluent = ethyl acetate, volume of organic eluent = 2.5 mL, extraction time = 25 min, desorption time = 25 min and sample pH = 6.5)

University of Malaya

Stability and reusability of the adsorbent is a very important parameter in practical applications and need to be thoroughly investigated. The reusability of MNP@FFAs-WPCO was examined after 5 usage cycles. Figure 4.42 shows that there is no significant decrease for the recoveries of the selected PAHs even after reusing five time, demonstrating the high stability and reusability of MNP@FFAs-WPCO for MSPE.

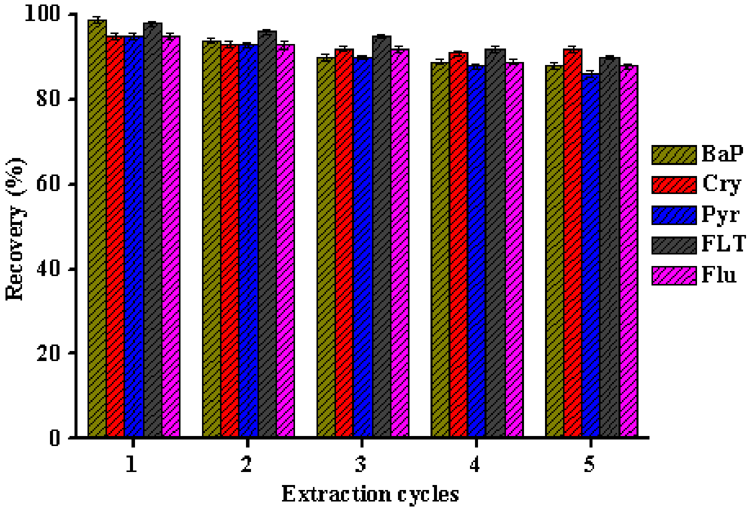

Figure 4.42: Reusability of the MNP@FFAs-WPCO for extraction of PAHs

Experiments revealed that the optimal extraction conditions for the extraction of PAHs are as follows; 25 mg adsorbent, 2.5 ml ethyl acetate as the desorption solvent, 25 min as the extraction/desorption time, sample solution pH 6.5 and 150 mL sample volume. Under optimized conditions, a series of the experiments was carried out and evaluated with regard to linearity, limit of detection, limit of quantification and precision to validate the developed method. Table 4.8 lists the comparison of analytical performances between MNP@FFAs-WPCO and MNP@FFAs-PCO. It can be seen that MNP@FFAs-WPCO-MSPE has a better linear range. In this case, for all tested PAHs, good linearity is exhibited with the coefficient of determination ranging from 0.9955 to 0.9998. The LOD and LOQ values for PAHs adsorption are found to range from 0.001 to 0.05 ng mL^{-1} and from 0.004 to 0.2 ng mL^{-1}, respectively while for the previously developed method, MNP@FFAs-PCO-MSPE have the LOD and LOQ values ranging from 0.01 to 0.05 ng mL^{-1} and 0.03 to 0.16 ng mL^{-1}, respectively. Therefore, it can be said that the present method MNP@FFAs-WPCO-MSPE is more sensitive in detecting selected PAHs as it has lower LOD and LOQ values compared to the previous method, MNP@FFAs-PCO-MSPE. This result is in line with our expectations as MNP@FFAs-WPCO has a larger surface area and better hydrophobicity compared to MNP@FFAs-PCO-MSPE. The reliability of the present method MNP@FFAs-WPCO-MSPE is good as the intra- day RSD% and inter-day RSD% are low, ranging from 2.9-6.5% and 1.5-2.5%, respectively. This has in implication that the current method can be used as a precise sensor for the determination of selected PAHs.

University of Malaya

Table 4.8: Analytical performance data of the proposed methods MNP@FFAs-WPCO-MSPE and MNP@FFAs-PCO-MSPE

	MNP@FFAs-WPCO						MNP@FFAs-PCO					
Analyte	Linearity				Precision		Linearity				Precision	
	LDR (ng mL^{-1})	R^2	LOD (ng mL^{-1})	LOQ (ng mL^{-1})	Intra-day (RSD% (*n*=7)	Inter-day (RSD% (*n*=3)	LDR (ng mL^{-1})	R^2	LOD (ng mL^{-1})	LOQ (ng mL^{-1})	Intra-day (RSD% *n*=7)	Inter-day (RSD% *n*=3)
Flu	0.1-100	0.9996	0.05	0.2	6.4	2.2	-	-	-	-	-	-
FLT	0.01-100	0.9955	0.009	0.03	6.5	1.5	0.1-100	0.9998	0.05	0.16	5.8	2.3
Pyr	0.01-100	0.9987	0.008	0.03	3.1	2.5	0.1-100	0.9998	0.03	0.08	3.8	3.1
Cry	0.01-50	0.9998	0.003	0.009	5.3	2.3	0.1-100	0.9998	0.02	0.07	4.2	1.6
BaP	0.01-100	0.9977	0.001	0.004	2.9	2.1	0.1-100	0.9998	0.01	0.03	3.9	1.1

University of Malaya

To demonstrate the applicability and reliability of the proposed method, the method was applied to treat real leachate and sludge collected from Jeram Landfill, Kuala Selangor. Again, as no PAHs are detected in these real samples, they were artificially spiked to the levels of 0.5 ng mL^{-1}, 5 ng mL^{-1} and 50 ng mL^{-1}. The results obtained for the recovery of PAHs using MNP@FFAs-WPCO is shown in Table 4.9. It could be seen that the recovery for all tested PAHs in leachate is in the range 82.8% to 116.6% with the RSDs (n = 5) ranging from 5.2% to 11.0%. The proposed method is thus presented as an excellent way for the determination of PAHs in real samples.

The developed method was also used for the determination of PAHs in sludge samples. Table 4.9 shows the recoveries for the spiked sludge to be in the range of 72.3%-119.9% with the RSDs (n = 5) ranging from 4.8% to 11.8%. These results imply that the method can be applied to preconcentrate PAHs that are found in trace levels in complex matrices. Figure 4.43 illustrates the typical HPLC-DAD chromatogram of the PAHs extracted by the proposed procedure from the leachate before and after the leachate was spiked with 50 ng mL^{-1} of each PAHs.

University of Malaya

Table 4.9: The recoveries and standard deviations of PAHs in real environmental samples with spiked concentration of 0.5 ng mL^{-1}, 5 ng mL^{-1} and 50 ng mL^{-1} for each analyte

Analyte	Spiked (ng mL^{-1})	Leachate (*n* = 5)		Sludge (*n*=5)	
		Recovery (%)	RSD (%)	Recovery (%)	RSD (%)
Flu	0.5	111.5	7.5	112.7	9.6
	5	94.0	9.7	98.3	9.6
	50	107.1	6.5	87.8	5.5
FLT	0.5	112.1	6.7	112.7	9.6
	5	116.6	11.0	103.6	8.6
	50	105.2	8.2	101.0	8.6
Pyr	0.5	115.3	6.0	117.6	4.8
	5	94.7	10.1	99.1	11.7
	50	82.8	6.1	95.1	9.9
Cry	0.5	100.4	7.6	116.7	11.2
	5	99.2	9.5	119.9	11.8
	50	105.8	6.7	107.2	11.7
BaP	0.5	100.0	9.0	116.4	11.7
	5	97.6	7.6	72.3	8.9
	50	110.6	5.2	73.4	7.9

University of Malaya

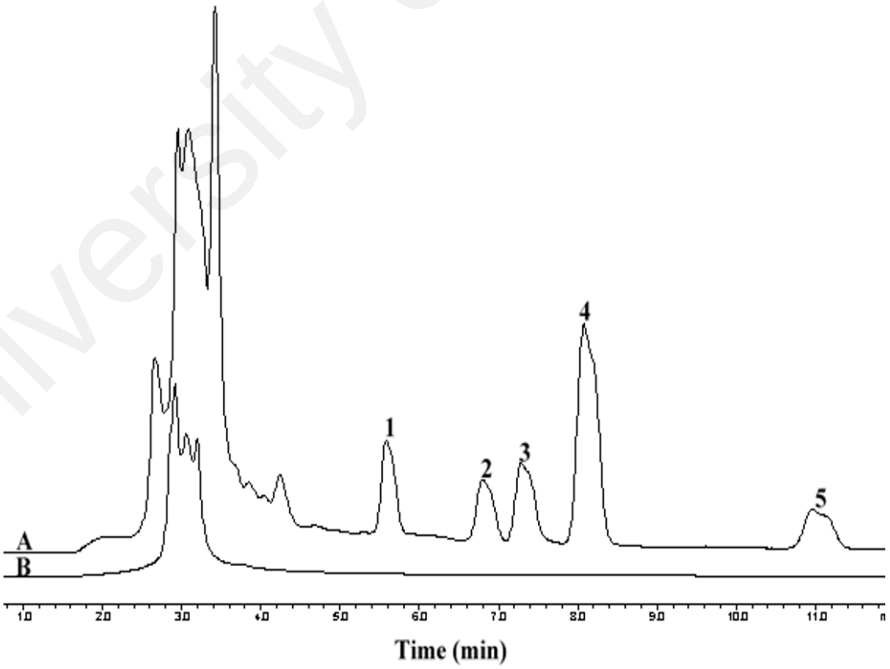

Figure 4.43: HPLC-DAD chromatograms of the PAHs after extraction using proposed MSPE: Non-spiked (A); and 50 ng mL^{-1} of each PAHs spiked leachate sample (B) (1) Flu (2) FLT, (3) Pyr, (4) Cry, and (5) BaP

The MNP@FFAs-PCO and MNP@FFAs-WPCO was evaluated by comparing the obtained results with results from similar works reported in literature. The extraction efficacies of MNP@FFAs-PCO and MNP@FFAs-WPCO adsorbents to adsorb PAHs were compared with other MSPE adsorbents published in literature (as shown in Table 4.10). The performances were evaluated in terms of %Recovery, %RSDs and LOD. The LOD of our methods are comparably low and have good PAHs adsorption that comparable to other reported works. The simple and economical fabrication of the MNP@FFAs-PCO and MNP@FFAs-WPCO adsorbents is the main advantage of the proposed adsorbent in comparison with other reported MSPE adsorbents for the determination of PAHs.

University of Malaya

Table 4.10: Comparison of %Recovery, %RSDs and LOD of the current work with other reported MSPE adsorbents

Matrix	Technique/ Adsorbent	%Recovery	%RSDs	LODs (ng mL^{-1})	Ref.
Aqueous samples	MSPE-GC / Magnetic C_{18} microspheres	35.0 - 99.0	< 10.0	0.8-36	(Liu *et al.*, 2009)
Lake water	MSPE-GC / Fe_3O_4-octadecylphosphonic acid	53.5 – 103.5	0.8 – 7.6	0.014 - 0.0644	(Ding *et al.*, 2010)
Tap – river – sea water	MSPE-HPLC / Fe_3O_4- Graphene Oxide	76.8 – 103.2	1.7 – 11.7	0.09 – 0.19	(Han *et al.*, 2012)
Tap-lake water	MSPE-HPLC/ g-C_3N_4/Fe_3O_4	80.0 – 99.8	1.6-5.5	0.05 – 0.1	(Wang *et al.*, 2015)
Leachate - sludge	MSPE-HPLC / Fe_3O_4- CN/IL	89.50 - 110.2	1.2 – 4.5	0.86 – 1.95	(Bakhshaei *et al.*, 2016)
Sea water	MSPE-GC/ G/ Fe_3O_4@PT	83.0 –107.0	4.3-11.2	0.03–80.0	(Mehdinia *et al.*, 2015)
Leachate - sludge	MSPE-HPLC / MNP@FFAs-PCO	81.1 – 119.3	3.1 – 13.6	0.01-0.05	This work
Leachate - sludge	MSPE-HPLC / MNP@FFAs-WPCO	72.3 – 119.9	4.8 – 11.8	0.001-0.05	This work

University of Malaya

4.3.2.2 Oil removal application

The oil adsorption capacity of MNP@FFAs-WPCO and MNP@FFAs-PCO is compared in Figure 4.44. As evident from the obtained result, the adsorption capacity of lubricating oil of MNP@FFAs-WPCO is higher than for MNP@FFAs-PCO. This is because MNP@FFAs-WPCO has a higher surface area and more hydrophobic sites for the adsorption of hydrophobic oils.

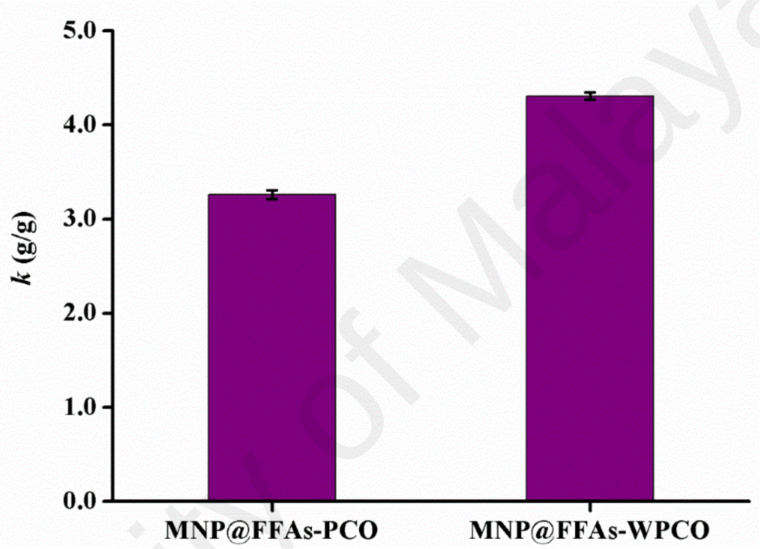

Figure 4.44: Comparison of the adsorption capacity of MNP@FFAs-WPCO and MNP@FFAs-PCO. (Amount of the adsorbents (*i.e.*, MNP@FFAs-PCO and MNP@FFAs-WPCO) = 15 mg, contact time = 60 min and pH of the aqueous solution = 7)

Several parameters such as weight of the adsorbent, pH of the solution and contact time on the adsorption of oil from water surface were investigated. All experiments were carried out in triplicate. The oil adsorbance capacity, k was used to evaluate the influence of these factors on oil removal efficacy.

The effect of adsorbent dosage on sorption efficacy of lubricating oil was examined by taking different quantities of MNP@FFAs-WPCO adsorbent ranging from 2 to 20 mg. As evident from Figure 4.45, the adsorption efficacy of oil increases with increase in the amount of adsorbent from 2 mg to 12 mg and does not change with further increase in

University of Malaya

dosage. Therefore, 12 mg MNP@FFAs-WPCO is taken as the optimum amount to use as it exhibits the highest oil adsorption capacity.

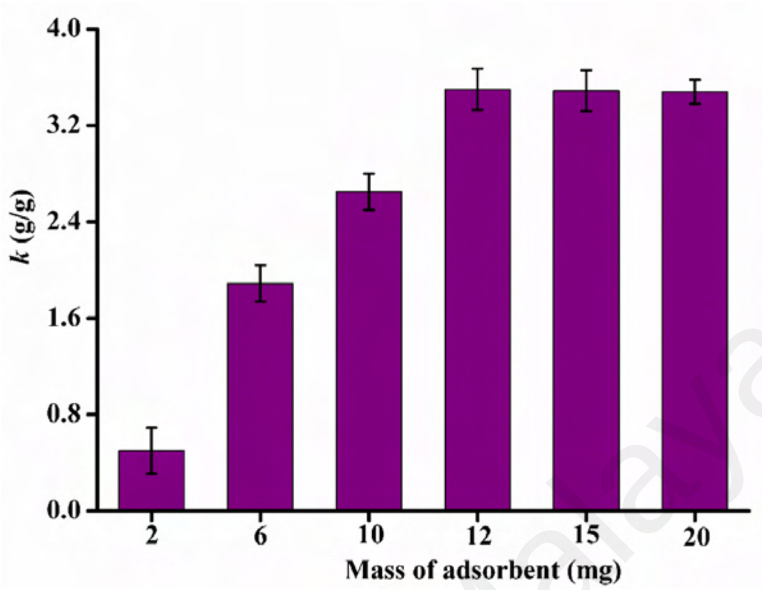

Figure 4.45: The effect of adsorbent dosage on the adsorption capacity of oil. (Contact time = 60 min and pH of the aqueous solution = 7)

The optimum contact time was determined by measuring the oil the MNP@FFAs-WPCO adsorbed after 10 to 60 min (Figure 4.46). The adsorption capacity of the oil increases with contact time up to 50 min and does not change after. Hence, 50 min of contact time is taken as the optimum time length to use in further studies.

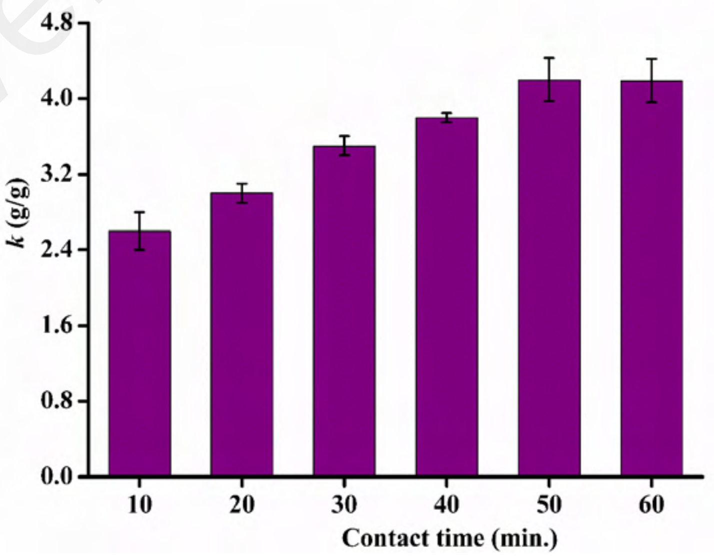

Figure 4.46: The effect of contact time on the adsorption capacity of oil. (Amount of MNP@FFAs-WPCO = 12 mg and pH of the aqueous solution = 7)

University of Malaya

The effect of pH on oil adsorption on MNP@FFAs-WPCO is shown in Figure 4.47. In this study, the effect of pH in the range between 3 and 8 on oil adsorption was examined. The results indicated that high oil adsorption capacity is the highest when the pH of the sample being treated is at pH 7. A similar finding was obtained when using MNP@FFAs-PCO as the oil adsorbing agent. Hence subsequent experiments adjust the pH of the sample to 7.

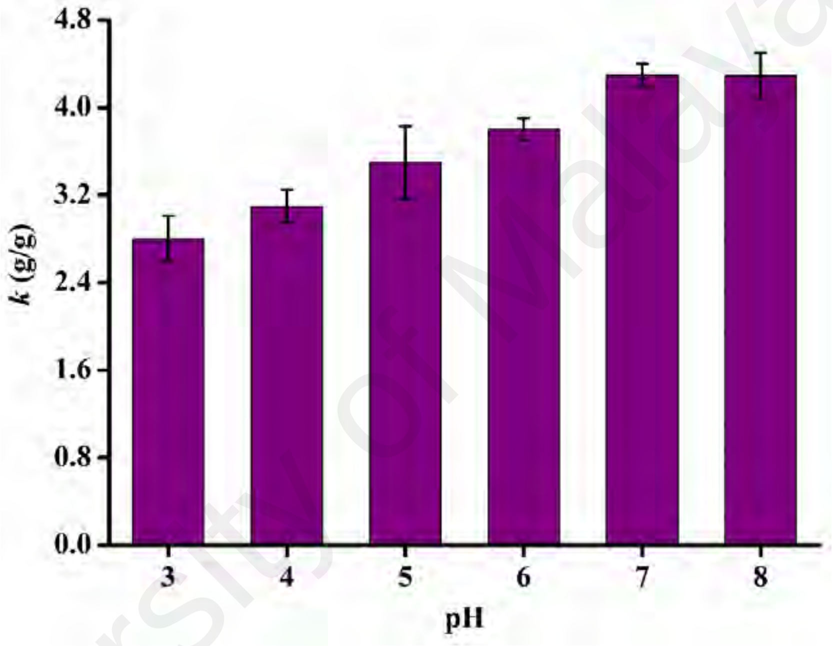

Figure 4.47: The effect of pH on the adsorption capacity of oil. (Amount of MNP@FFAs-WPCO = 12 mg and contact time = 50 min)

The reusability of the adsorbent is a key requirement in oil clean-up applications. Figure 4.48 shows the reusability of MNP@FFAs-WPCO as an adsorbent for lubricating oil sorption. It was found that the regenerated MNP@FFAs-WPCO can be reused at least 6 times and still be able to adsorb 3.11 times of oil higher than its own weight.

University of Malaya

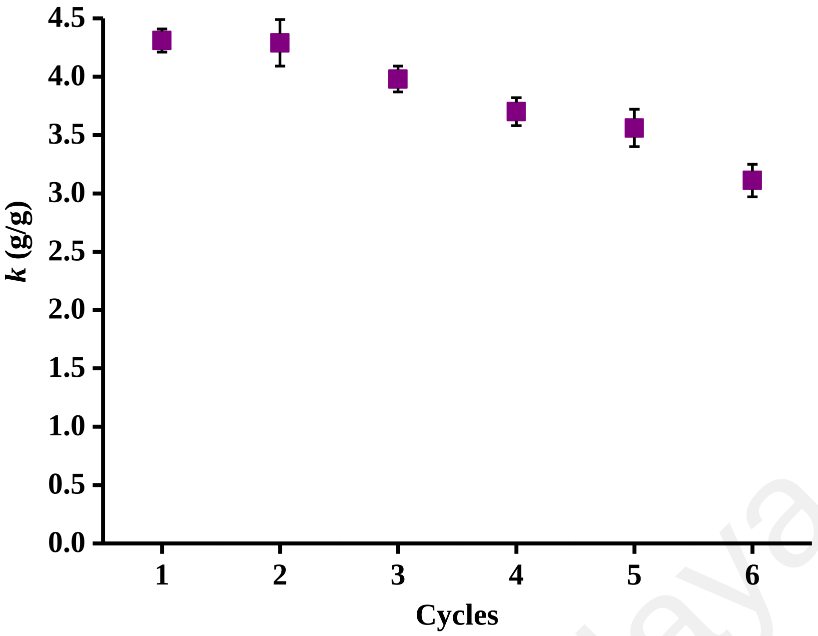

Figure 4.48: Oil-adsorption capacity of MNP@FFAs-WPCO after different oil-removal cycles

Elemental, FT-IR and TGA studies were carried out to prove the phenomena of residue oil adsorption by MNP@FFAs-WPCO and the results were compared with that for MNP@FFAs-PCO. The elemental study (Figure 4.49(A-C)) shows that the weight% of C in oil loaded MNP@FFAs-WPCO (92.67%) is much higher compared to %C found in bare MNP@FFAs-WPCO (26.3%) and oil loaded MNP@FFAs-PCO (42.73%). Furthermore, it can be seen from Figure 4.49(D) that the amount of oil adsorption on the MNP@FFAs-WPCO is more significant as the alkane bands at 2853.43 and 2919.01 cm^{-1} appear more intense for the oil loaded MNP@FFAs-WPCO compared to that for the oil loaded MNP@FFAs-PCO and bare MNP@FFAs-WPCO. The elemental and FT-IR studies affirm that the oil adsorbed by MNP@FFAs-WPCO is more than that adsorbed by MNP@FFAs-PCO. TGA thermograms of oil loaded MNP@FFAs-WPCO and MNP@FFAs-PCO (Figure 4.49(E)) reveal no weight loss associated with water loss at 100 °C implying that the oil loaded MNP@FFAs-WPCO and MNP@FFAs-PCO only adsorbed oil during adsorption study.

University of Malaya

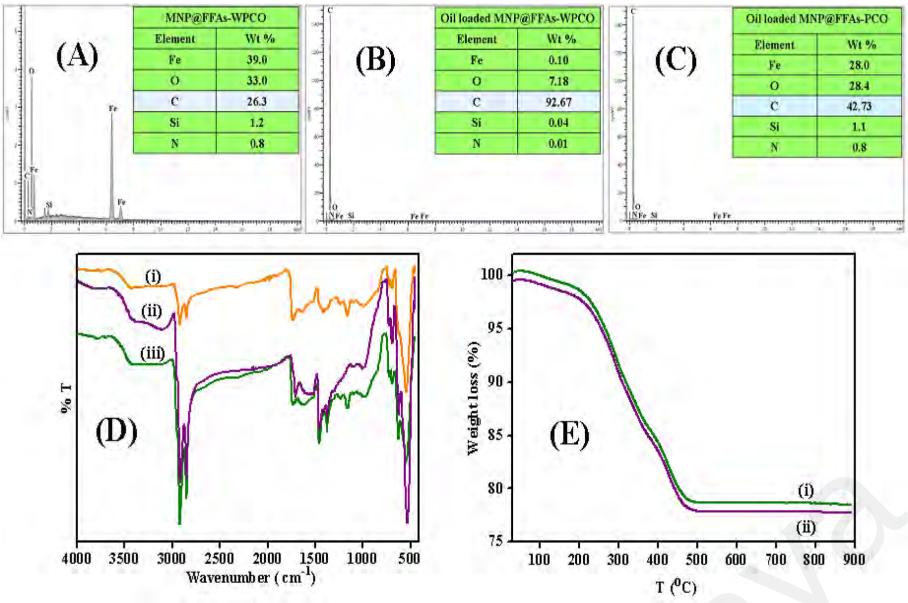

Figure 4.49: EDX spectra of (A) MNP@FFAs-WPCO; (B) oil loaded of MNP@FFAs-WPCO and (C) oil loaded of MNP@FFAs-PCO; (D) FT-IR spectra of (i) MNP@FFAs-WPCO; (ii) oil loaded of MNP@FFAs-PCO and (iii) oil loaded of MNP@FFAs-WPCO; (D) TGA thermogram of (i) oil loaded of MNP@FFAs-WPCO and (ii) oil loaded of MNP@FFAs-PCO

We further examined the adsorption capacity of MNP@FFAs-WPCO towards various domestic and commercial oil (including lubricating oil, corn oil and palm oil). Our studies revealed that the newly prepared MNP@FFAs-WPCO exhibit high adsorption capacities ranging from 2.66 to 4.31 g/g (Figure 4.50). Oil uptake capacity of the adsorbent as a function of viscosity of the adsorbed oil is shown previously in Table 4.5.

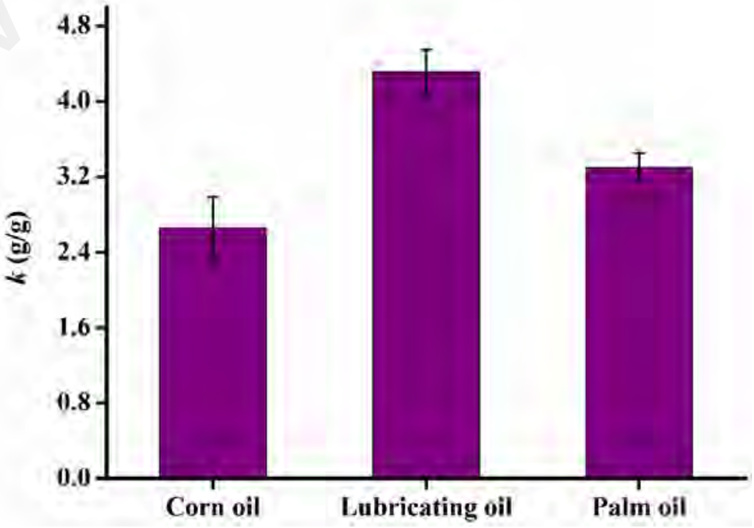

Figure 4.50: Oil adsorption capacity of the MNP@FFAs-WPCO. (Amount of MNP@FFAs-WPCO = 12 mg, contact time = 50 min and pH of the aqueous solution = 7)

University of Malaya

The performance of the developed adsorbents in this work, MNP@FFAs-WPCO and MNP@FFAs-PCO is compared with other adsorbents reported in literature (Table 4.11). Our proposed adsorbents, MNP@FFAs-WPCO and MNP@FFAs-PCO have higher oil uptake capacity compared to other reported adsorbents. The comparison result well demonstrated the fabricated adsorbents have potential as an adsorbing agents for oil spill clean-up because of their hydrophobic properties which enhance the oil uptake capacity. Additionally, the proposed method offered many advantages such as simplicity, easy removal and operation, suggesting the proposed adsorbent is a good tool for water remediation.

University of Malaya

Table 4.11: Comparison of the oil sorption uptake of various reported adsorbents

Adsorbent	Experimental oil	Sorption capacity (g/g)	Ref.
Lauric acid treated oil palm leaves	Crude oil	1.18	(Sidik *et al*., 2012)
Hydrophobic aerogels	Crude oil	2.80	(Wang *et al*., 2010)
Polystyrene coated magnetic nanocomposites (Fe_3O_4@PS)	Lubricating oil	3.00	(Chen *et al*., 2013)
Hydrophobized vermicullite	Standard mineral oil	0.023	(Mysore *et al*., 2005)
Hydrophobic aquaphyte-*Salvinia* sp. (HAS)	Crude oil	1.39	(Ribeiro *et al*., 2003)
MNP@FFAs-PCO	Lubricating oil	3.50	This study
MNP@FFAs-WPCO	Lubricating oil	4.31	This study

University of Malaya

In the present investigation, free fatty acids directly obtained from waste palm cooking oil functionalized magnetic nanoparticles (MNP@FFAs-WPCO) is successfully synthesized and characterized. It is a better performing adsorbent compared to MNP@FFAs-PCO as it has lower LOD values for the PAHs used in this study and better oil sorption capacity. This is because of the higher specific surface area and better hydrophobicity of MNP@FFAs-WPCO.

Due to excellent performance of MNP@FFAs-WPCO in trapping hydrophobic organic contaminants, its application is extended for the simultaneous determination of various organic pollutants in real samples. Since organic contaminants present in the complex matrix have a wide range of polarities, therefore, the MNP@FFAs-WPCO is integrated with graphene oxide which has an abundance of oxygen-containing functional groups to ensure the new adsorbent has good affinities toward various targeted organic contaminants and aqueous matrices. Thus, the new adsorbent, free fatty acids from waste palm cooking oil functionalized magnetic nanoparticles immobilized on graphene oxide (MNP@FFAs-WPCO-GO) was designed. The properties and its application for the simultaneous determination PAHs and PAEs in apple, cabbage and landfill sludge samples are discussed in Section 4.4.

University of Malaya

4.4 Free fatty acids from waste palm cooking oil functionalized magnetic nanoparticles immobilized on the surface of graphene oxide (MNP@FFAs-WPCO-GO) and its application

4.4.1 Characterizations of MNP@FFAs-WPCO-GO

The surface characteristics of the MNP@FFAs-WPCO-GO were analyzed using various instruments to confirm the successful synthesis of this adsorbent. In this study, Fourier transform infrared (FT-IR) spectroscopic analysis was used to study the surface chemistry of the prepared materials. The FT-IR spectra of the synthesized GO, MNP@FFAs-WPCO and MNP@FFAs-WPCO-GO are shown in Figure 4.51(A-C). The spectrum of GO shows the presence of oxygen containing functional groups due to presence of C=O and C-O groups at 1725, 1623 and 1375 cm^{-1}. The presence of other bands around 1194 and 3268 cm^{-1} are most probably due to the presence of epoxy, O-H stretching vibration and absorbed water molecules (Ma *et al.*, 2012). The spectrum of MNP@FFAs-WPCO shows the presence of alkane bands and C=O at 2922, 2858 and 1748 cm^{-1}, respectively confirming the functionalization of free fatty acids on MNPs. The spectrum obtained for MNP@FFAs-WPCO-GO shows all the relevant peaks for both GO and MNP@FFAs-WPCO confirming the successful introduction of MNP@FFAs-WPCO on GO.

University of Malaya

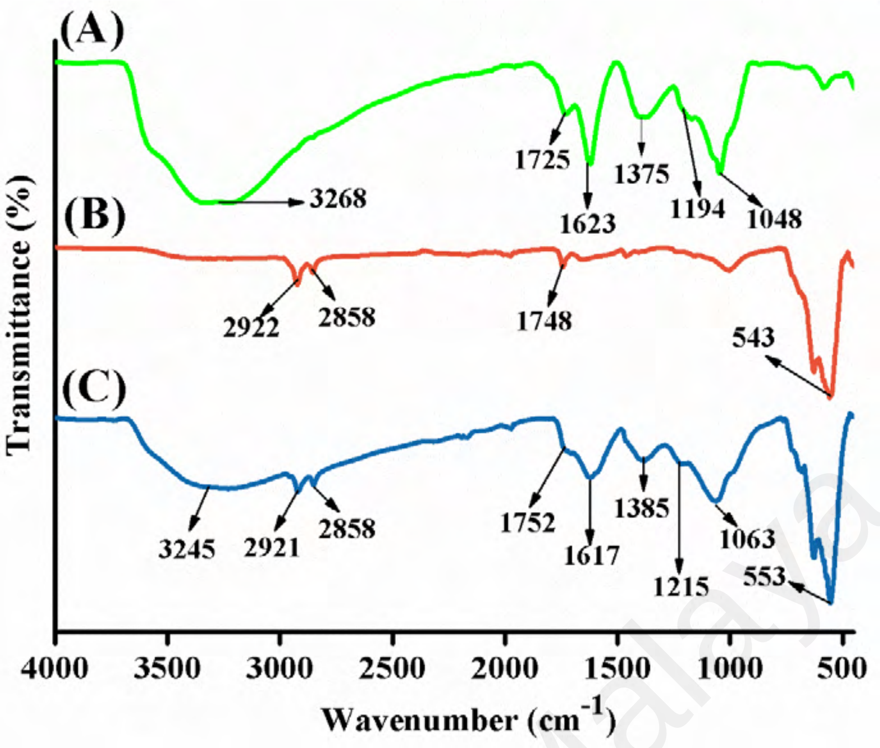

Figure 4.51: FT-IR spectra of (A) GO; (B) MNP@FFAs-WPCO and (C) MNP@FFAs-WPCO-GO

XRD analysis was used in order to study the crystallinity of the fabricated materials. The phase structures of the GO, MNP@FFAs-WPCO and MNP@FFAs-WPCO-GO are shown in Figure 4.52(A-C). The spectrum of GO shows the appearance of the diffraction peak at $2\theta = 10^\circ$ which refers to the (002) plane, suggesting the crystalline structure of GO sheet (Yang *et al.*, 2011). MNP@FFAs-WPCO also showed crystalline cubic spinel structure as all the diffraction peaks ($2\theta = 30.42^\circ, 35.59^\circ, 43.42^\circ, 53.63^\circ, 57.35^\circ$ and 63.02°, which corresponds to (220), (311), (400), (422), (511) and (440)) planes matching the standard XRD pattern of Fe_3O_4 (JCPDS 88-0866) (Marquez *et al.*, 2009). The synthesis of MNP@FFAs-WPCO-GO is confirmed by the emergence of the main diffraction peaks of MNP@FFAs-WPCO and GO.

University of Malaya

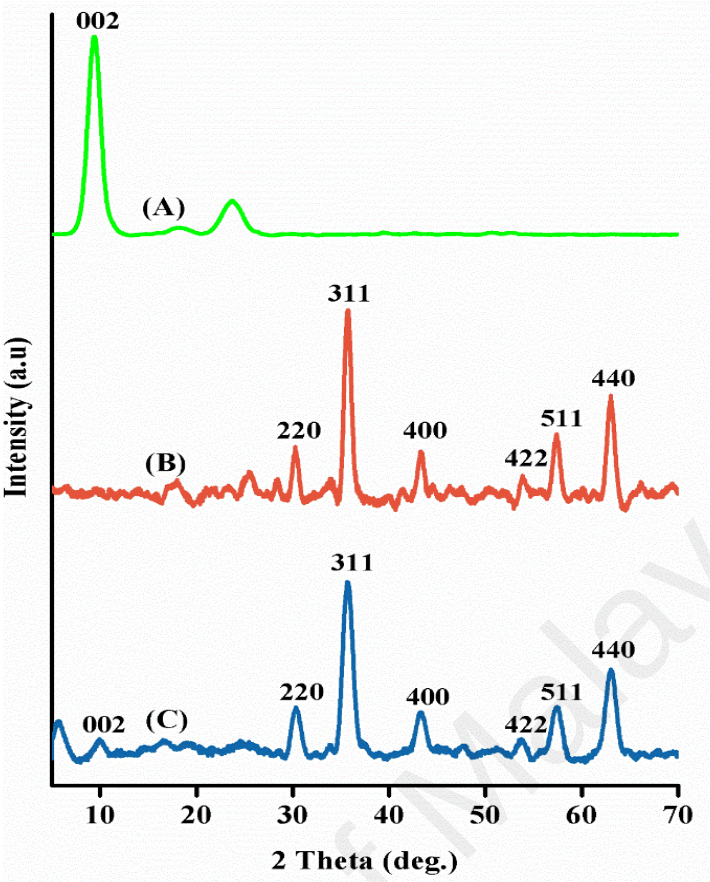

Figure 4.52: XRD patterns of (A) GO; (B) MNP@FFAs-WPCO and (C) MNP@FFAs-WPCO-GO

University of Malaya

EDX analysis was used to measure the elemental compositions of the designed MNP@FFAs-WPCO-GO and MNP@FFAs-WPCO (Figure 4.53(A-B)). The spectrum of MNP@FFAs-WPCO showed the presence of 26.3% of C and 33.0% of O. The spectrum of MNP@FFAs-WPCO-GO shows higher percentage of C (47.7%) and O (33.6%) than for MNP@FFAs-WPCO alone, implying that MNP@FFAs-WPCO was successfully introduced into GO layer.

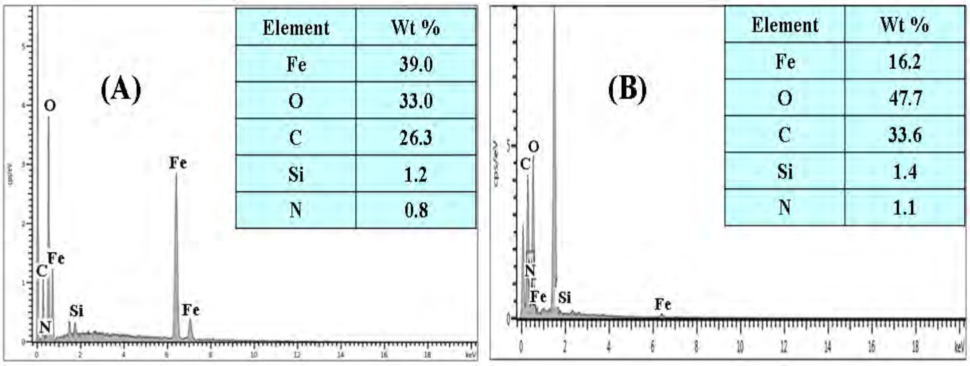

(A)

Element	Wt %
Fe	39.0
O	33.0
C	26.3
Si	1.2
N	0.8

(B)

Element	Wt %
Fe	16.2
O	47.7
C	33.6
Si	1.4
N	1.1

Figure 4.53: EDX spectra of (A) MNP@FFAs-WPCO and (B) MNP@FFAs-WPCO-GO

TGA analysis was performed to characterize the thermal behaviour of the fabricated adsorbents and the results are shown in Figure 4.54(A-B) and Table 4.12. The MNP@FFAs-WPCO shows a 5.82% weight loss due to the breakdown of 3-aminopropyl and free fatty acids moieties from the surface of MNPs at temperature 200 to 440 °C. For MNP@FFAs-WPCO-GO, there is a weight loss of about 6.01% when increasing the temperature from 30 to 150 °C. This is due to the loss of residual water from GO sheets (Eigler *et al*., 2012). Furthermore, a weight loss of 7.80% was observed at temperature 250 to 430 °C due to the pyrolysis of oxygen-containing groups from the GO layers (McAllister *et al*., 2007) and decomposition of organic groups which are 3-aminopropyl and free fatty acid moieties. Finally, there is a well-defined weight loss about 10.1% at 500 to 600 °C associated with the combustion of the carbon skeleton (Lotfi *et al*., 2016).

University of Malaya

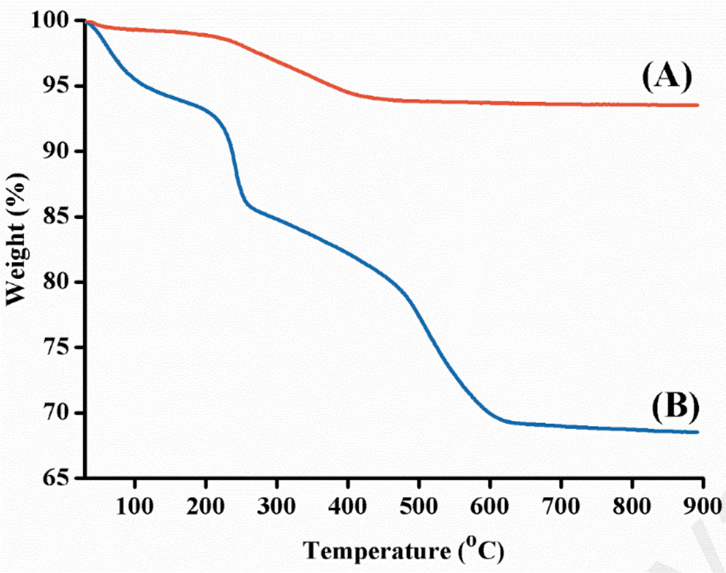

Figure 4.54: TGA curves of (A) MNP@FFAs-WPCO and (B) MNP@FFAs-WPCO-GO

Table 4.12: TGA analysis of MNP@FFAs-WPCO and MNP@FFAs-WPCO-GO

Sample	Region (°C)	Weight loss (%)	Assignment
MNP@FFAs-WPCO	(200 - 440)	5.82	3-aminopropyl & free fatty acids moieties
MNP@FFAs-WPCO-GO	(30 – 150)	6.01	Residual water from GO sheets
	(250 – 430)	7.80	Oxygen-containing groups from GO layers, 3-aminopropyl & free fatty acids groups
	(500 – 600)	10.1	Carbon skeleton

The morphologies of the prepared materials were investigated by FESEM and TEM analyses and the results are shown in Figure 4.55. The morphological study of GO sheet (Figure 4.55A) have both smooth and wrinkled surfaces (Ziaei *et al.*, 2014). The image in Figure 4.55B and D show that the prepared adsorbent, MNP@FFAs-WPCO is spherical in shape and have a rough surface. The morphological images for MNP@FFAs-WPCO-GO show the MNP@FFAs-WPCO particles well deposited onto the surface of GO sheets (Figure 4.55C and E), confirming its successful synthesis.

University of Malaya

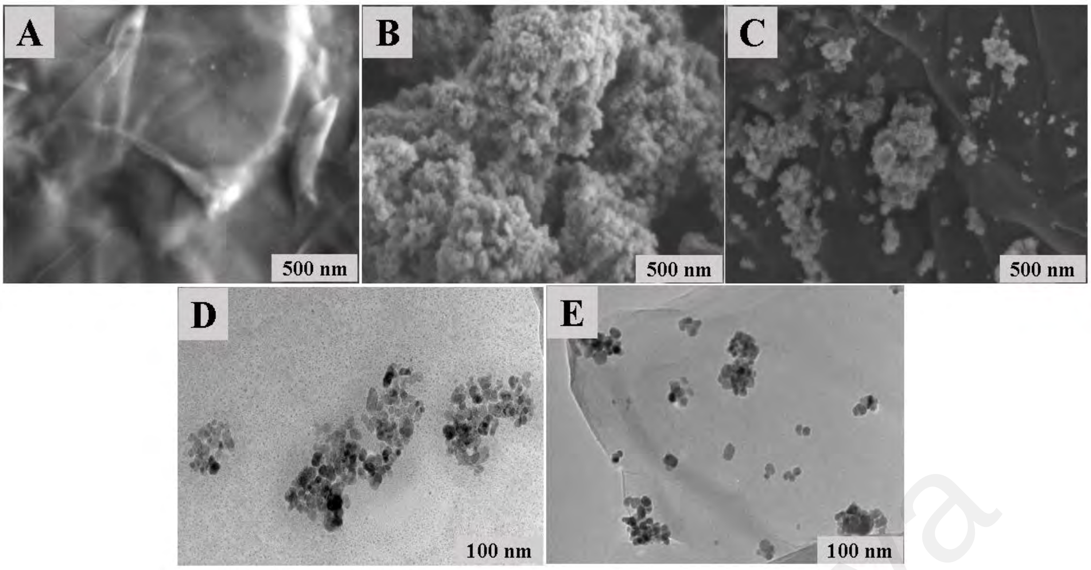

Figure 4.55: FESEM images of (A) GO; (B) MNP@FFAs-WPCO and (C) MNP@FFAs-WPCO-GO and TEM images of (D) MNP@FFAs-WPCO and (E) MNP@FFAs-WPCO-GO

The magnetic property of all the obtained nanoparticles was examined using VSM analysis. All prepared adsorbents (Figure 4.56(A-B)) exhibited S-like pattern for magnetization hysteresis loops, revealing the superparamagnetic behavior of these materials. The saturation magnetization values of MNP@FFAs-WPCO and MNP@FFAs-WPCO-GO are 53.28 emu g^{-1} and 30.64 emu g^{-1}, respectively. The lower saturation magnetization values for MNP@FFAs-WPCO-GO compared to MNP@FFAs-WPCO indicate the presence of non- magnetic layer of GO shielding the surface of MNP@FFAs-WPCO.

University of Malaya

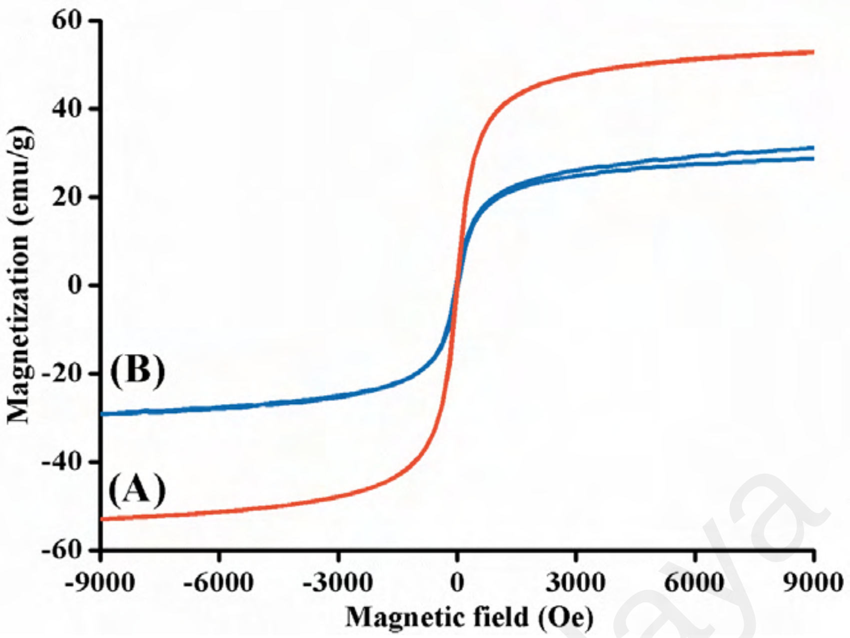

Figure 4.56: The magnetization hysteresis loops of (A) MNP@FFAs-WPCO and (B) MNP@FFAs-WPCO-GO

4.4.2 Application of the MNP@FFAs-WPCO-GO

The structure and composition studies on the prepared MNP@FFAs-WPCO-GO using FT-IR, XRD, EDX, TGA, FESEM, TEM and VSM prove the successful synthesis of this new adsorbent. The developed MNP@FFAs-WPCO-GO is applied as MSPE adsorbent for simultaneous determination of selected PAHs and phthalate esters (PAEs) from apple, cabbage and landfill sludge samples.

In order to improve extraction performance of the targeted PAEs and PAHs, different ratios of MNP@FFAs-WPCO to GO were tested to find the optimum one to synthesis new adsorbent, MNP@FFAs-WPCO-GO. As can be seen in Figure 4.57(A-B), as the ratio of GO is increased, the extraction efficiencies of all studied PAHs are decrease. This is because GO contains carboxylic, epoxy and hydroxyl functional groups which enhance the dispersion of MNP@FFAs-WPCO in aqueous media. Thus, increasing the ratio of GO to MNP@FFAs-WPCO reduces the hydrophobicity and prevents MNP@FFAs-WPCO from float on water surface to adsorb PAHs molecules floating at the air-water interface. In contrast, the increase pattern are observed for extraction efficiencies of all

University of Malaya

the selected PAEs. This is because GO can interact with PAEs through additional hydrogen bonding and π-π interaction. When the ratio of GO to MNP@FFAs-WPCO is decreased, PAHs extraction is enhanced due to stronger hydrophobicity of MNP@FFAs-WPCO causing the adsorbent to remain floating on the water surface to adsorb PAHs molecules more effectively. However, a decrease pattern in PAEs adsorption was also observed. This is due to the MNP@FFAs-WPCO floating only on the surface of water and cannot interact well with PAEs in aqueous media as PAEs are polar compare to PAHs. After some careful considerations, the ratio 2:1 (MNP@FFAs-WPCO:GO) was chosen to develop the MNP@FFAs-WPCO-GO. The extraction performance of the developed MNP@FFAs-WPCO-GO was then compared with MNP@FFAs-WPCO.

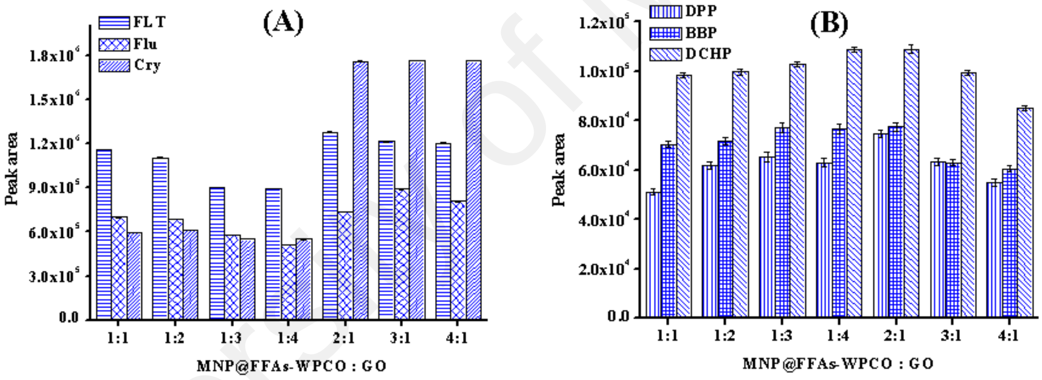

Figure 4.57: The study mass ratio of MNP@FFAs-WPCO to GO on the extraction efficiency of (A) PAEs and (B) PAHs. (Desorption solvent = methanol, volume of desorption solvent = 1.5 mL, extraction time = 10 min, desorption time = 10 min, sample pH = 6.5 and sample volume = 15 mL)

A comparative study was carried out in order to compare the extraction performance of the newly synthesized MNP@FFAs-WPCO-GO with MNP@FFAs-WPCO. Figure 4.58(A-B) shows MNP@FFAs-WPCO-GO is a better adsorbent for PAHs and PAEs than MNP@FFAs-WPCO. This result can be explained by the structure of MNP@FFAs-WPCO-GO which offers strong π–π interactions, hydrogen bonding, and hydrophobic interaction with all targeted analytes (Figure 4.59) meanwhile MNP@FFAs-WPCO can

University of Malaya

only interact with the targeted adsorbates through hydrophobic interactions. Thus MNP@FFAs-WPCO-GO is employed in the following studies.

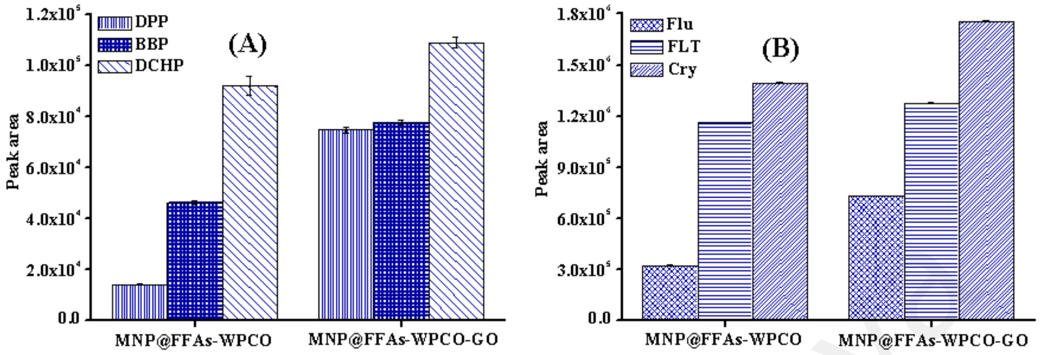

Figure 4.58: Comparison of the extraction efficiencies of (A) PAEs and (B) PAHs between MNP@FFAs-WPCO and MNP@FFAs-WPCO-GO. (Amount of the adsorbents (*i.e.*, MNP@FFAs-WPCO and MNP@FFAs-WPCO-GO) = 15 mg, desorption solvent = methanol, volume of desorption solvent = 1.5 mL, extraction time = 10 min, desorption time = 10 min, sample pH = 6.5 and sample volume = 15 mL)

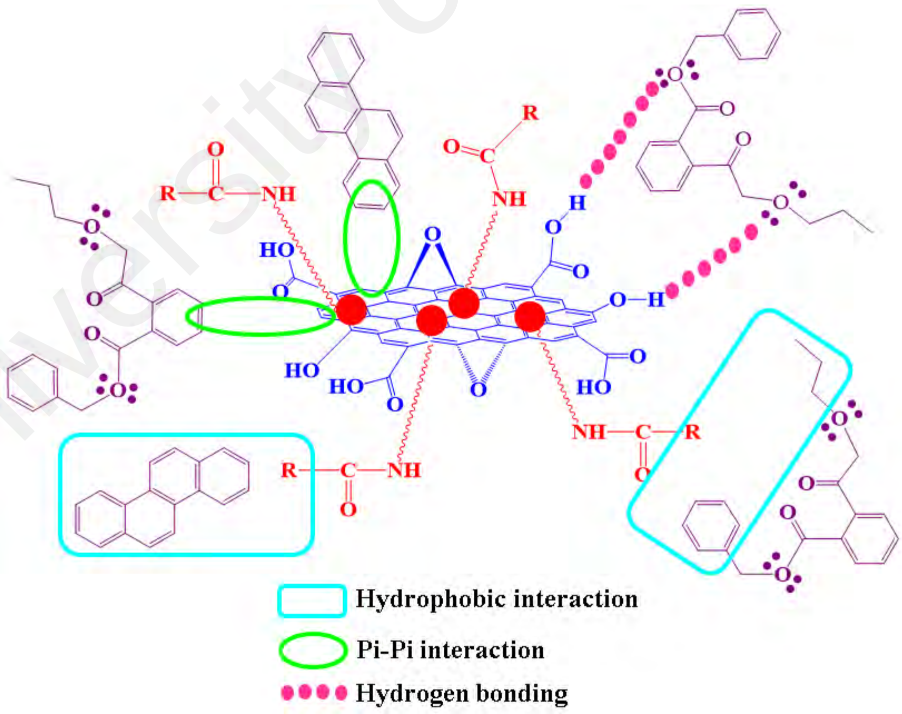

Figure 4.59: Proposed mechanism of interactions between MNP@FFAs-WPCO-GO and mixture of PAHs and PAEs

University of Malaya

In order to achieve optimum MSPE conditions using the developed adsorbent, detailed studies were carried out to investigate the effect of adsorbent amount, desorption solvent type and volume, extraction and desorption times, sample pH and solution volume. A standard aqueous solution spiked with 1 μg mL^{-1} containing a mixture of PAEs (DPP, BBP and DCHP) and PAHs (Flu, FLT and Cry) was used as the sample to be treated.

It is necessary to get the optimum adsorbent dose in order to maximize the interactions between studied analytes and adsorption sites of adsorbent in the solution. To investigate the performance of MNP@FFAs-WPCO-GO, the effect of dosage of adsorbent on extraction performance was investigated in the range of 10 to 30 mg. Figure 4.60 shows that the extraction efficacy increase remarkably with increasing MNP@FFAs-WPCO-GO up to 20 mg simply due to more binding sites being present (Ibrahim *et al*., 2010). Increasing the dosage to 25 or 30 mg does not increase extraction any further as the accessible active sites for PAEs and PAHs adsorption on MNP@FFAs-WPCO-GO becomes fully occupied. Hence, 20 mg MNP@FFAs-WPCO-GO is selected as the optimum dosage to use in subsequent studies.

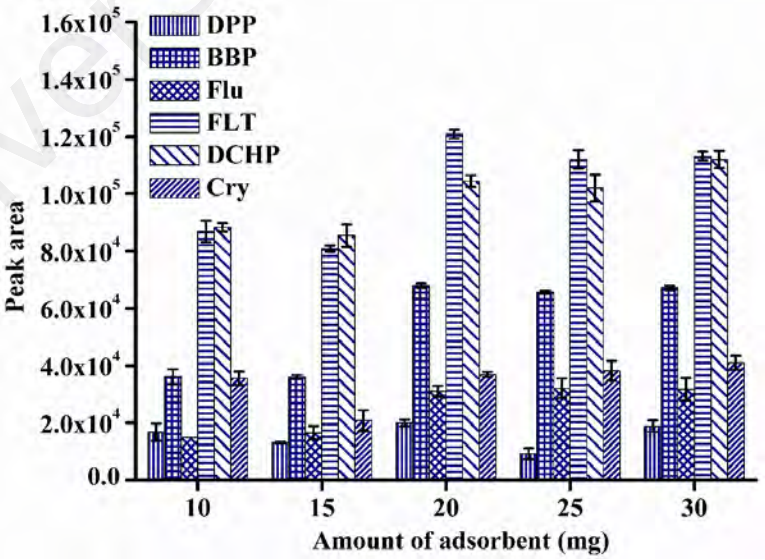

Figure 4.60: The effect of adsorbent dosage on the extraction efficiency of mixture PAEs and PAHs. (Desorption solvent = methanol, volume of desorption solvent = 1.5 mL, extraction time = 10 min, desorption time = 10 min, sample pH = 6.5 and sample volume = 15 mL)

University of Malaya

In order to desorb PAHs and PAEs from the adsorbent, several organic eluents (acetone, toluene, ethyl acetate, *n*-hexane, acetonitrile and methanol) were investigated as the desorption solvent. The obtained results reveal that acetone is the best organic solvent to desorb PAEs-PAHs from MNP@FFAs-WPCO-GO (Figure 4.61(A)). This result might be due to the ability of acetone to break hydrogen bonds and hydrophobic interactions between PAHs and PAEs, and MNP@FFAs-WPCO-GO. The result obtained in this work is similar with the results reported in other published works (Luo *et al*., 2012; Wu *et al*., 2012). Then, the optimum volume of acetone to use is investigated from the range 0.5 mL to 2.5 mL. As shown in Figure 4.61(B), 2.0 mL acetone is sufficient to completely desorb all PAHs and PAEs. Hence, 2.0 mL acetone is selected for optimum desorption solvent volume for further MSPE experiments.

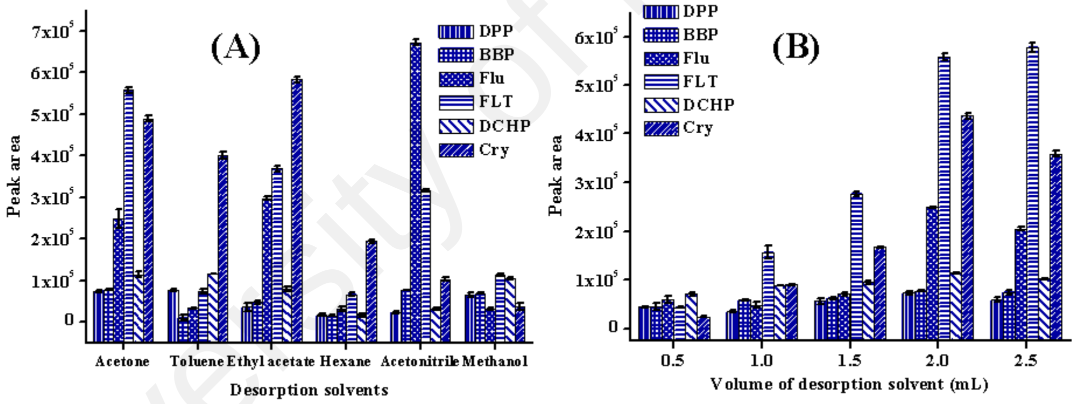

Figure 4.61: The effect of (A) organic eluent (Amount of MNP@FFAs-WPCO-GO = 20 mg, volume of desorption solvent = 1.5 mL, extraction time = 10 min, desorption time = 10 min, sample pH = 6.5 and sample volume = 15 mL) and (B) Volume of organic eluent (Amount of MNP@FFAs-WPCO-GO = 20 mg, desorption solvent = acetone, extraction time = 10 min, desorption time = 10 min, sample pH = 6.5 and sample volume = 15 mL) on the extraction efficiency of mixture PAEs and PAHs

The extraction and desorption time play an important role in the adsorption and desorption process. In order to achieve good extraction efficiency, the extraction time was varied from 5 min to 30 min in order to find the optimum time to use. As evident from Figure 4.62(A), 10 min resulted in the best extraction efficacies for all studied PAEs-

University of Malaya

PAHs mixture. No significant improvement is observed when the extraction time is prolonged to 30 min. This phenomenon may be attributed to the fact that there are many accessible sites to interact with the PAEs-PAHs at the beginning, and extraction proceeds easily. As time went on, more active sites become occupied, so the extraction rate becomes slower (Huang *et al*., 2015). After 10 mins, the active sites saturate and the extraction rate no longer increases. Therefore, 10 min is chosen as the optimum extraction time. The desorption time was also varied from 3 to 15 min in order to find the optimum time to use (Figure 4.62(B)). The result reveals that as the desorption time is increased from 3 to 10 min, the desorption rate for all analytes increases and further increase in the desorption time does not significantly increase the extraction efficacies. This phenomenon can be explained by the large interfacial area between the solid adsorbent and desorption solvent allowing the desorption rate to stabilize rapidly (Luo *et al*., 2012). Thus, 10 min is chosen as the optimum extraction and desorption time in following experiments.

University of Malaya

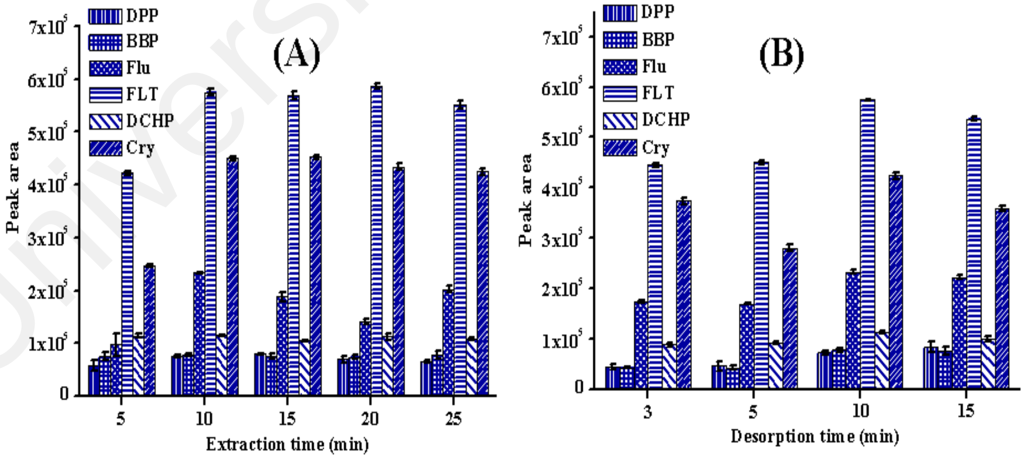

Figure 4.62: The effects of (A) extraction time (Amount of MNP@FFAs-WPCO-GO = 20 mg, desorption solvent = acetone, volume of desorption solvent = 2.0 mL, desorption time = 10 min, sample pH = 6.5 and sample volume = 15 mL) and (B) desorption time (Amount of MNP@FFAs-WPCO-GO = 20 mg, desorption solvent = acetone, volume of desorption solvent = 2.0 mL, extraction time = 10 min, sample pH = 6.5 and sample volume = 15 mL) on the extraction efficiency of mixture PAEs and PAHs

pH of sample solution is an important parameter to consider as it greatly affects the surface charge and binding sites of the adsorbent and the stability of the target analytes during the extraction process. In this study, the sample pH was varied from 3 to 9 and the effect on PAEs-PAHs extraction was examined. Figure 4.63 shows that there is no obvious variation for the recoveries of the targeted mixture of PAEs-PAHs when the solution pH was varied in the range of 3-9. The adsorption of PAHs and PAEs are unaffected by the surface charge of the adsorbent as they are neutral molecules under ordinary conditions (Zhang *et al*., 2010). This is in good agreement with the experiment results obtained in a work published by Zhang *et al*. (2010). Hence, pH 6.5 which is the natural pH of the sample is used in subsequent experiments.

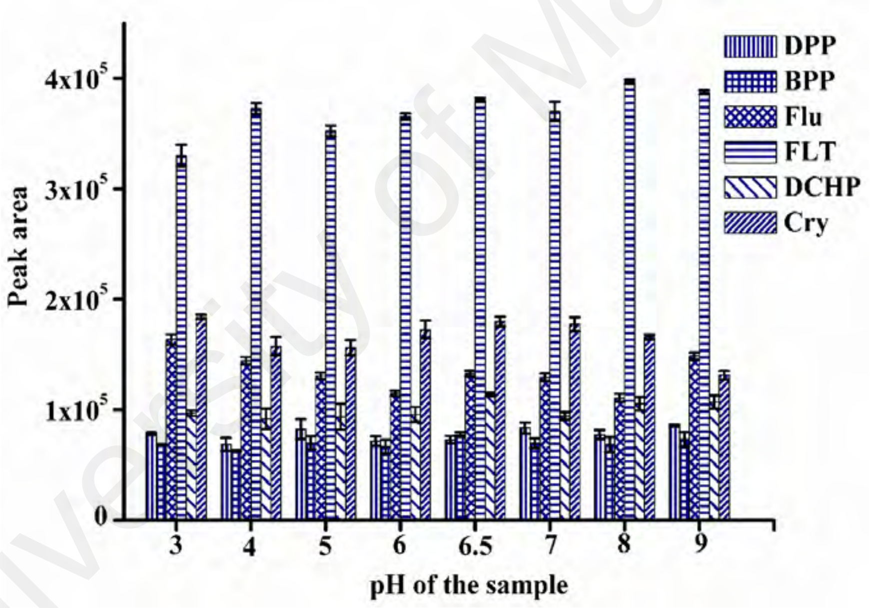

Figure 4.63: The effect of solution pH on the extraction efficiency of mixture PAEs and PAHs. (Amount of MNP@FFAs-WPCO-GO = 20 mg, desorption solvent = acetone, volume of desorption solvent = 2.0 mL, extraction time = 10 min, desorption time = 10 min and sample volume = 15 mL)

The sample volume of the target analytes also affects the efficacy of extraction. In this study, the effect of sample volume ranging from 15 to 250 mL was studied. Figure 4.64 shows that as the sample volume is increased up to 200 mL, extraction efficacy becomes higher. Further increase in sample volume does not alter the extraction efficacy due to the

University of Malaya

active sites on MNP@FFAs-WPCO-GO becoming saturated. 200 mL is therefore chosen as optimum sample loading.

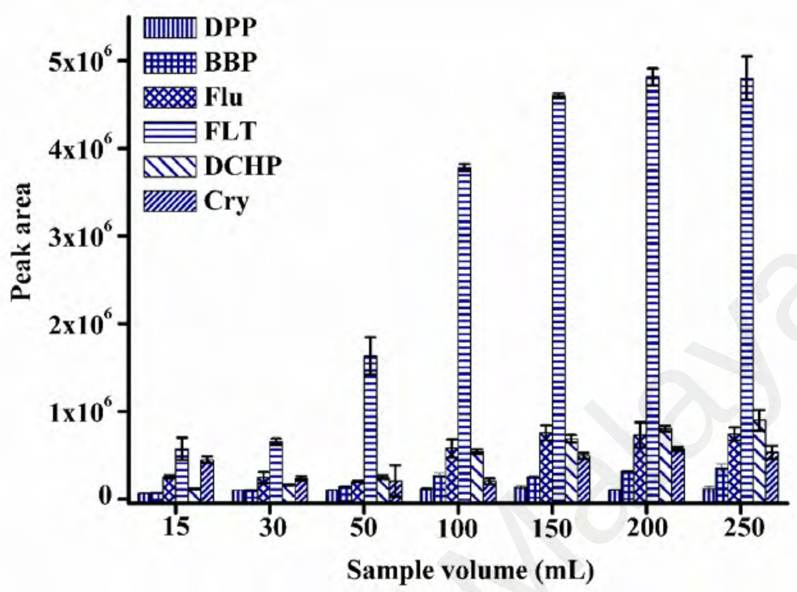

Figure 4.64: The effect of sample volume on the extraction efficiency of mixture PAEs and PAHs. (Amount of MNP@FFAs-WPCO-GO = 20 mg, desorption solvent = acetone, volume of desorption solvent = 2.0 mL, extraction time = 10 min, desorption time = 10 min and sample pH = 6.5)

Reusability is an important factor to consider when estimating the efficacy of a magnetic sorbent. In order to evaluate the reusability of the MSPE sorbent, spent MNP@FFAs-WPCO-GO was washed with acetone several times and then dried before being used in subsequent MSPE experiments. As Figure 4.65 shows, the prepared MNP@FFAs-WPCO-GO is reusable at least five times without obvious loss in the adsorption capacity and magnetic property, suggesting the regeneration efficacy and stability of the MSPE adsorbent.

University of Malaya

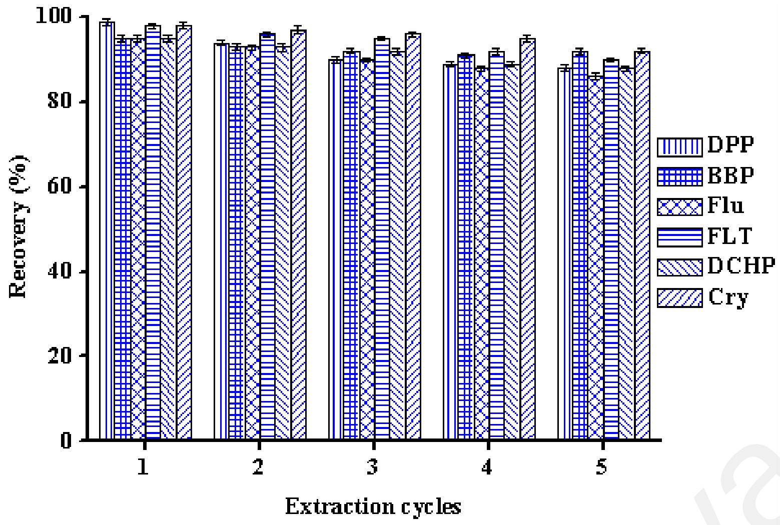

Figure 4.65: Reusability of the MNP@FFAs-WPCO-GO for extraction of mixture PAEs and PAHs

On the basis of the above conditions, the optimum extraction conditions is therefore as follows; 20 mg MNP@FFAs-WPCO-GO particles is added into 200 mL sample solution. Extraction is allowed to proceed for 10 min and then the adsorbent is removed. The adsorbed PAHs and PAEs is then desorbed using 2.0 mL acetone for 10 min.

The quantitative parameters of the developed method such as linear range, LOD, LOQ and precision was then validated by experiment and tabulated in Table 4.13. The coefficient of determination is found to be satisfactory, ranging from 0.9900 to 0.9948 with the linear range of PAEs and PAHs being between 1-1000 ng mL^{-1} and 0.1-1000 ng mL^{-1}, respectively. The LOD and LOQ were determined when the signal-to-noise ratio is 3 and 10, respectively. In this study, The LODs for the selected PAEs and PAHs are 0.56-0.97 ng mL^{-1} and 0.02-0.93 ng mL^{-1}, respectively while the LOQ for PAEs and PAHs are in the range of 1.86 to 3.2 ng mL^{-1} and 0.07 to 3.10 ng mL^{-1}, respectively. Additionally, the results for the extraction of PAEs and PAHs are reproducible as their intra-day RSDs are low, being in the range of 2.4 to 5.4% and 2.4 to 3.5%, respectively and the inter-day RSDs, in the range of 2.0 to 4.5% and 2.1 to 4.1%, respectively.

University of Malaya

Table 4.13: Analytical performance for HPLC-DAD determination of PAEs and PAHs using MNP@FFAs-WPCO-GO

Analyte	Linearity LDR(ng mL^{-1})	R^2	LOD (ng mL^{-1})	LOQ (ng mL^{-1})	Precision Intra-day (RSD% n = 7)	Precision Inter-day (RSD% n = 3)
DPP	1-1000	0.9923	0.97	3.2	2.4	2.0
BBP	1-1000	0.9904	0.56	1.86	5.4	3.8
DCHP	1-1000	0.9944	0.94	3.14	3.7	4.5
Flu	1-1000	0.9928	0.93	3.10	2.4	4.1
FLT	0.1-1000	0.9900	0.04	0.13	2.7	2.1
Cry	0.1-1000	0.9948	0.02	0.07	3.5	3.5

The potential application of MNP@FFAs-WPCO–GO material for the determination of the selected PAHs and PAEs in real samples such as cabbage, apple and landfill sludge samples was investigated. No PAEs and PAHs were found in these real samples. Table 4.14 shows the recoveries of PAEs and PAHs from various matrices are in the range of 81.5% -118.2% with good RSDs (n=5) less than 10% and 86.7% to 118.8% with acceptable RSDs (n=5) ranging from 1.5% to 10.4%, respectively. The result is a testament to the accuracy of the currently developed method. The typical HPLC-DAD chromatogram of blank and spiked landfill sludge is displayed in Figure 4.66. The proposed extraction method was also applied for the analysis of various apples samples, including USA Red Rome, US Royal Gala, US Red Del, USA Jonagold, China Fuji apples and landfill sludge samples from different areas such as Taman Beringin and Bukit Beruntung. However, no PAEs and PAHs were detected in all samples, suggesting that the presence of PAEs and PAHs in the samples were below the LOD of the current method, MSPE/HPLC-MNP@FFAs-WPCO-GO.

University of Malaya

Table 4.14: The recoveries and standard deviations of PAEs and PAHs in real apple, cabbage and landfill sludge samples

Analyte	Spiked (ng mL^{-1})	Apple ($n = 5$)		Cabbage ($n = 5$)		Landfill sludge ($n = 5$)	
		Recovery (%)	RSD (%)	Recovery (%)	RSD (%)	Recovery (%)	RSD (%)
DPP	1000	81.5	2.3	98.7	3.7	91.0	4.4
	100	111.1	3.2	111.7	4.8	101.2	7.0
	50	104.5	6.4	108.2	4.0	114.7	3.6
BBP	1000	84.1	2.1	107.6	2.1	85.2	3.5
	100	100.3	5.0	103.7	6.0	115.7	4.4
	50	84.0	6.8	117.6	9.9	108.6	3.0
DCHP	1000	83.3	4.6	103.0	7.2	101.0	4.7
	100	105.0	9.5	114.3	6.5	100.5	7.0
	50	104.0	6.6	96.9	6.	118.2	5.0
Flu	1000	86.7	8.3	106.9	5.4	101.0	4.7
	100	105.3	7.3	87.7	7.9	115.1	4.1
	50	107.6	3.8	113.4	5.7	118.3	4.0
FLT	100	114.8	1.5	94.8	5.0	93.5	4.5
	10	118.8	2.0	106.7	8.7	105.7	9.1
	1	114.0	2.2	104.3	10.4	110.8	8.3
Cry	100	110.4	6.7	101.4	6.1	110.7	9.6
	10	105.7	7.8	90.8	11.0	112.3	3.0
	1	98.9	9.5	93.0	4.7	102.2	6.1

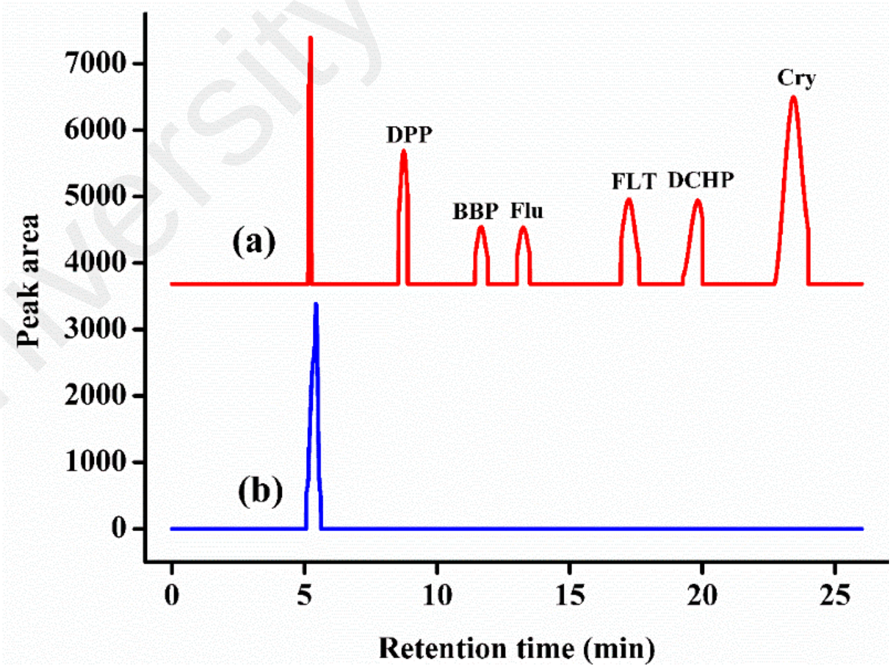

Figure 4.66: Chromatogram of landfill sludge using MNP@FFAs-WPCO-GO as the MSPE adsorbent spiked with (a) 100 ng mL^{-1} of DPP, BBP, Flu and DCHP and 10 ng mL^{-1} of FLT and Cry and (b) unspiked landfill sludge

University of Malaya

The performance of the present system (MSPE/HPLC-DAD/ MNP@FFAs-WPCO-GO) was compared with works in literature with respect to recovery and LOD. The present work is the first attempt for magnetic solid phase extraction of simultaneous determination of PAHs and PAEs in apple, cabbage and landfill sludge samples. Table 4.15 reveal that the present method used in this study have lower LODs and comparable recoveries with other reported MSPE adsorbents.

University of Malaya

Table 4.15: Comparison of the developed MSPE adsorbent with other literature MSPE adsorbents for determination of PAEs and PAHs

Analyte	Technique/adsorbent	Matrix	%Recovery	LODs (ng mL^{-1})	Ref.
PAHs	MSPE-HPLC/MNP@CN/IL	Leachate-sludge	89.50-110.2	0.40–0.59	(Bakhshaei *et al*., 2016)
PAHs	MSPE-GC/OPA-MMNPs	Tap water-river water-hospital sewage	61.9-119.1	0.014-0.07	(Ding *et al*., 2010)
PAHs	MSPE-HPLC/Fe_3O_4-GO	Tap water-river water-seawater	76.8-103.2	0.09-0.19	(Han *et al*., 2012)
PAEs	MSPE-HPLC/G-Fe_3O_4	Water and beverage	82.0-106.0	0.01-0.04	(Wu *et al*., 2012)
PAEs	MSPE-HPLC/Fe_3O_4@SiO_2-G	River water-reservoir water-soybean milk	87.2-109.0	0.15-0.30	(Wang *et al*., 2013)
PAEs	MSPE-GC/MNP@P3TArH	Bottled mineral water-bottled fresh milk	68-101	0.08-0.468	(Baharin *et al*., 2016)
PAEs-PAHs	MSPE-HPLC/ MNP@FFAs-WPCO-GO	Fruit-vegetable-sludge	81.5-118.8	0.02-0.97	This study

University of Malaya

The proposed adsorbent shows excellent adsorption capacity for PAEs and PAHs as it provides many adsorption sites through hydrogen bonding, hydrophobic, and π–π interactions. When combined with HPLC-DAD, the MSPE- MNP@FFAs-WPCO-GO method can be used to detect selected PAEs and PAHs with LOD as low as 0.56-0.97 ng mL^{-1} and 0.02-0.93 ng mL^{-1}, respectively. Satisfactory recoveries are obtained for PAEs and PAHs from various matrices are in the range of 81.5% -118.2% with good RSDs (n=5) less than 10% and 86.7% to 118.8% with acceptable RSDs (n=5) ranging from 1.5% to 11.0%, respectively. The reusability test revealed that MNP@FFAs-WPCO-GO have good stability and can be reused consistently up to five times. These remarkable features make MNP@FFAs-WPCO-GO a potential adsorbent for the separation, purification, and pre-concentration of environmental pollutants from complex matrices.

University of Malaya

CHAPTER 5: CONCLUSIONS AND FUTURE DIRECTION

5.1 Conclusion

New adsorbents MNP@FFAs-PCO, MNP@FFAs-WPCO and MNP@FFAs-WPCO-GO for the adsorption of organic pollutants. In the present investigation, MNP@FFAs-PCO and MNP@FFAs-WPCO were successfully characterized and applied as a MSPE adsorbent for the enrichment of targeted PAHs in landfill leachate and sludge samples prior to HPLC-DAD detection. Due to good hydrophobic interaction of the fabricated adsorbents with studied PAHs, high adsorption capacity and extraction efficiency were achieved during extraction process. The obtained LOD of all selected PAHs for MNP@FFAs-PCO and MNP@FFAs-WPCO were in the range of 0.01-0.05 ng mL^{-1} and 0.001 to 0.05 ng mL^{-1}, respectively with limit of quantification (LOQ) in the range of 0.03-0.16 ng mL^{-1} and 0.004-0.2 ng mL^{-1}, respectively. The application of MNP@FFAs-PCO and MNP@FFAs-WPCO for environmental samples were successfully studied on the leachate and sludge from landfill site. The MNP@FFAs-PCO recorded good recovery (81.1-119.3%) with satisfactory precision (%RSD: 3.1–13.6), meanwhile MNP@FFAs-WPCO showed satisfactory recovery (72.3–119.9%) with acceptable precision (%RSD: 4.8–11.8).

Additionally, the current study revealed that the magnetically retrievable MNP@FFAs-PCO and MNP@FFAs-WPCO are also promising adsorbents for removal of oil from aqueous solution because of their strong hydrophobic framework. The results showed that MNP@FFAs-PCO and MNP@FFAs-WPCO could adsorb 3.50 times and 4.31 times of oil higher than their own weight, respectively. Moreover, they are environment durability which enable them to work even under harsh environment. The recyclability result showed that MNP@FFAs-PCO and MNP@FFAs-WPCO can still adsorb oil 2.3 times and 3.11 times of their own weight, respectively even after 6th cycle.

University of Malaya

The MNP@FFAs-WPCO is shown to be an excellent MSPE adsorbent as it has a low LOD for selected PAHs and good oil sorption capacity compared to MNP@FFAs-PCO. This is because of its larger surface area and higher hydrophobicity of MNP@FFAs-WPCO which improved the adsorption of oil and PAHs on its framework.

MNP@FFAs-WPCO is then immobilized onto GO to form MNP@FFAs-WPCO-GO. The proposed adsorbent provided hydrogen bonding, π-π and hydrophobic interactions which improves the extraction capabilities for PAHs and PAEs. The developed method showed excellent adsorption capacity towards PAEs and PAHs as it provided adsorption sites through hydrogen bonding, hydrophobic and π–π interactions. The MSPE-MNP@FFAs-WPCO-GO method provided low LODs (0.02 – 0.93 ng mL^{-1} for PAHs) and (0.56 – 0.97 ng mL^{-1} for PAEs) and LOQs in the range of (0.07 to 3.10 ng mL^{-1} for PAHs) and (1.86 to 3.20 ng mL^{-1} for PAEs). The application of MNP@FFAs-WPCO-GO was successfully studied on apple, cabbage and landfill sludge samples. High recoveries (81.5 – 118.2% for PAEs) and (86.7 – 118.8% for PAHs) with satisfactory precision (%RSD: 2.1 to 9.9 for PAEs; 1.5 to 11.0 for PAHs) were obtained.

5.2 Future direction

A further study on the use of MNP@FFAs-PCO, MNP@FFAs-WPCO and MNP@FFAs-WPCO-GO to adsorb other organic contaminants should be carried out. In addition, the coating agent used in this study could be used to coat other solid supports so that it can be employed for other sample preparation technique. This alternative is very important into developing various analytical techniques for the determination of trace organic contaminants in real samples.

University of Malaya

REFERENCES

Ahmad, A. L., Sumathi, S., & Hameed, B. H. (2005). Adsorption of residue oil from palm oil mill effluent using powder and flake chitosan: equilibrium and kinetic studies. *Water Research*, *39*(12), 2483-2494.

Ahmadi, F., Mahmoudi-Yamchi, T., & Azizian, H. (2018). Super paramagnetic core–shells anchored onto silica grafted with C_8/NH_2 nano-particles for ultrasound-assisted magnetic solid phase extraction of imipramine and desipramine from plasma. *Journal of Chromatography B*, *1077*, 52-59.

Asuha, S., Suyala, B., Siqintana, X., & Zhao, S. (2011). Direct synthesis of Fe_3O_4 nanopowder by thermal decomposition of Fe–urea complex and its properties. *Journal of Alloys and Compounds*, *509*(6), 2870-2873.

Awalludin, M. F., Sulaiman, O., Hashim, R., & Nadhari, W. N. A. W. (2015). An overview of the oil palm industry in Malaysia and its waste utilization through thermochemical conversion, specifically via liquefaction. *Renewable and Sustainable Energy Reviews*, *50*, 1469-1484.

Baharin, S. N. A., Muhamad Sarih, N., & Mohamad, S. (2016). Novel Functionalized Polythiophene-Coated Fe_3O_4 Nanoparticles for Magnetic Solid-Phase Extraction of Phthalates. *Polymers*, *8*(5), 117.

Bai, L., Mei, B., Guo, Q. Z., Shi, Z. G., & Feng, Y. Q. (2010). Magnetic solid-phase extraction of hydrophobic analytes in environmental samples by a surface hydrophilic carbon-ferromagnetic nanocomposite. *Journal of Chromatography A*, *1217*(47), 7331-7336.

Bakhshaei, S., Kamboh, M. A., Nodeh, H. R., Zain, S. M., Rozi, S. K. M., Mohamad, S., & Mohialdeen, I. A. M. (2016). Magnetic solid phase extraction of polycyclic aromatic hydrocarbons and chlorophenols based on cyano-ionic liquid functionalized magnetic nanoparticles and their determination by HPLC-DAD. *RSC Advances*, *6*(80), 77047-77058.

Ballesteros-Goḿ z, A., & Rubio, S. (2009). Hemimicelles of alkyl carboxylates chemisorbed onto magnetic nanoparticles: study and application to the extraction of carcinogenic polycyclic aromatic hydrocarbons in environmental water samples. *Analytical Chemistry*, *81*(21), 9012-9020.

Banerjee, A., Gokhale, R., Bhatnagar, S., Jog, J., Bhardwaj, M., Lefez, B., Hannoyer, B., & Ogale, S. (2012). MOF derived porous carbon–Fe_3O_4 nanocomposite as a high

University of Malaya

performance, recyclable environmental superadsorbent. *Journal of Materials Chemistry*, *22*(37), 19694-19699.

Bhattacharyya, K. G., & Gupta, S. S. (2006). Pb (II) uptake by kaolinite and montmorillonite in aqueous medium: influence of acid activation of the clays. *Colloids and Surfaces A: Physicochemical and Engineering Aspects*, *277*(1), 191-200.

Bianchi, F., Chiesi, V., Casoli, F., Luches, P., Nasi, L., Careri, M., & Mangia, A. (2012). Magnetic solid-phase extraction based on diphenyl functionalization of Fe_3O_4 magnetic nanoparticles for the determination of polycyclic aromatic hydrocarbons in urine samples. *Journal of Chromatography A*, *1231*, 8-15.

Can, K., Ozmen, M., & Ersoz, M. (2009). Immobilization of albumin on aminosilane modified superparamagnetic magnetite nanoparticles and its characterization. *Colloids and Surfaces B: Biointerfaces*, *71*(1), 154-159.

Chen, F., Xie, S., Zhang, J., & Liu, R. (2013). Synthesis of spherical Fe_3O_4 magnetic nanoparticles by co-precipitation in choline chloride/urea deep eutectic solvent. *Materials Letters*, *112*, 177-179.

Chen, M., Jiang, W., Wang, F., Shen, P., Ma, P., Gu, J., Mao, J., & Li, F. (2013). Synthesis of highly hydrophobic floating magnetic polymer nanocomposites for the removal of oils from water surface. *Applied Surface Science*, *286*, 249-256.

Chu, Y., & Pan, Q. (2012). Three-dimensionally macroporous Fe/C nanocomposites as highly selective oil-absorption materials. *ACS Applied Materials & Interfaces*, *4*(5), 2420-2425.

Cortazar, E., Zuloaga, O., Sanz, J., Raposo, J. C., Etxebarria, N., & Fernandez, L. A. (2002). MultiSimplex optimisation of the solid-phase microextraction–gas chromatographic–mass spectrometric determination of polycyclic aromatic hydrocarbons, polychlorinated biphenyls and phthalates from water samples. *Journal of Chromatography A*, *978*(1), 165-175.

Dias, A. M. G. C., Hussain, A., Marcos, A. S., & Roque, A. C. A. (2011). A biotechnological perspective on the application of iron oxide magnetic colloids modified with polysaccharides. *Biotechnology Advances*, *29*(1), 142-155.

Ding, J., Gao, Q., Luo, D., Shi, Z. G., & Feng, Y. Q. (2010). *n*-Octadecylphosphonic acid grafted mesoporous magnetic nanoparticle: Preparation, characterization, and application in magnetic solid-phase extraction. *Journal of Chromatography A*, *1217*(47), 7351-7358.

University of Malaya

Długosz, J. (2013). Selected methods of treatment of leachate from municipal landfills– for review. *Archives of Waste Management and Environmental Protection*, *15*(2), 59-68.

Du, X., He, J., Zhu, J., Sun, L., & An, S. (2012). Ag-deposited silica-coated Fe_3O_4 magnetic nanoparticles catalyzed reduction of p-nitrophenol. *Applied Surface Science*, *258*(7), 2717-2723.

Eigler, S., Dotzer, C., Hirsch, A., Enzelberger, M., & Müller, P. (2012). Formation and decomposition of CO_2 intercalated graphene oxide. *Chemistry of Materials*, *24*(7), 1276-1282.

Farah, J. Y., El-Gendy, N. S., & Farahat, L. A. (2007). Biosorption of Astrazone Blue basic dye from an aqueous solution using dried biomass of Baker's yeast. *Journal of Hazardous Materials*, *148*(1), 402-408.

Feás, C. P., Alonso, M. B., Pena-Vazquez, E., Hermelo, P. H., & Bermejo-Barrera, P. (2008). Phthalates determination in physiological saline solutions by HPLC–ES-MS. *Talanta*, *75*(5), 1184-1189.

Feng, B., Hong, R. Y., Wang, L. S., Guo, L., Li, H. Z., Ding, J., Zhang, Y., & Wei, D. G. (2008). Synthesis of Fe_3O_4/APTES/PEG diacid functionalized magnetic nanoparticles for MR imaging. *Colloids and Surfaces A: Physicochemical and Engineering Aspects*, *328*(1), 52-59.

Font, H., Adrian, J., Galve, R., Estévez, M. C., Castellari, M., Gratacós-Cubarsí, M., Sanchez-Baeza, F., & Marco, M. P. (2008). Immunochemical assays for direct sulfonamide antibiotic detection in milk and hair samples using antibody derivatized magnetic nanoparticles. *Journal of Agricultural and Food Chemistry*, *56*(3), 736-743.

Ge, B., Zhang, Z., Zhu, X., Ren, G., Men, X., & Zhou, X. (2013). A magnetically superhydrophobic bulk material for oil removal. *Colloids and Surfaces A: Physicochemical and Engineering Aspects*, *429*, 129-133.

Ge, F., Li, M. M., Ye, H., & Zhao, B. X. (2012). Effective removal of heavy metal ions Cd^{2+}, Zn^{2+}, Pb^{2+}, Cu^{2+} from aqueous solution by polymer-modified magnetic nanoparticles. *Journal of Hazardous Materials*, *211*, 366-372.

Gill, C. S., Price, B. A., & Jones, C. W. (2007). Sulfonic acid-functionalized silica-coated magnetic nanoparticle catalysts. *Journal of Catalysis*, *251*(1), 145-152.

Gu, J., Jiang, W., Wang, F., Chen, M., Mao, J., & Xie, T. (2014). Facile removal of oils from water surfaces through highly hydrophobic and magnetic polymer nanocomposites. *Applied Surface Science*, *301*, 492-499.

University of Malaya

Han, Q., Wang, Z., Xia, J., Chen, S., Zhang, X., & Ding, M. (2012). Facile and tunable fabrication of Fe_3O_4/graphene oxide nanocomposites and their application in the magnetic solid-phase extraction of polycyclic aromatic hydrocarbons from environmental water samples. *Talanta*, *101*, 388-395.

Hao, L., Wang, C., Ma, X., Wu, Q., Wang, C., & Wang, Z. (2014). Magnetic three-dimensional graphene solid-phase extraction coupled with high performance liquid chromatography for the determination of phthalate esters in fruit juice. *Analytical Methods*, *6*(15), 5659-5665.

He, F., Fan, J., Ma, D., Zhang, L., Leung, C., & Chan, H. L. (2010). The attachment of Fe_3O_4 nanoparticles to graphene oxide by covalent bonding. *Carbon*, *48*(11), 3139-3144.

Hsu, R. S., Chang, W. H., & Lin, J. J. (2010). Nanohybrids of magnetic iron-oxide particles in hydrophobic organoclays for oil recovery. *ACS Applied Materials & Interfaces*, *2*(5), 1349-1354.

Huang, Y., Wang, Y., Pan, Q., Wang, Y., Ding, X., Xu, K., Li. N., & Wen, Q. (2015). Magnetic graphene oxide modified with choline chloride-based deep eutectic solvent for the solid-phase extraction of protein. *Analytica Chimica Acta*, *877*, 90-99.

Ibrahim, S., Wang, S., & Ang, H. M. (2010). Removal of emulsified oil from oily wastewater using agricultural waste barley straw. *Biochemical Engineering Journal*, *49*(1), 78-83.

Isha, A., Yusof, N. A., Ahmad, M., Suhendra, D., Yunus, W. M. Z. W., & Zainal, Z. (2006). A chemical sensor for trace V(V) ion determination based on fatty hydroxamic acid immobilized in polymethylmethacrylate. *Sensors and Actuators B: Chemical*, *114*(1), 344-349.

Isha, A., Yusof, N. A., Ahmad, M., Suhendra, D., Yunus, W. M. Z. W., & Zainal, Z. (2007). Optical fibre chemical sensor for trace vanadium (V) determination based on newly synthesized palm based fatty hydroxamic acid immobilized in polyvinyl chloride membrane. *Spectrochimica Acta Part A: Molecular and Biomolecular Spectroscopy*, *67*(5), 1398-1402.

Jadhav, S. V., Nikam, D. S., Khot, V. M., Thorat, N. D., Phadatare, M. R., Ningthoujam, R. S., Salunkhe, A.B., & Pawar, S. H. (2013). Studies on colloidal stability of PVP-coated LSMO nanoparticles for magnetic fluid hyperthermia. *New Journal of Chemistry*, *37*(10), 3121-3130.

Jang, J. H., & Lim, H. B. (2010). Characterization and analytical application of surface modified magnetic nanoparticles. *Microchemical Journal*, *94*(2), 148-158.

University of Malaya

Janoszka, B., Warzecha, L., Blaszczyk, U., & Bodzek, D. (2004). Organic compounds formed in thermally treated high-protein food. Part I: Polycyclic aromatic hydrocarbons. *Acta Chromatographica*, 115-128.

Japir, A. A. W., Salimon, J., Derawi, D., Bahadi, M., & Yusop, M. R. (2016, November). Separation of free fatty acids from high free fatty acid crude palm oil using short-path distillation. In *AIP Conference Proceedings* (Vol. 1784, No. 1, p. 030001). AIP Publishing.

Jawad, A. H., Islam, M. A., & Hameed, B. H. (2017). Cross-linked chitosan thin film coated onto glass plate as an effective adsorbent for adsorption of reactive orange 16. *International Journal of Biological Macromolecules*, *95*, 743-749.

Jiao, Y., Fu, S., Ding, L., Gong, Q., Zhu, S., Wang, L., & Li, H. (2012). Determination of trace leaching phthalate esters in water by magnetic solid phase extraction based on magnetic multi-walled carbon nanotubes followed by GC-MS/MS. *Analytical Methods*, *4*(9), 2729-2734.

Ju, J. H., Lee, I. S., Sim, W. J., Eun, H., & Oh, J. E. (2009). Analysis and evaluation of chlorinated persistent organic compounds and PAHs in sludge in Korea. *Chemosphere*, *74*(3), 441-447.

Kassaee, M. Z., Motamedi, E., & Majdi, M. (2011). Magnetic Fe_3O_4-graphene oxide/polystyrene: fabrication and characterization of a promising nanocomposite. *Chemical Engineering Journal*, *172*(1), 540-549.

Kazerouni, N., Sinha, R., Hsu, C. H., Greenberg, A., & Rothman, N. (2001). Analysis of 200 food items for benzo[a] pyrene and estimation of its intake in an epidemiologic study. *Food and Chemical Toxicology*, *39*(5), 423-436.

Kim, E. H., Lee, H. S., Kwak, B. K., & Kim, B. K. (2005). Synthesis of ferrofluid with magnetic nanoparticles by sonochemical method for MRI contrast agent. *Journal of Magnetism and Magnetic Materials*, *289*, 328-330.

Kim, K. H., Jahan, S. A., Kabir, E., & Brown, R. J. (2013). A review of airborne polycyclic aromatic hydrocarbons (PAHs) and their human health effects. *Environment International*, *60*, 71-80.

Knothe, G., & Steidley, K. R. (2009). A comparison of used cooking oils: a very heterogeneous feedstock for biodiesel. *Bioresource Technology*, *100*(23), 5796-5801.

Konieczka, P., & Namiesnik, J. (2016). *Quality Assurance and Quality Control in the Analytical Chemical Laboratory: A Practical Approach*. CRC Press.

University of Malaya

Kulkarni, M. G., & Dalai, A. K. (2006). Waste cooking oil an economical source for biodiesel: a review. *Industrial & Engineering Chemistry Research*, *45*(9), 2901-2913.

Kumar, R., Inbaraj, B. S., & Chen, B. H. (2010). Surface modification of superparamagnetic iron nanoparticles with calcium salt of poly (γ-glutamic acid) as coating material. *Materials Research Bulletin*, *45*(11), 1603-1607.

Lam, M. K., Lee, K. T., & Mohamed, A. R. (2010). Homogeneous, heterogeneous and enzymatic catalysis for transesterification of high free fatty acid oil (waste cooking oil) to biodiesel: a review. *Biotechnology Advances*, *28*(4), 500-518.

Li, M., Jiao, C., Yang, X., Wang, C., Wu, Q., & Wang, Z. (2017). Magnetic N-doped mesoporous carbon as an adsorbent for the magnetic solid-phase extraction of phthalate esters from soft drinks. *Journal of Separation Science*, *40*(8), 1637-1643.

Li, X. S., Zhu, G. T., Luo, Y. B., Yuan, B. F., & Feng, Y. Q. (2013). Synthesis and applications of functionalized magnetic materials in sample preparation. *TrAC Trends in Analytical Chemistry*, *45*, 233-247.

Li, X., Chen, G., Ma, Y., Feng, L., Zhao, H., Jiang, L., & Wang, F. (2006). Preparation of a super-hydrophobic poly (vinyl chloride) surface via solvent–nonsolvent coating. *Polymer*, *47*(2), 506-509.

Li, Y., Chu, J., Qi, J., & Li, X. (2011). An easy and novel approach for the decoration of graphene oxide by Fe3O4 nanoparticles. *Applied Surface Science*, *257*(14), 6059-6062.

Liu, J. F., Zhao, Z. S., & Jiang, G. B. (2008). Coating Fe_3O_4 magnetic nanoparticles with humic acid for high efficient removal of heavy metals in water. *Environmental Science & Technology*, *42*(18), 6949-6954.

Liu, Q., Shi, J., Cheng, M., Li, G., Cao, D., & Jiang, G. (2012). Preparation of graphene-encapsulated magnetic microspheres for protein/peptide enrichment and MALDI-TOF MS analysis. *Chemical Communications*, *48*(13), 1874-1876.

Liu, Q., Shi, J., Wang, T., Guo, F., Liu, L., & Jiang, G. (2012). Hemimicelles/admicelles supported on magnetic graphene sheets for enhanced magnetic solid-phase extraction. *Journal of Chromatography A*, *1257*, 1-8.

Liu, Y., Li, H., & Lin, J. M. (2009). Magnetic solid-phase extraction based on octadecyl functionalization of monodisperse magnetic ferrite microspheres for the determination of polycyclic aromatic hydrocarbons in aqueous samples coupled with gas chromatography–mass spectrometry. *Talanta*, *77*(3), 1037-1042.

University of Malaya

Lotfi, Z., Mousavi, H. Z., & Sajjadi, S. M. (2016). Covalently bonded double-charged ionic liquid on magnetic graphene oxide as a novel, efficient, magnetically separable and reusable sorbent for extraction of heavy metals from medicine capsules. *RSC Advances*, *6*(93), 90360-90370.

Lu, A. H., Salabas, E. E., & Schüth, F. (2007). Magnetic nanoparticles: synthesis, protection, functionalization, and application. *Angewandte Chemie International Edition*, *46*(8), 1222-1244.

Luo, X., Zhang, F., Ji, S., Yang, B., & Liang, X. (2014). Graphene nanoplatelets as a highly efficient solid-phase extraction sorbent for determination of phthalate esters in aqueous solution. *Talanta*, *120*, 71-75.

Luo, Y. B., Yu, Q. W., Yuan, B. F., & Feng, Y. Q. (2012). Fast microextraction of phthalate acid esters from beverage, environmental water and perfume samples by magnetic multi-walled carbon nanotubes. *Talanta*, *90*, 123-131.

Ma, Y. X., Li, Y. F., Zhao, G. H., Yang, L. Q., Wang, J. Z., Shan, X., & Yan, X. (2012). Preparation and characterization of graphite nanosheets decorated with Fe_3O_4 nanoparticles used in the immobilization of glucoamylase. *Carbon*, *50*(8), 2976-2986.

Mahmoud, M. E., Ahmed, S. B., Osman, M. M., & Abdel-Fattah, T. M. (2015). A novel composite of nanomagnetite-immobilized-baker’s yeast on the surface of activated carbon for magnetic solid phase extraction of Hg (II). *Fuel*, *139*, 614-621.

Mahpishanian, S., Sereshti, H., & Baghdadi, M. (2015). Superparamagnetic core–shells anchored onto graphene oxide grafted with phenylethyl amine as a nano-adsorbent for extraction and enrichment of organophosphorus pesticides from fruit, vegetable and water samples. *Journal of Chromatography A*, *1406*, 48-58.

Maity, D., & Agrawal, D. C. (2007). Synthesis of iron oxide nanoparticles under oxidizing environment and their stabilization in aqueous and non-aqueous media. *Journal of Magnetism and Magnetic Materials*, *308*(1), 46-55.

Marquez, F., Morant, C., Sanz, J. M., & Elizalde, E. (2009). Attachment of magnetite nanoparticles on carbon nanotubes bundles and their response to magnetic fields. *Journal of Nanoscience and Nanotechnology*, *9*(6), 3810-3814.

McAllister, M. J., Li, J. L., Adamson, D. H., Schniepp, H. C., Abdala, A. A., Liu, J., Alonso, M.H., Milius, D.V., Car, R., & Aksay, I. A. (2007). Single sheet functionalized graphene by oxidation and thermal expansion of graphite. *Chemistry of Materials*, *19*(18), 4396-4404.

University of Malaya

Mehdinia, A., Khodaee, N., & Jabbari, A. (2015). Fabrication of graphene/Fe_3O_4@ polythiophene nanocomposite and its application in the magnetic solid-phase extraction of polycyclic aromatic hydrocarbons from environmental water samples. *Analytica Chimica Acta*, *868*, 1-9.

Mirshahghassemi, S., Ebner, A. D., Cai, B., & Lead, J. R. (2017). Application of high gradient magnetic separation for oil remediation using polymer-coated magnetic nanoparticles. *Separation and Purification Technology*, *179*, 328-334.

Moazed, H., & Viraraghavan, T. (2005). Use of organo-clay/anthracite mixture in the separation of oil from oily waters. *Energy Sources*, *27*(1-2), 101-112.

Moazzen, M., Ahmadkhaniha, R., Gorji, M. E. H., Yunesian, M., & Rastkari, N. (2013). Magnetic solid-phase extraction based on magnetic multi-walled carbon nanotubes for the determination of polycyclic aromatic hydrocarbons in grilled meat samples. *Talanta*, *115*, 957-965.

Mohamad, S., Wan Yunus, W. M. Z., Haron, M. J., Rahman, A., & Zaki, M. (2008). Extraction and separation of molybdenum (VI) from acidic media by fatty hydrazides. *Journal of Chemical Technology and Biotechnology*, *83*(11), 1565-1569.

Mürbe, J., Rechtenbach, A., & Töpfer, J. (2008). Synthesis and physical characterization of magnetite nanoparticles for biomedical applications. *Materials Chemistry and Physics*, *110*(2), 426-433.

Mysore, D., Viraraghavan, T., & Jin, Y. C. (2005). Treatment of oily waters using vermiculite. *Water Research*, *39*(12), 2643-2653.

Ngah, W. W., & Hanafiah, M. A. K. M. (2008). Biosorption of copper ions from dilute aqueous solutions on base treatedrubber (Hevea brasiliensis) leaves powder: kinetics, isotherm, and biosorption mechanisms. *Journal of Environmental Sciences*, *20*(10), 1168-1176.

Nodeh, H. R., Ibrahim, W. A. W., Ali, I., & Sanagi, M. M. (2016). Development of magnetic graphene oxide adsorbent for the removal and preconcentration of As (III) and As (V) species from environmental water samples. *Environmental Science and Pollution Research*, *23*(10), 9759-9773.

Nodeh, H. R., Ibrahim, W. A. W., Sanagi, M. M., & Aboul-Enein, H. Y. (2016). Magnetic graphene-based cyanopropyltriethoxysilane as an adsorbent for simultaneous determination of polar and non-polar organophosphorus pesticides in cow's milk. *RSC Advances*, *6*(30), 24853-24864.

Nurerk, P., Kanatharana, P., & Bunkoed, O. (2017). Polyaniline-coated magnetite nanoparticles incorporated in alginate beads for the extraction and enrichment of

University of Malaya

polycyclic aromatic hydrocarbons in water samples. *International Journal of Environmental Analytical Chemistry*, *97*(2), 145-158.

Pan, S. D., Zhou, L. X., Zhao, Y. G., Chen, X. H., Shen, H. Y., Cai, M. Q., & Jin, M. C. (2014). Amine-functional magnetic polymer modified graphene oxide as magnetic solid-phase extraction materials combined with liquid chromatography–tandem mass spectrometry for chlorophenols analysis in environmental water. *Journal of Chromatography A*, *1362*, 34-42.

Patnaik, P. (2010). *Handbook of Environmental Analysis: Chemical Pollutants in Air, Water, Soil, and Solid Wastes*. CRC Press.

Petcharoen, K., & Sirivat, A. (2012). Synthesis and characterization of magnetite nanoparticles via the chemical co-precipitation method. *Materials Science and Engineering: B*, *177*(5), 421-427.

Peters, C. A., Knightes, C. D., & Brown, D. G. (1999). Long-term composition dynamics of PAH-containing NAPLs and implications for risk assessment. *Environmental Science & Technology*, *33*(24), 4499-4507.

Rajakovic, V., Aleksic, G., Radetic, M., & Rajakovic, L. (2007). Efficiency of oil removal from real wastewater with different sorbent materials. *Journal of Hazardous Materials*, *143*(1), 494-499.

Ribeiro, T. H., Rubio, J., & Smith, R. W. (2003). A dried hydrophobic aquaphyte as an oil filter for oil/water emulsions. *Spill Science & Technology Bulletin*, *8*(5), 483-489.

Ricardo, A. I. C., Bernardo, F. J. G., Zougagh, M., Martín-Doimeadios, R. C. R., & Ríos, Á. (2017). Magnetic nanoparticles—carbon nanotubes hybrid composites for selective solid-phase extraction of polycyclic aromatic hydrocarbons and determination by ultra-high performance liquid chromatography. *Analytical and Bioanalytical Chemistry*, *409*(21), 5125-5132.

Saleem, J., Riaz, M. A., & Gordon, M. (2018). Oil sorbents from plastic wastes and polymers: A review. *Journal of Hazardous Materials*, *341*, 424-437.

Salimon, J., Abdullah, B. M., & Salih, N. (2011). Hydrolysis optimization and characterization study of preparing fatty acids from Jatropha curcas seed oil. *Chemistry Central Journal*, *5*(1), 67.

Seddon, K. R., Stark, A., & Torres, M. J. (2000). Influence of chloride, water, and organic solvents on the physical properties of ionic liquids. *Pure and Applied Chemistry*, *72*(12), 2275-2287.

University of Malaya

Sen, T., Sebastianelli, A., & Bruce, I. J. (2006). Mesoporous Silica − Magnetite Nanocomposite: Fabrication and Applications in Magnetic Bioseparations. *Journal of the American Chemical Society*, *128*(22), 7130-7131.

Senturk, H. B., Ozdes, D., Gundogdu, A., Duran, C., & Soylak, M. (2009). Removal of phenol from aqueous solutions by adsorption onto organomodified Tirebolu bentonite: Equilibrium, kinetic and thermodynamic study. *Journal of Hazardous Materials*, *172*(1), 353-362.

Shahabuddin, S., Muhamad Sarih, N., Mohamad, S., & Joon Ching, J. (2016). SrtiO3 nanocube-doped polyaniline nanocomposites with enhanced photocatalytic degradation of methylene blue under visible light. *Polymers*, *8*(2), 27.

Sharma, Y. C., Singh, B., & Korstad, J. (2011). Advancements in solid acid catalysts for ecofriendly and economically viable synthesis of biodiesel. *Biofuels, Bioproducts and Biorefining*, *5*(1), 69-92.

Shen, J., Hu, Y., Shi, M., Li, N., Ma, H., & Ye, M. (2010). One step synthesis of graphene oxide− magnetic nanoparticle composite. *The Journal of Physical Chemistry C*, *114*(3), 1498-1503.

Sheng, G., Li, Y., Yang, X., Ren, X., Yang, S., Hu, J., & Wang, X. (2012). Efficient removal of arsenate by versatile magnetic graphene oxide composites. *RSC Advances*, *2*(32), 12400-12407.

Sidik, S. M., Jalil, A. A., Triwahyono, S., Adam, S. H., Satar, M. A. H., & Hameed, B. H. (2012). Modified oil palm leaves adsorbent with enhanced hydrophobicity for crude oil removal. *Chemical Engineering Journal*, *203*, 9-18.

Sokker, H. H., El-Sawy, N. M., Hassan, M. A., & El-Anadouli, B. E. (2011). Adsorption of crude oil from aqueous solution by hydrogel of chitosan based polyacrylamide prepared by radiation induced graft polymerization. *Journal of Hazardous Materials*, *190*(1), 359-365.

Srinivasan, A., & Viraraghavan, T. (2010). Oil removal from water by fungal biomass: a factorial design analysis. *Journal of Hazardous Materials*, *175*(1), 695-702.

Suhendra, D., Yunus, W. W., Haron, M. J., Basri, M., & Silong, S. (2010). Separation and preconcentration of copper (II) ion by fatty hydroxamic acids immobilized onto amberlite XAD–4 Resin. *Indonesian Journal of Chemistry*, *6*(2), 165-169.

Sung, H. H., Kao, W. Y., & Su, Y. J. (2003). Effects and toxicity of phthalate esters to hemocytes of giant freshwater prawn, Macrobrachium rosenbergii. *Aquatic Toxicology*, *64*(1), 25-37.

University of Malaya

Tahmasebi, E., & Yamini, Y. (2012). Facile synthesis of new nano sorbent for magnetic solid-phase extraction by self-assembling of bis-(2,4,4-trimethylpentyl)-dithiophosphinic acid on Fe_3O_4@ Ag core@ shell nanoparticles: characterization and application. *Analytica Chimica Acta*, *756*, 13-22.

Takafuji, M., Ide, S., Ihara, H., & Xu, Z. (2004). Preparation of poly (1-vinylimidazole)-grafted magnetic nanoparticles and their application for removal of metal ions. *Chemistry of Materials*, *16*(10), 1977-1983.

Tartaj, P., Morales, M. P., Gonzalez-Carreno, T., Veintemillas-Verdaguer, S., & Serna, C. J. (2005). Advances in magnetic nanoparticles for biotechnology applications. *Journal of Magnetism and Magnetic Materials*, *290*, 28-34.

Taufiqurrahmi, N., Mohamed, A. R., & Bhatia, S. (2011). Production of biofuel from waste cooking palm oil using nanocrystalline zeolite as catalyst: Process optimization studies. *Bioresource Technology*, *102*(22), 10686-10694.

Tsumura†*, Y., Ishimitsu, S., Saito, I., Sakai §, H., Tsuchida §, Y., & Tonogai, Y. (2003). Estimated daily intake of plasticizers in 1-week duplicate diet samples following regulation of DEHP-containing PVC gloves in Japan. *Food Additives & Contaminants*, *20*(4), 317-324.

Venkatanarasimhan, S., & Raghavachari, D. (2013). Epoxidized natural rubber–magnetite nanocomposites for oil spill recovery. *Journal of Materials Chemistry A*, *1*(3), 868-876.

Wan, J., Chen, X., Wang, Z., Yang, X., & Qian, Y. (2005). A soft-template-assisted hydrothermal approach to single-crystal Fe_3O_4 nanorods. *Journal of Crystal Growth*, *276*(3), 571-576.

Wang, D., Silbaugh, T., Pfeffer, R., & Lin, Y. S. (2010). Removal of emulsified oil from water by inverse fluidization of hydrophobic aerogels. *Powder Technology*, *203*(2), 298-309.

Wang, M., Cui, S., Yang, X., & Bi, W. (2015). Synthesis of gC_3N_4/Fe_3O_4 nanocomposites and application as a new sorbent for solid phase extraction of polycyclic aromatic hydrocarbons in water samples. *Talanta*, *132*, 922-928.

Wang, W., Ma, R., Wu, Q., Wang, C., & Wang, Z. (2013). Fabrication of magnetic microsphere-confined graphene for the preconcentration of some phthalate esters from environmental water and soybean milk samples followed by their determination by HPLC. *Talanta*, *109*, 133-140.

Wang, W., Ma, R., Wu, Q., Wang, C., & Wang, Z. (2013). Magnetic microsphere-confined graphene for the extraction of polycyclic aromatic hydrocarbons from

University of Malaya

environmental water samples coupled with high performance liquid chromatography–fluorescence analysis. *Journal of Chromatography A*, *1293*, 20-27.

Wang, Y., Wang, S., Niu, H., Ma, Y., Zeng, T., Cai, Y., & Meng, Z. (2013). Preparation of polydopamine coated Fe3O4 nanoparticles and their application for enrichment of polycyclic aromatic hydrocarbons from environmental water samples. *Journal of Chromatography A*, *1283*, 20-26.

Wattie, B., Dumont, M. J., & Lefsrud, M. (2018). Synthesis and properties modified feather keratin-based motor oil sorbing cryogels with high oil holding capacity. *Journal of Polymers and the Environment*, *26*(1), 59-65.

Wilhelm, C., Billotey, C., Roger, J., Pons, J. N., Bacri, J. C., & Gazeau, F. (2003). Intracellular uptake of anionic superparamagnetic nanoparticles as a function of their surface coating. *Biomaterials*, *24*(6), 1001-1011.

Wise, S. A., Sander, L. C., & Schantz, M. M. (2015). Analytical methods for determination of polycyclic aromatic hydrocarbons (PAHs)—a historical perspective on the 16 US EPA priority pollutant PAHs. *Polycyclic Aromatic Compounds*, *35*(2-4), 187-247.

Wu, J., Wang, C., Liang, X., Yang, X., Wang, C., Wu, Q., & Wang, Z. (2017). Magnetic spherical carbon as an efficient adsorbent for the magnetic extraction of phthalate esters from lake water and milk samples. *Journal of Separation Science*, *40*(10), 2207-2213.

Wu, Q., Liu, M., Ma, X., Wang, W., Wang, C., Zang, X., & Wang, Z. (2012). Extraction of phthalate esters from water and beverages using a graphene-based magnetic nanocomposite prior to their determination by HPLC. *Microchimica Acta*, *177*(1-2), 23-30.

Wu, W., He, Q., & Jiang, C. (2008). Magnetic iron oxide nanoparticles: synthesis and surface functionalization strategies. *Nanoscale Research Letters*, *3*(11), 397.

Yan, Z., He, M., Chen, B., Gui, B., Wang, C., & Hu, B. (2017). Magnetic covalent triazine framework for rapid extraction of phthalate esters in plastic packaging materials followed by gas chromatography-flame ionization detection. *Journal of Chromatography A*, *1525*, 32-41.

Yan, Z., Yuan, J., Zhu, G., Zou, Y., Chen, C., Yang, S., & Yao, S. (2013). A new strategy based on cholesterol-functionalized iron oxide magnetic nanoparticles for determination of polycyclic aromatic hydrocarbons by high-performance liquid chromatography with cholesterol column. *Analytica Chimica Acta*, *780*, 28-35.

University of Malaya

Yang, J., Li, J. Y., Qiao, J. Q., Lian, H. Z., & Chen, H. Y. (2014). Solid phase extraction of magnetic carbon doped Fe3O4 nanoparticles. *Journal of Chromatography A*, *1325*, 8-15.

Yang, J., Wu, M., Chen, F., Fei, Z., & Zhong, M. (2011). Preparation, characterization, and supercritical carbon dioxide foaming of polystyrene/graphene oxide composites. *The Journal of Supercritical Fluids*, *56*(2), 201-207.

Yang, P., Chen, J., Wang, Z., Qiao, X., Cai, X., Tian, F., & Ge, L. (2007). Contributions of deposited particles to pine needle polycyclic aromatic hydrocarbons. *Journal of Environmental Monitoring*, *9*(11), 1248-1253.

Yang, X., Chen, C., Li, J., Zhao, G., Ren, X., & Wang, X. (2012). Graphene oxide-iron oxide and reduced graphene oxide-iron oxide hybrid materials for the removal of organic and inorganic pollutants. *RSC Advances*, *2*(23), 8821-8826.

Yang, X., Zhang, X., Ma, Y., Huang, Y., Wang, Y., & Chen, Y. (2009). Superparamagnetic graphene oxide–Fe3O4 nanoparticles hybrid for controlled targeted drug carriers. *Journal of Materials Chemistry*, *19*(18), 2710-2714.

Yusoff, M. M., Raoov, M., Yahaya, N., & Salleh, N. M. (2017). An ionic liquid loaded magnetically confined polymeric mesoporous adsorbent for extraction of parabens from environmental and cosmetic samples. *RSC Advances*, *7*(57), 35832-35844.

Zakaria, M. P., Takada, H., Tsutsumi, S., Ohno, K., Yamada, J., Kouno, E., & Kumata, H. (2002). Distribution of polycyclic aromatic hydrocarbons (PAHs) in rivers and estuaries in Malaysia: a widespread input of petrogenic PAHs. *Environmental Science & Technology*, *36*(9), 1907-1918.

Zeng, F., Cui, K., Xie, Z., Wu, L., Liu, M., Sun, G., Lin. Y., Luo. D., & Zeng, Z. (2008). Phthalate esters (PAEs): emerging organic contaminants in agricultural soils in peri-urban areas around Guangzhou, China. *Environmental Pollution*, *156*(2), 425-434.

Zhang, L., He, R., & Gu, H. C. (2006). Oleic acid coating on the monodisperse magnetite nanoparticles. *Applied Surface Science*, *253*(5), 2611-2617.

Zhang, Q., Saleh, A. S., Chen, J., & Shen, Q. (2012). Chemical alterations taken place during deep-fat frying based on certain reaction products: a review. *Chemistry and Physics of Lipids*, *165*(6), 662-681.

Zhang, S., Niu, H., Cai, Y., & Shi, Y. (2010). Barium alginate caged Fe_3O_4@ C_{18} magnetic nanoparticles for the pre-concentration of polycyclic aromatic

University of Malaya

hydrocarbons and phthalate esters from environmental water samples. *Analytica Chimica Acta*, *665*(2), 167-175.

Zhang, S., Niu, H., Hu, Z., Cai, Y., & Shi, Y. (2010). Preparation of carbon coated Fe_3O_4 nanoparticles and their application for solid-phase extraction of polycyclic aromatic hydrocarbons from environmental water samples. *Journal of Chromatography A*, *1217*(29), 4757-4764.

Zhao, X., Shi, Y., Cai, Y., & Mou, S. (2008). Cetyltrimethylammonium bromide-coated magnetic nanoparticles for the preconcentration of phenolic compounds from environmental water samples. *Environmental Science & Technology*, *42*(4), 1201-1206.

Zhou, H., Wu, C., Meng, A., Zhang, Y., & Williams, P. T. (2014). Effect of interactions of biomass constituents on polycyclic aromatic hydrocarbons (PAH) formation during fast pyrolysis. *Journal of Analytical and Applied Pyrolysis*, *110*, 264-269.

Zhou, Q., Lei, M., Wu, Y., & Yuan, Y. (2017). Magnetic solid phase extraction of typical polycyclic aromatic hydrocarbons from environmental water samples with metal organic framework MIL-101 (Cr) modified zero valent iron nano-particles. *Journal of Chromatography A*, *1487*, 22-29.

Zhou, Y. B., Tang, X. Y., Hu, X. M., Fritschi, S., & Lu, J. (2008). Emulsified oily wastewater treatment using a hybrid-modified resin and activated carbon system. *Separation and Purification Technology*, *63*(2), 400-406.

Zhu, Q., Tao, F., & Pan, Q. (2010). Fast and selective removal of oils from water surface via highly hydrophobic core− shell Fe_2O_3@ C nanoparticles under magnetic field. *ACS Applied Materials & Interfaces*, *2*(11), 3141-3146.

Ziaei, E., Mehdinia, A., & Jabbari, A. (2014). A novel hierarchical nanobiocomposite of graphene oxide–magnetic chitosan grafted with mercapto as a solid phase extraction sorbent for the determination of mercury ions in environmental water samples. *Analytica Chimica Acta*, *850*, 49-56.

University of Malaya

LIST OF PUBLICATIONS AND PAPERS PRESENTED

Publications:

Rozi, S. K. M., Bakhshaei, S., Manan, N. S. A., & Mohamad, S. (2016). Superhydrophobic magnetic nanoparticle-free fatty acid regenerated from waste cooking oil for the enrichment of carcinogenic polycyclic aromatic hydrocarbons in sewage sludges and landfill leachates. *RSC Advances*, *6*(90), 87719-87729.

Rozi, S. K. M., Nodeh, H. R., Kamboh, M. A., Manan, N. S. A., & Mohamad, S. (2017). Novel Palm Fatty Acid Functionalized Magnetite Nanoparticles for Magnetic Solid-Phase Extraction of Trace Polycyclic Aromatic Hydrocarbons from Environmental Samples. *Journal of Oleo Science*, *66*(7), 771-784.

Rozi, S. K. M., Shahabuddin, S., Manan, N. S. A., Mohamad, S., Kamal, S. A. A., & Rahman, S. A. (2018). Palm Fatty Acid Functionalized Fe_3O_4 Nanoparticles as Highly Selective Oil Adsorption Material. *Journal of Nanoscience and Nanotechnology*, *18*(5), 3248-3256.

Proceedings/presentations:

Siti Khalijah Mahmad Rozi, Ninie Suhana Abdul Manan & Sharifah Mohamad, "Superhydrophobic magnetic nanoparticle-free fatty acid regenerated from waste cooking oil for the enrichment of carcinogenic polycyclic aromatic hydrocarbons in sewage sludges and landfill leachates", 16th Asia Pacific International Symposium On Microscale Separations and Analysis (2016), Johor Bahru, Johor, Malaysia.

Siti Khalijah Mahmad Rozi, Ninie Suhana Abdul Manan & Sharifah Mohamad, "Superhydrophobic Free Fatty Acid Functionalized Fe_3O_4 Nanoparticles from Waste Cooking Oil for Enhanced Oil-Water Separation", The 29th Malaysian Analytical Chemistry Symposium, (2016), Penang, Malaysia.

University of Malaya